MECHANICAL PROPERTIES OF SODIUM AND POTASSIUM ACTIVATED METAKAOLIN-BASED GEOPOLYMERS

A Thesis

by

HYUNSOO KIM

Submitted to the Office of Graduate Studies of
Texas A&M University
in partial fulfillment of the requirements for the degree of

MASTER OF SCIENCE

August 2010

Major Subject: Materials Science and Engineering

MECHANICAL PROPERTIES OF SODIUM AND POTASSIUM ACTIVATED METAKAOLIN-BASED GEOPOLYMERS

A Thesis

by

HYUNSOO KIM

Submitted to the Office of Graduate Studies of
Texas A&M University
in partial fulfillment of the requirements for the degree of

MASTER OF SCIENCE

Approved by:

Chair of Committee,	Miladin Radovic
Committee Members,	Zoubeida Ounaies
	Victor Ugaz
Head of Department,	Ibrahim Karaman

August 2010

Major Subject: Materials Science and Engineering

ABSTRACT

Mechanical Properties of Sodium and Potassium Activated Metakaolin-Based Geopolymers.

(August 2010)

Hyunsoo Kim, B.S., Korea Military Academy, Korea

Chair of Advisory Committee: Dr. Miladin Radovic

Geopolymers (GPs) are a new class of inorganic polymers that have been considered as good candidate materials for many applications, including fire resistant and refractory panels, adhesives, and coatings, waste encapsulation material, etc. The aim of this study is to establish relationship between structural and mechanical properties of geopolymers with different chemical compositions. The metakaolin-based geopolymers were prepared by mechanically mixing metakaolin and alkaline silicate aqueous solutions to obtain samples with SiO_2/Al_2O_3 molar ratio that ranges from 2.5 to 5, and Na/Al or K/Al atomic ratios equal to 1. Geopolymer samples were cured in a laboratory oven at 80°C and ambient pressure for different times in the sealed containers. Structural characterization of the samples with different chemical compositions was carried out using X-Ray Diffraction (XRD), Fourier Transform Infrared (FTIR) spectroscopy, Nuclear Magnetic-Resonance (NMR) spectroscopy and Scanning Electron Microscopy (SEM) with Energy Dispersive Spectroscopy (EDS). The mechanical characterization included Micro-indentation, Vickers indentation and fracture toughness measurement, as well as compressive testing.

It was found that structure and mechanical properties of GPs depend on their chemical composition. The Na-GPs with ratio 3 have a highest compressive strength and Young's modulus of 39 MPa and 7.9 GPa, respectively. The results of mechanical testing are discussed in more detail in this thesis and linked to structural properties of processed geopolymers.

DEDICATION

To my parents and brother

ACKNOWLEDGMENTS

I would like to express my appreciation to my advisor Dr. Miladin Radovic at Texas A&M University, for his encouragement, and support throughout the research. I would also like to thank my committee members, Dr. Victor Ugaz and Dr. Zoubeida Ounaies, for their help with my research. It has been a great experience to receive their valuable insight and suggestions towards the improvement of my work.

My sincere thanks also goes to Marci Lizcano for providing help with synthesis of geopolymers and analysis of experimental results. I would like to also thank Dr. Vladimir Bakhmoutov, ByungSoo Ham, and WoonKyu Baek, for their help with NMR, Microindentation, and Vickers indentation testing. I would like to thank Republic of Korea Army for financial support during my study.

NOMENCLATURE

ATR-FTIR	Attenuated Total Reflectance FTIR
E	Young's Modulus
EDS	Energy-Dispersive Spectroscopy
FTIR	Fourier Transform Infrared Spectroscopy
GPs	Geopolymers
HV	Vickers Hardness Number
K-GPs	K (Potassium) Activated Geopolymers
K_{IC}	Fracture Toughness
MAS-NMR	Magic-Angle Spinning NMR
MK	Metakaolin
Na-GPs	Na (Sodium) Activated Geopolymers
NMR	Nuclear Magnetic Resonance Spectroscopy
PPM	Parts Per Million
PSS	Poly (sialate-siloxo)
S	Probability of Survival
SE	Secondary Electron
SEM	Scanning Electron Microscopy
TAMU	Texas A&M University
XRD	X-Ray Diffraction Resonance
δ	Chemical Shifts

TABLE OF CONTENTS

LISTS OF FIGURES

Page

Page

Page

LISTS OF TABLES

CHAPTER I

INTRODUCTION

1.1. Geopolymers

Geopolymers recently emerged as a new class of inorganic aluminosilicate polymeric materials. These materials were synthesized for the first time in 1940 by A. O. Purdon [1] and again in the late 1950's by Glukhovsky [2]. The term geopolymer was introduced by Davidovits [3] in the early 70's to denote their inorganic nature ("geo") and structural similarity to organic polymers ("polymers"), and is commonly used nowadays [3, 4].

These inorganic polymers are processed by polycondensation of aluminum and silicon monomeric or oligomeric species in metal alkali-activated solutions [3]. The GP precursors can be obtained from different aluminosilicate sources such as clays, Metakaolin, and industrial waste (fly-ash or furnace slug). Alkali hydroxide solutions are added to the aluminosilicate source to activate the dissolution and polymerization process. The activating solutions are based on aqueous solutions of alkali hydroxides and the most commonly used metal alkaline activators are Na and K [5]. However, other metals from group I and II of the periodic table as well as NH_4^+, and H_3O^+ may also be utilized for synthesis [6, 7]. The silicon content of the final product can be manipulated by the addition of SiO_2 to the alkaline aqueous solution. After mixing, K-silicate and Na-silicate solutions with aluminosilicate sources, the material is placed in molds and cured usually at temperatures below 100 ºC for various periods of time [8]. According to

This thesis follows the style of IEEE/TMS Journal of Electronic Materials.

Davidovits, the resulting GP structure can be characterized as a 3-D matrix of tetrahedrally coordinated Si and Al species. The negatively charged aluminum anions are balance by the positively charged metal cations in the 3-D network structure of geopolymers [3].

1.2. Properties and Applications

Previous work have shown that properties of GPs, can vary significantly depending on processing environments, Si/Al molar ratios, type of aluminosilicate source, water content, etc. All those studies have shown that GPs have good thermally stability up to 1000-1200 °C [9], chemical resistivity [10], fire resistivity [3], compressive strength, low shrinkage, abrasion resistance, adhesion to various substrates, and low thermal conductivity [8, 11, 12].

When considering these various properties, the applications for GP technology become evident. Several applications of geopolymers and their composites have been proposed and utilized so far [3, 8]. GPs have been considered for toxic waste management [13-15], construction materials [16], biomaterials [17], concrete binders [11, 18], and adhesives [19, 20]. Moreover, some of these applications may provide solutions to environmental concerns when dealing with CO_2 emissions involved in Portland cement processing [11, 21] and industrial waste [22, 23].

1.3. Motivation

Geopolymers are well known for their enhanced compressive strength compared to concrete [11, 24-26]. The mechanical properties of these materials are critical if GPs are to be commercially utilized. Many studies have been carried out in an effort to enhance

the mechanical properties of GPs [4, 27-29]. However, the effects of chemical composition, processing parameters, and resulting microstructure on mechanical properties remains obscure.

The goal of this thesis is to elucidate the mechanical behavior of GPs as a result of these parameters. This study investigates the effects of the SiO_2/Al_2O_3 molar ratio and metal activators (Na and K) on the mechanical properties of metakaolin-based GPs. The molar ratios considered are SiO_2/Al_2O_3= 2.5, 3, 4, and 5 with H_2O/Al_2O_3= 11 and 13. Atomic ratios at Na/Al and K/Al were held constant and equal to 1, that is stoichiometric ratio required to keep negative charges of Al tetrahedral balanced. Additionally, the effects of different curing and ageing times on the mechanical properties of GPs were investigated. The samples were cured for 24 and 48 hrs at 80ºC in sealed containers. Also, Na-GPs with ratio SiO_2/Al_2O_3= 4, K-GPs with ratio SiO_2/Al_2O_3= 2.5 and 4 were aged for 10 days in air at ambient temperature before testing.

In order to verify that the materials were geopolymers, material characterization studies were carried out using X-ray diffraction (XRD), Fourier Transform Infrared spectroscopy (FTIR), Nuclear Magnetic-Resonance (NMR) spectroscopy, and Scanning Electron Microscopy (SEM) with Energy Dispersive Spectroscopy (EDS).

Furthermore, characterization of the mechanical properties was carried out in order to determine effects of chemical composition, curing times and ageing on the hardness, elastic moduli, fracture toughness and compressive strength of GPs. The observed changes in mechanical properties are linked to the structural characteristics of the process GPs.

1.4. Thesis Organization

This thesis consists of five chapters. In Chapter II, thesis reviews published literature on structure, processing and mechanical properties of Metakaolin-based geopolymers as well as a general history of geopolymer research. Chapter III provides details of the experimental methods and materials used throughout the research. Chapter IV describes and discusses experiment results, while Chapter V provides conclusions and recommendations for future work.

CHAPTER II

LITERATURE REVIEW

2.1. A History of Geopolymers

The term “Geopolymer” (GP) was introduced by Joseph Davidovits to refer to a new class of X-ray amorphous structure of aluminosilicate binders [5]. GPs are processed by hydro-thermal synthesis of aluminosilicates in alkaline or alkaline silicate solutions [30]. The term ‘geo’ refers to the inorganic property of the material, while the term ‘polymer’ refers to the similarity of the GP structure to organic polymers [3, 4]. GPs can be processed from a large variety of aluminosilicate sources and alkaline activating solutions [31].

Research in GPs initially concentrated on their applications as alternative cement to ordinary Portland Cements (OPCs) [32]. Although synthesis is similar, chemical bonding in OPCs differs from GPs in that its former are formed by reactions of calcium oxide and silicon dioxide to form calcium-silicate hydrates [33] while GPs are formed by polycondensation of Al and Si species. The synthesis and structure in geopolymer technology is still poorly understood. However, theoretical concepts have been proposed and are discussed in the subsequent sections of this chapter.

2.2. Geopolymer Synthesis

2.2.1. Precursors

GPs precursors can be obtained from a wide range of aluminosilicate sources, such

as calcium slag [34], fly ashes [35], industrial coal ash [36], and clays [37], kaolinite and metakaolin [27, 31, 35, 37]. Metakaolin has been widely used in the construction industry as cement binders due to advanced reaction, activation [38] and higher purity when compared to other aluminosilicate sources.

2.2.1.1. Metakaolin

Metakaolin is a calcined kaolinite. Dehydroxylation in kaolinite occurs when Al-O-H bonds break releasing hydroxyl groups (-OH) and hydrogen that later form water molecule. Surface hydroxyl groups break away easier than the hydroxyl groups within the material as a result of longer bond length on the surface [12]. Calcining results not only in the removal of water from the kaolinite but also increases reactivity to alkaline activators, namely metakaolin [39]. Calcining temperatures range from 500 to 750 °C for 2 to 10 hours [39-41] and results in formation of X-ray amorphous metakaolin. However, the calcinations process can sometimes result in the formation of crystalline phases such as spinnel, cristobalite, mullite that is are deleterious for processing geopolymers due to their lower reactivity in alkaline solutions [42]. **Figure 2-1** shows structure of layered, uncreated aluminosilicate source that might be present in GPs as a result of incomplete reaction [31].

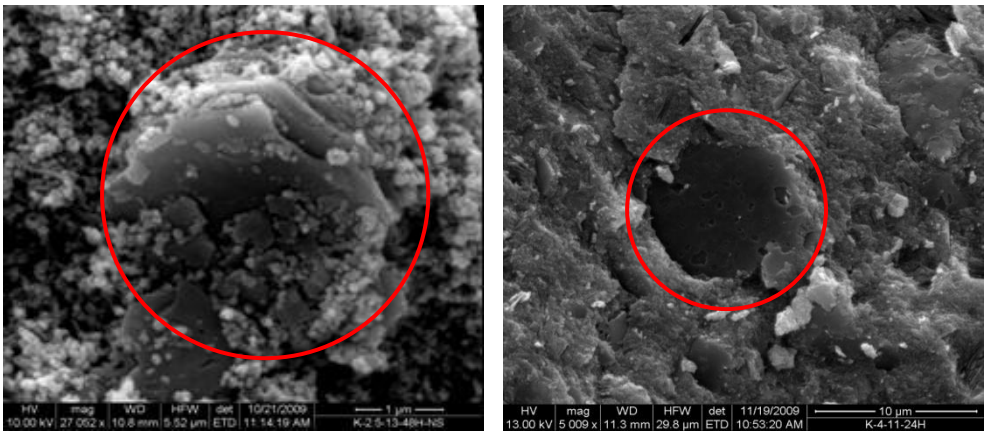

Figure 2 - 1: Layered, uncreated aluminosilicate source in GPs

2.2.2. Alkaline Activators and Dissolution of Si & Al Species

The alkaline activators are responsible for two simultaneous processes; dissolution into Al and Si monomerics species and polymerization. While OH^- groups are believed to play a main role in dissolution of Si and Al species, the presence of alkali ions are crucial for the polycondseation of those species into the 3-D polymeric network. Another function of the alkaline metal activator is to keep the AlO_4^- anions neutral. The most common metal cations used as activating solutions are Na and K [27-29, 41, 43-46]. Aqueous solutions of NaOH, KOH as well as sodium or potassium silicates can be prepared and used to synthesize GPs. When the alkaline solution with high pH (usually pH of 13~14) is added to the precursor, Si^{4+} and Al^{3+} components are hydrolyzed forming mostly $[SiO(OH)_3]^-$, $[SiO_2(OH)_2]^{2-}$ and $[Al(OH)_4]^-$ monomeric species [6]. The following equations describe the dissolution and hydrolysis of Si and Al species [7].

$Al_2O_3 + 3H_2O + 2OH^- \rightarrow 2[Al(OH)_4]^-$ ……. (2.1)

$SiO_2 + H_2O + OH^- \rightarrow [SiO(OH)_3]^-$ ……..…. (2.2)

$SiO_2 + 2OH^- \rightarrow [SiO_2(OH)_2]^{2-}$ ……. (2.3)

The degree of MK dissolution depends on the dissolution rate, the temperature during the dissolution, the reactivity of the MK source and the OH^- concentration [7]. MK has been shown to have a higher dissolution rate of Al and Si species than other materials, resulting in faster geopolymerization process. Furthermore, it was shown that addition of NaOH results in faster dissolution rates when compared to KOH [47].

2.2.3. Condensation & Polymerization and Resulting Atomic Structure

The condensation process is believed to occur simultaneously with the dissolution process [40]. It has been suggested that during this process $[SiO_2(OH)_2]^{2-}$, $[SiO(OH)_3]^-$ and $[Al(OH)_4]^-$ are attracted by a hydroxyl group within the monomeric species. The two monomeric species link together and share an O atom and release an H_2O molecule [6]. The resulting network of silicon-oxygen-aluminate consists of SiO_4 and AlO_4^- tetrahedral that share corner oxygens [48]. Thus, geopolymers can be classified as Poly(sialates) with following chemical formula [48]:

$$M_p[(SiO_2)_z AlO_2]_p \cdot wH_2O \quad \text{……..…….……...…} \quad (2.4)$$

where M is the metal cation, p is the degree of poly-condensation, w is amounts of bonded water or ratio of hydration, and z is 1, 2, 3, etc. The poly (sialate) building units

forms ring and chain polymers with Al^{3+}, Si^{4+} in IV-fold coordination connected in amorphous to semi-crystalline 3-D networks. The basic building units of geopolymers are described as **Figure 2-2**:

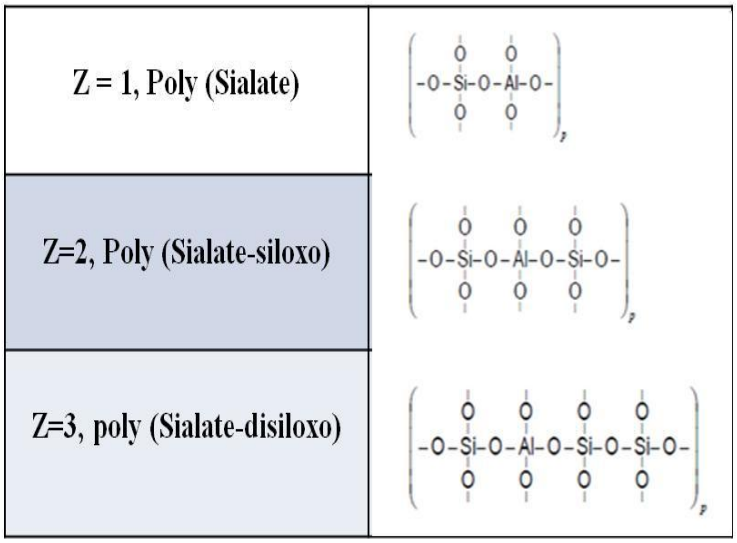

Figure 2 - 2: Davidovits' building units of GPs [48]

Although Davidivits [48] was the first one to describe the structure of geopolymers, using the structural analogy between this class of materials and organic polymers, he was unable to fully characterize and verify their structure experimentally. However, significant break trough in experimental characterization of geopolymers and verification of Davidovits model has been achieved in the studies published by Sauer et al [49], and Provis et al [12].

Faimon, et al [50] has proposed the geopolymerization process shown in **Figure 2-3 (a)**. According to this model, source materials dissolute into Al and Si monomers, and turns into unidentified secondary mineral by automatic process [50]. However, this study is limited to only a single Si/Al molar ratio of 2.

Provis, et al [10] later explained the geopolymerization process based on Faimon work as it is schematically shown in **Figure 2-3 (b)**. They proposed that unstable aluminosilicate sources in alkali solutions dissolve forming Si monomers, Al monomers, and polymerized Si olygomers, Si and Al monomers polycondensate in olygomeric species and for aluminosilicate gel. Depending on processing conditions and compositions, those aluminosilicate species can further polycondensate in amorphous 3-D networks (Gel II) or crystallize in zeolite structures [10].

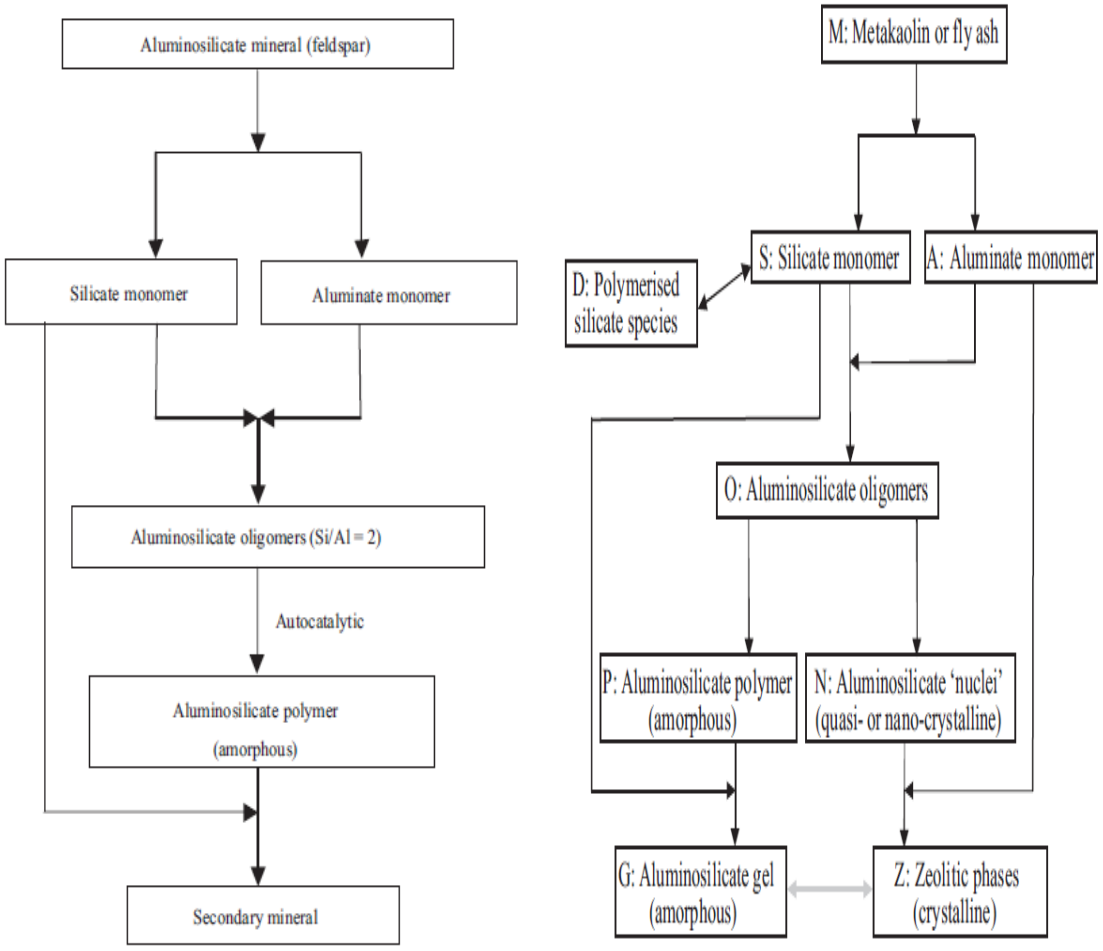

Figure 2 - 3: Geopolymerization process: (a) Faimon [50], (b) Provis [10]

Yao, et al [40] has suggested that the geopolymerization process can be divided into three stages: (1) deconstruction, (2) polymerization and (3) stabilization as showed schematically in **Figure 2-4**. Although these stages are shown separately, they are believed to be occur simultaneously.

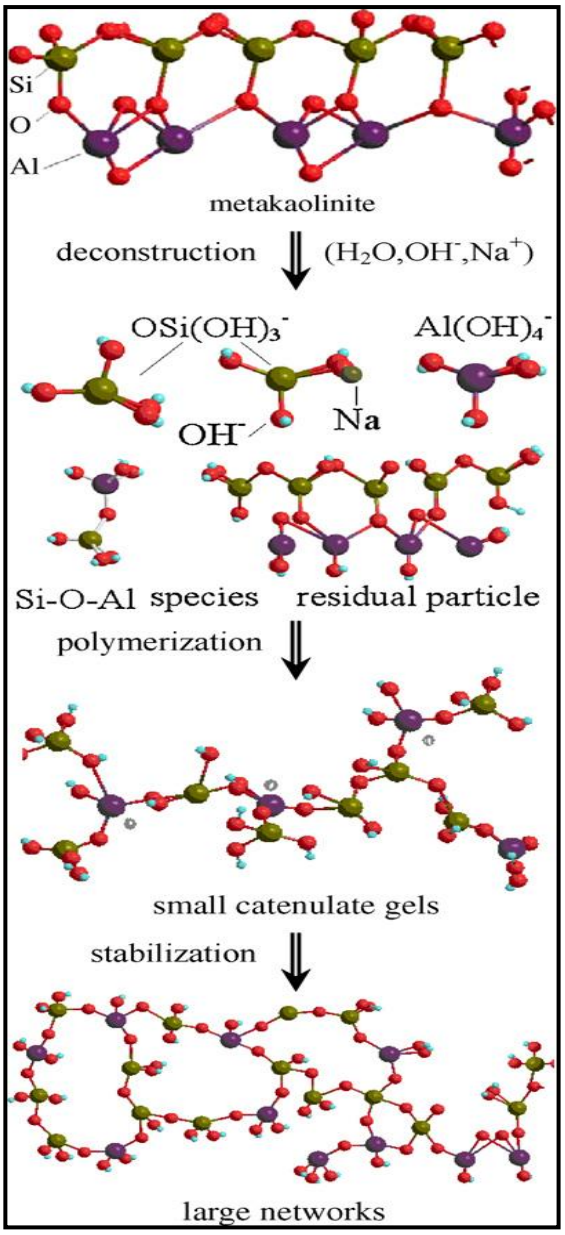

Figure 2 - 4: Schematic representation of Geopolymerization [40]

2.3. Material Characterization Methods

Various characterization methods can be used to identify amorphous and semi-crystalline features in geopolymeric materials. They are described in the following sections.

2.3.1. X-ray Diffraction

X-ray diffraction is an important tool for identifying, characterizing, and quantifying minerals. It is widely used for examination of crystalline materials. The wavelengths of X-rays range from 0.1 to 20 Å which is in the order of atomic unit cells [51]. When an X-ray interacts with atomic structures of the same magnitude, it is diffracted. The diffracted X-rays are depicted as peaks, diffuse halos or combination of both for crystalline, amorphous and semi-crystalline materials respectively [52].

Geopolymers are often X-ray amorphous; however, it may simply mean that the crystalline features do not interact with X-rays and may be nano-crystalline with short order atomic arrangements rather than truly amorphous [8, 52]. **Figure 2-5** shows examples of the diffraction patterns for crystalline and non-crystalline SiO_2. In the non-crystalline state, X-ray diffraction has a broad diffuse halo rather than sharp diffraction peaks. Typical characteristic halos for potassium and sodium GPs are shown in **Figure 2-6**. The diffuse halo is often observed between $2\theta = 20^{o}$- 40^{o} with a peak at $2\theta_{max} = 27^{o}$ - 29^{o} [8, 53, 54].

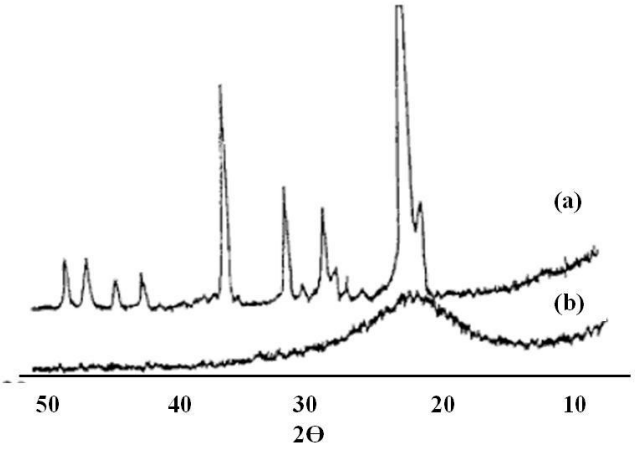

Figure 2 - 5: XRD for (a) crystalline and (b) non-crystalline SiO_2 [55]

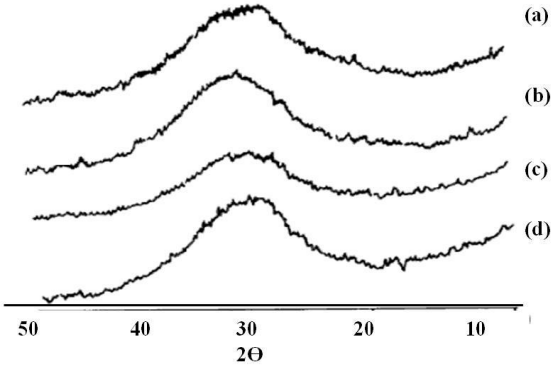

Figure 2 - 6: XRD for (Na, K)-PSS (a and b), K-PSS(c and d) [48]

XRD cannot solely be used to characterize geopolymer structures due to their inherent amorphous nature; however it is a useful tool that gives an indication of whether or not a material may be a geopolymer warranting further examination.

2.3.2. Fourier Transform Infra-red Spectroscopy, FTIR

Fourier Transform Infrared Spectroscopy (FTIR) has been used to investigate aluminosilicate materials [56]. It is a practical technique to characterize the structure of GPs in conjunction with XRD. FTIR can be used to identify functional chemical groups within the GP matrix [20, 57-59] through analysis of the absorption and transmission speactra of molecular structures in mid-infrared frequency range (400 to 4000 cm^{-1}). Absorption occurs when the vibration frequencies of a bond are the same as the infrared frequency. The vibrations of atoms and molecules are unique and are in essence a fingerprint which can be used to characterize materials [60, 61].

The IR spectra for poly (sialate), poly (sialate-silixo) are assigned to internal vibrations of Si-O-Si, and Si-O-Al bonds as shown in **Figure 2-7**. The Si/Al molar ratios affect mostly the stretching modes of the bonds and may shift to lower frequencies with increasing 4-coordinated aluminum [5].

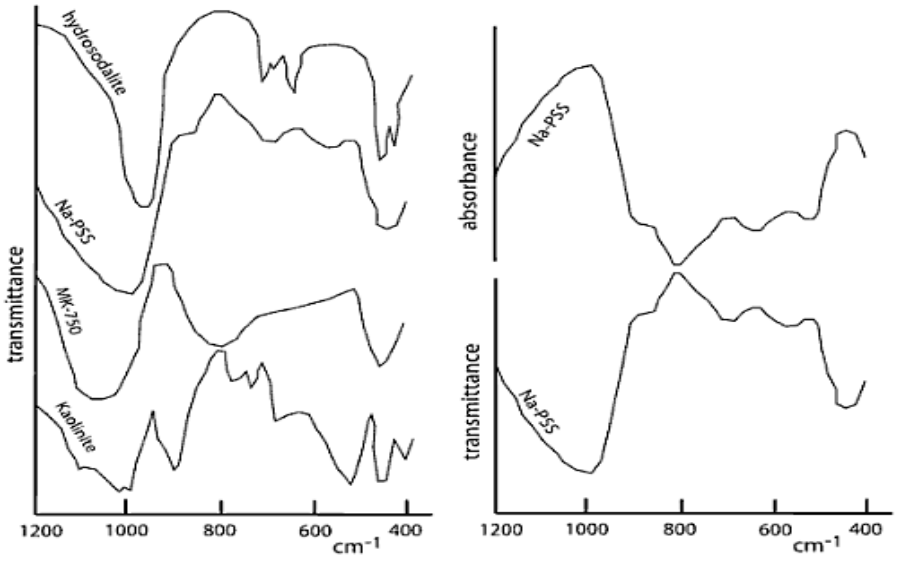

Figure 2 - 7: IR spectra for aluminosilicates and GPs (left),

IR spectra for Na-poly(sialate-siloxo) (right) [5]

The bands for kaolinite and metakaolin or calcined kaolin (MK-750) [5] stay the same at 1080-1100 cm^{-1}. Sodium activated geopolymerization of MK-750 has low the wave number about 80 to 90 cm^{-1}. This indicates changes in the microstructure after polymerization. Davidovits suggests that the shift towards lower wave numbers is due to environmental changes of Si-O bonds in which SiO_4 units have been replaced by AlO_4^- [5]. Additionally, the calcined MK-750 shifts to lower wave numbers for 4-coordinated Al (798 cm^{-1}) from the 6-coordinated Al (914 cm^{-1}) in the kaolinite. The main (Si, Al-O) bands are given in **Table 2-1** as investigated by Barbosa, et al [31].

Table 2 - 1: IR characteristic bands and corresponding species of GPs [31]

Bands	Ranges
Si-O	1080-1100 cm^{-1} (symmetrical vibration)
Si(Al)-O	1008 cm^{-1} (asymmetrical vibration)
Al-OH	914 cm^{-1} (6 coordinated Al-OH stretching vibration)
Si-OH	840 cm^{-1} (bending vibration)
Al-O	798 cm^{-1} (4 coordinated Al-O stretching vibration)
Si-O	694 cm^{-1} (symmetrically stretching vibration)
Si-O-Al	540 cm^{-1} (bending vibration)
Si-O	469 cm^{-1} (in-plane bending vibration)

2.3.3. Magic-Angle Spinning NMR Spectroscopy

Nuclear Magnetic Resonance spectroscopy (NMR) is a powerful tool in material characterization. Based on the magnetic spin of nuclei in atomic structures, atomic molecular properties can be explored with magnetic nuclear spins [62]. The nuclei in isotopes will resonate when they are exposed to an external magnetic field and electromagnetic field. The resonance frequency is proportional to the magnetic field and

characteristic of nuclei. The resonance of the nuclei can vary depending on its location i.e. neighboring atoms. These variations, referred to as chemical shifts (δ), are result of smaller magnetic fields from neighboring bonding electrons, which in turn modify the external magnetic field in the vicinity of a molecule. The chemical shifts are measured on the order of parts per million (ppm) [63].

NMR is commonly used in the study of geopolymers. In particular, ^{29}SI NMR and ^{27}Al NMR is usually carried out to give insight into Si-O-Si and Si-O-Al bonding in silico-aliminate materials [5]. Conventionally, $Q_n(mX)$, is used to describe the structural units of aluminosilicate materials. In this notation, Q represents the central atom of investigation either Si or Al, *n* denotes the number of covalent bonds, *m* is the number of *X* atoms (Si or Al) surrounding Q [48, 57, 64]. An example of the $Q_n(mX)$ notation where X= Al and n = 4 is shown in **Figure 2-8** for a 3-D tetrahedral structures commonly observed in GPs structures.

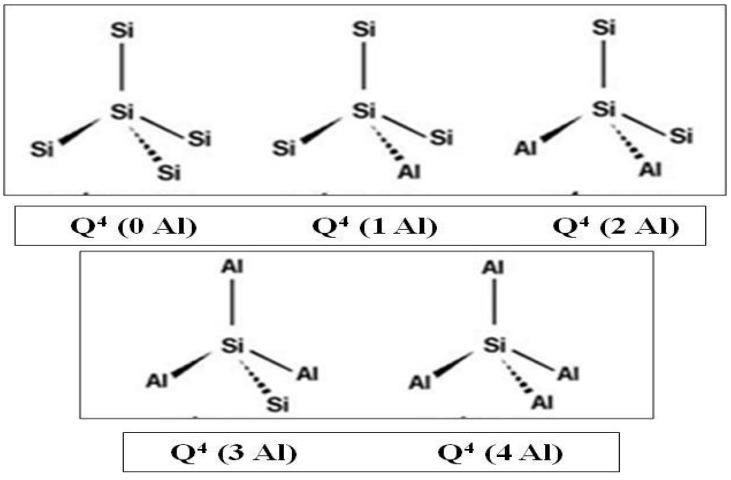

Figure 2 - 8: Q_n(mAl) notations [48]

2.3.3.1 ^{27}Al MAS-NMR Spectroscopy

It has been shown that 4-coordinated aluminum resonates at about 50 ± 20 ppm, and 6-coordinated aluminum resonates at approximately 0 ± 10 ppm from $[Al(H_2O)_6]^{3+}$ [5, 65]. Other chemical shifts are given in **Table 2-2** for various aluminosilicates [5]. Klinowski (1984) [66] found that tetravalent aluminum resonates at 60 – 80 ppm from the 6-coordinated Al in $[Al(H_2O)_6]^{6+}$. The Loewenstein aluminum avoidance that states that no two Al tetrahedra can be linked by an oxygen bridge in 3D-framework sites [67] was confirmed by some NMR studies

Table 2 - 2: Al-coordination and ^{27}Al chemical shift [68]

Name	Formula	Coordination	Chemical shift(ppm)
Anorthoclase	$(Na,K)AlSi_3O_8$	4	54
Orthoclase	$KAlSi_3O_8$	4	53
Sanidine	$KAlSi_3O_8$	4	57
K-Feldspar	$KAlSi_3O_8$	4	54
Nephiline	$NaAlSiO_4$	4	52
Calcium aluminate	$Ca_3Al_4O_7$	4	71
Sodium aluminate	$NaAlO_2$	4	76
Muscovite	$KAl_2Si_3O_{11}H_2O$	6, 4	-1, 63
Biotite	$K(Mg,Fe)_3AlSi_3O_{11}H_2O$	4	65

Several AlQ resonances were indentified in the spectra recently. Typical AlQ_n geopolymeric units are shown in **Figure 2-9** [5].

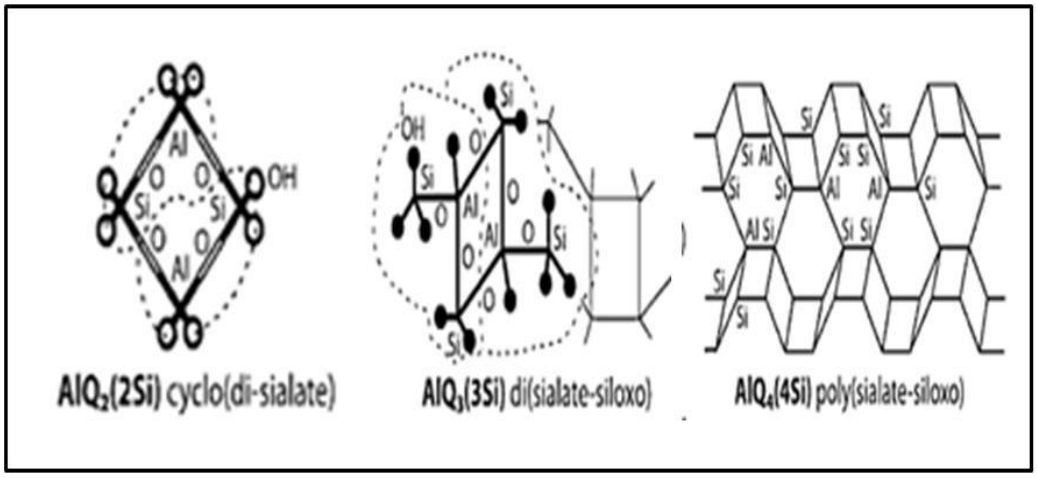

Figure 2 - 9: AlQ_n building units in geopolymeric reactions [5]

Figure 2-10 shows ^{27}Al MAS-NMR spectroscopy of K-PSS. The ^{27}Al chemical shifts is in the range of 55 ppm from $[Al(H_2O)_6]^{6+}$. This indicates a tetrahedrally coordinated AlQ_4 (4Si) type. The deficiency of other resonance and exceedingly narrow resonance at 55 ppm, eliminates any rest singular building units such as a dimmer and trimer [5].

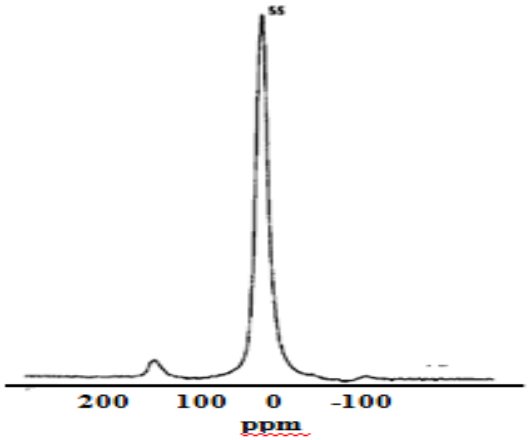

Figure 2 - 10: ^{27}Al NMR spectroscopy for K-PSS [48]

^{27}Al MAS-NMR spectroscopy does not explain the various frameworks of GPs materials such as those based on poly-sialate, poly(sialate-siloxo), poly(sialate-disiloxo) polymeric building units [5]. ^{29}Si MAS-NMR spectroscopy is then used to explain these structures that ^{27}Al MAS-NMR spectroscopy does not provide [5]. However, ^{27}Al MAS-NMR can provide confirmation of geopolymerization if 4-coordinated Al is observed.

2.4. Mictostructure of Geopolymers

P. Duxson, et al. [69], Kriven, et al. [70] , Zhang, et al. [71] carried out comprehensive studies on the microstructure of metakaolin-based geopolymers. The microstructural features of GPs are important for understanding mechanical properties of GPs. For example, **Figure 2-11** shows that compressive strength and Young's modulus highly related to chemical compositions of GPs. Additionally, P. Duxson [69] suggested the chemical compositions of GPs related to their microstructure.

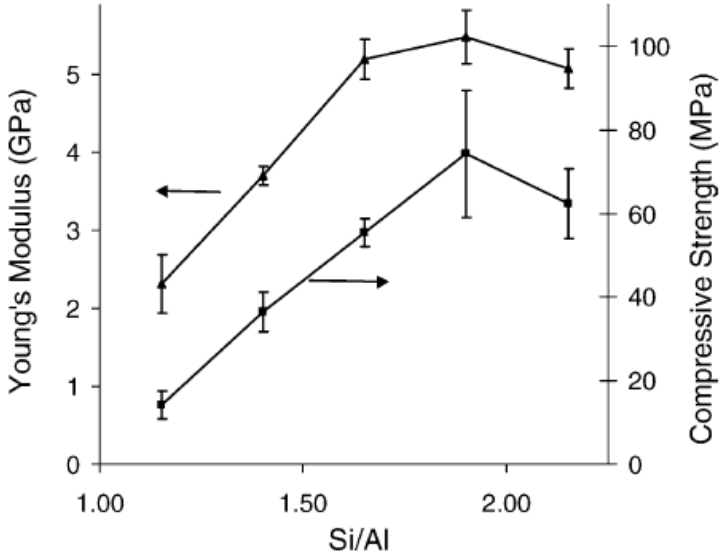

Figure 2 – 11: Young's modulus and Max compressive strength of GPs [69]

Figure 2-12 shows SEM microstructural images of Na-GPs. Low ratio of Si/Al results in less compact structure and more separated binder phases than higher ratios. Higher Si/Al ratio has relatively homogeneous structures [69]. The less compacted structure of GPs with low Si/Al ratio usually results in cracking during polishing, making preparation of those samples for microscopy quite difficult [72]. **Figure 2-12** also shows GPs with high Si/Al ratio have smaller number of quite large pores when compared to samples with lower Si/Al ratio [69]. However, porosity in GPs is poorly understood because of different complications with experimental characterization of pores size distribution [12].

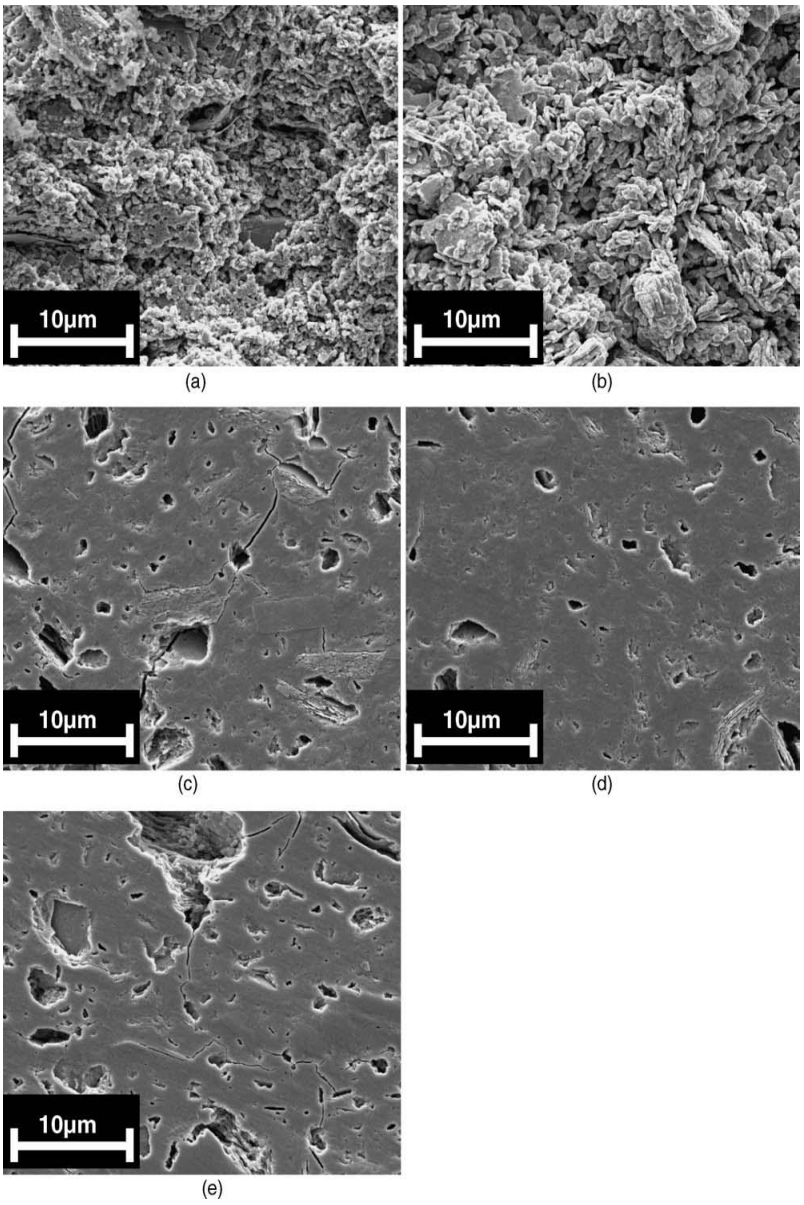

Figure 2 - 12: Microstructure of Na-GPs with raio of Si/Al = (a) 1.15, (b) 1.40, (c) 1.65, (d) 1,90, (e) 2.15 [69]

2.5. Mechanical Properties of GPs

In the past, geopolymers were usually considered as a class of materials with very poor mechanical properties, especially strength in compression, tension and bending. Thus, mechanical properties of this novel class of inorganic polymers have been ignored in the past. However, interest in using geopolymers in many engineering applications recently became the main driving force for intensive studies on their mechanical properties. Many studies demonstrated that geopolymers, although mechanically relatively weak materials, have specific strength and stiffness that are comparable to those of many other conventional materials because they have low density (1.65 – 1.95 g/cm^3) [73].

In the past five years, several reports on the mechanical properties of metakaolin derived geopolymer have been published. Most of those papers report on the effect of chemistry and processing conditions on the mechanical properties of geopolymers. However, results published in various papers cannot be easily compared because of large number of processing variables that are different in those studies. Despite difficulties in comparing results for different studies, some general conclusions can be drawn from previous studies and they are briefly discussed in the reminder of this section.

Rowles, et al. [74] studied the compressive strength of GPs synthesized using sodium silicate solutions and MK. The Na-GPs with ratio Si/Al=1~3, Na/Al=0.5~2 were cured at 75 °C for 24 hours and aged for 7 days [74] and **Figure 2-13** summarizes results of their research. According to those results, the compressive strength depends on amounts of Na, Si, and Al. The highest compressive strength of 67 MPa was measured

for GPs with Si/Al ratio of 2.5 and Na/Al of 1.3 after ageing of 7 days [74].

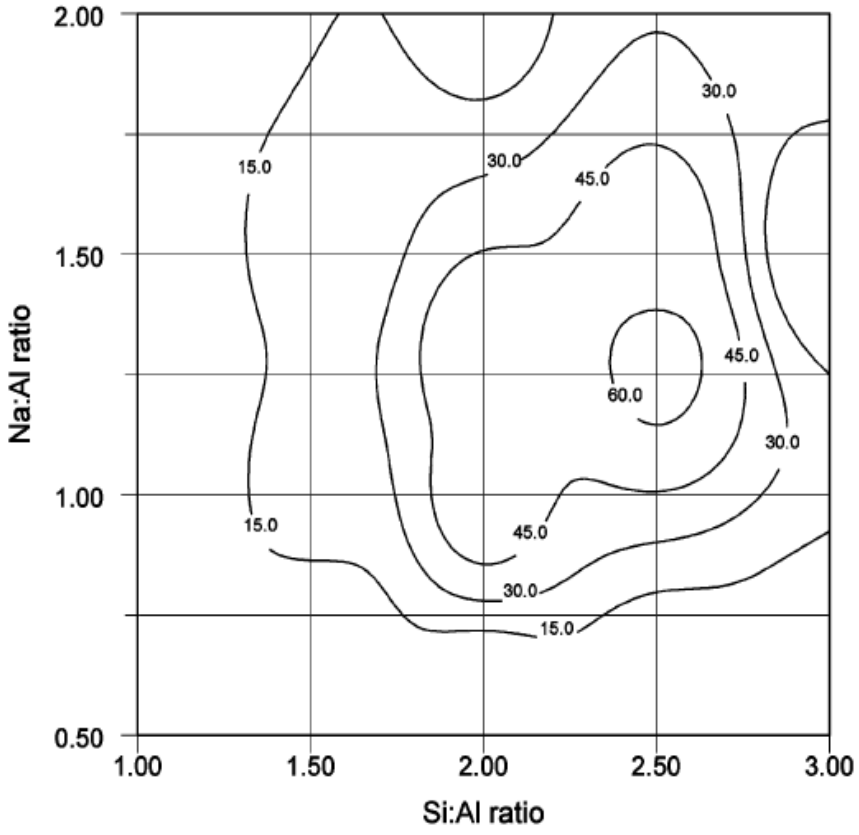

Figure 2 - 13: Compressive strength contours for Na-GPs [74]

P. Duxson, et al. [28] reported on the effect of types of alkali and Si/Al ratio on the mechanical properties of metakaolin-based GPs. The GPs with different alkali type (Na, K) and Si/Al ratios in the range of 1.15 ~ 2.15 were studied after 7 ~ 28 days of ageing

[28]. They also reported on the densities of examined samples. The results of their work show overall density of GPs decrease with increasing Si/Al ratios. The most important results of this study are summarized in **Figure 2-14** and **Figure 2-15** that show the effect of Si/Al ratio and ageing time on strength and Young's modulus

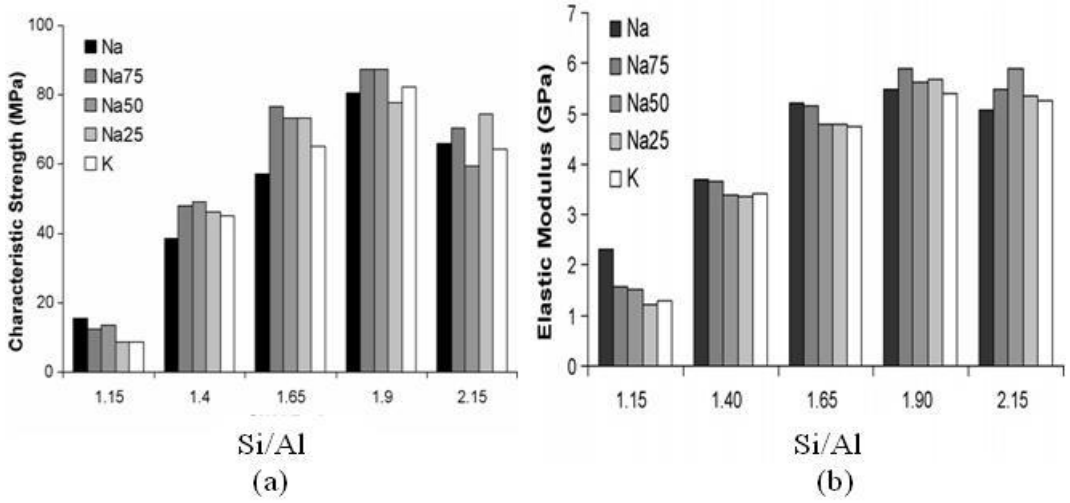

Figure 2 - 14: Results from aging 7 days: (a) compressive strength, (b) elastic modulus as a function of Si/Al ratio acoording to P. Duxson et al [28]. Na75, Na 50 and Na25 are mixed-alkali samples with Na/[K+Na] ratio = 0.25~0.75. K, Na stands for geopolymers processed using KOH, NaOH as alkali activator respectively [28]

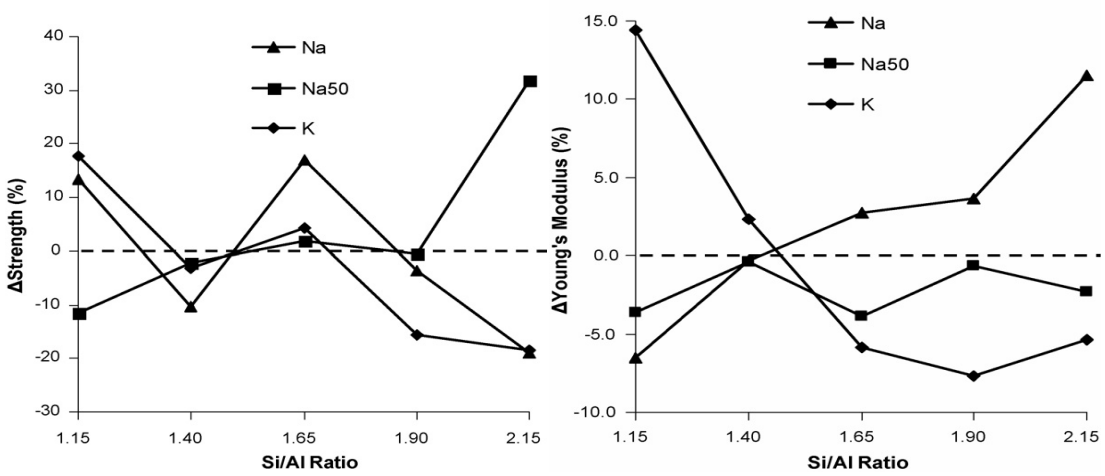

(a) (b)

Figure 2 - 15: Changes of (a) compressive strength, (b) Young's modulus between aging 7 and 28 days [28]

Wang, et al. [73] studied synthesis and mechanical properties of metakaolinite-based GP processed with various concentrations of NaOH solution. **Figure 2-16** summarizes results of their study. They found that flexural and compressive strength of GPs increases with the increase of concentration of NaOH solution from 4 to 12mol/L and sodium silicate solution with ratio of $SiO_2/NaO_2 = 3.2$. They also showed that density of the samples increases with increasing concentration of NaOH, and concluded that the apparent increase in flexural and compressive strength with increasing concentration of NaOH is most likely caused by increased density of the samples. They also showed [**Figure 2-16 (d), (f)**] that ageing time up to 40 days has little effect on density and strength of the samples.

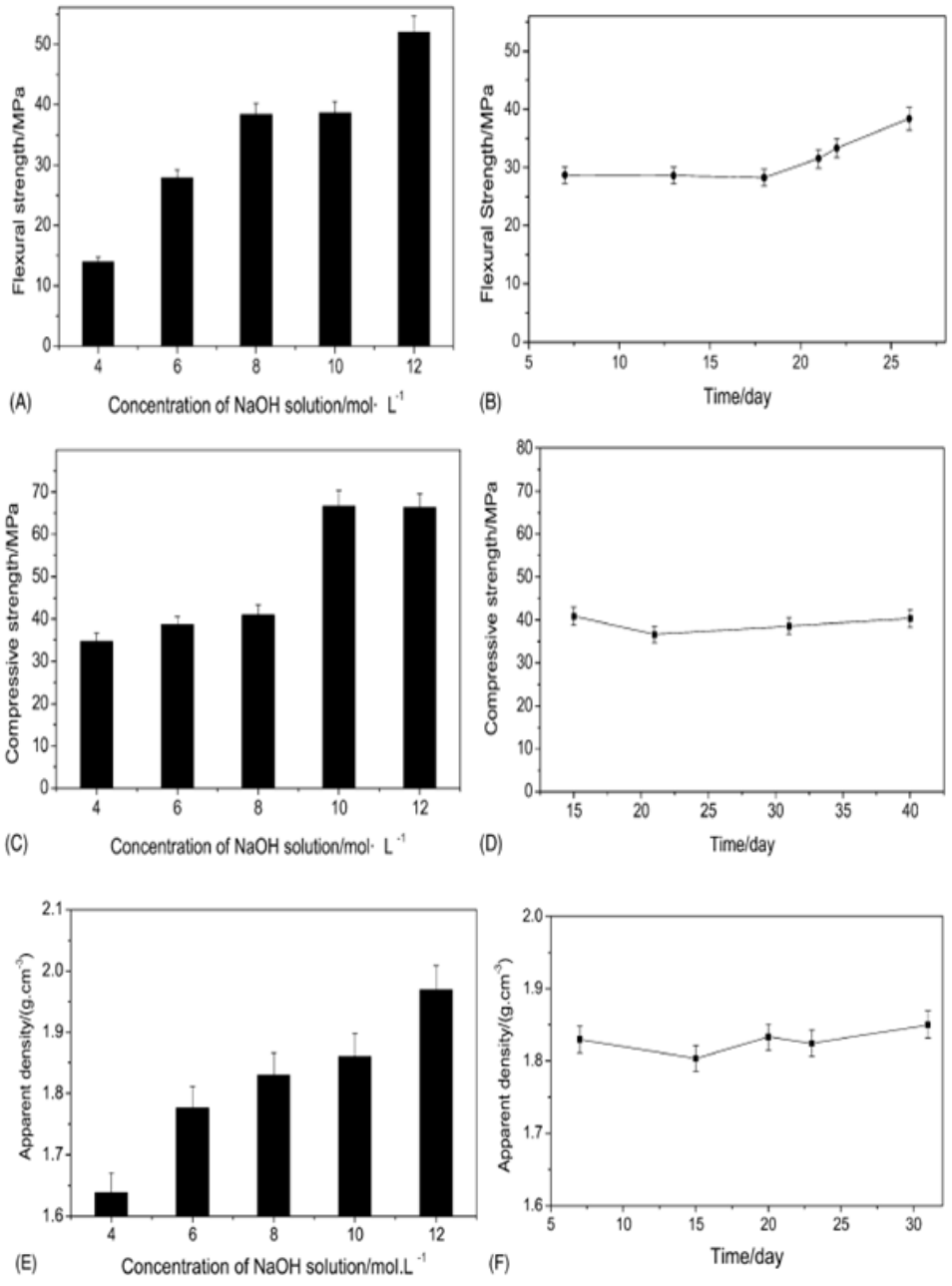

Figure 2 - 16: (a-b) flexural strength, (c-d) compressive strength, and (e-f) density as a function of NaOH solutions and ageing time according to Wang et al. [73]

B. A. Latella, et al. [29] studied mechanical properties of metakaolin-based geopolymers with molar ratios of Si/Al = 2 and Na/Al = 1. **Figure 2-17** summarizes results of fracture toughness measurements for geopolymers processed by using several different precursors, namely: SAGP - sodium aluminate ($NaAlO_2$), Ludox (SiO_2) and metakaolin (MK); FSGP -NaOH, fumed silica and MK; LGP: Ludox, NaOH and MK; and SGP - sodium silicate and MK [29]. They measured fracture toughness (K_{IC}) and Young's modulus (E) of GPs using optical measuring device (MicroVu, Model 9050A) and a non-destructive impulse excitation techniques respectively [29]. They concluded that porosity is the crucial microstructural variable controlling the mechanical properties of the GPs [29], in addition to presence of impurities and uncreated phases.

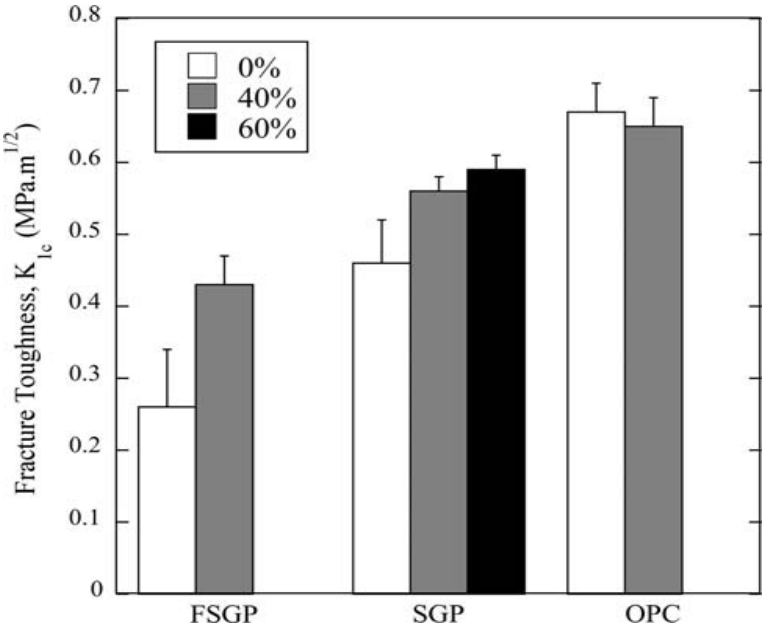

Figure 2 - 17: Results of Latella' research [29]

Lecomte, et al. [37] studied hardness of GPs using Vickers indentation with 5 Kg loads. They reported the highest hardness values of K-GPs to be 200 MPa. Furthermore, they found that the different Si/Al ratio and different types of precursors does not have effect on hardness values of geopolymers [37]. **Figure 2-18** shows a typical example of Vickers indentation of GPs.

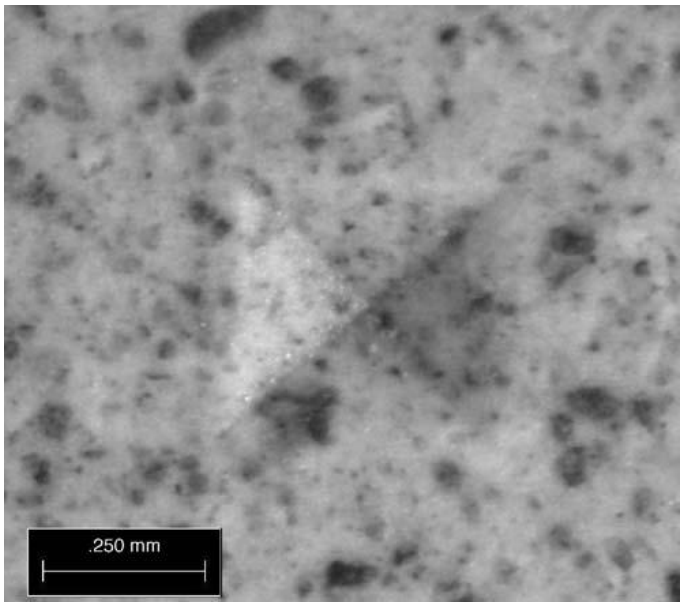

Figure 2 - 18: Vickers indentation in GPs [75]

Belena, et al. [76] studied nanoindentation of Na-GPs. Na-GPs prepared with ratio of SiO_2/Al_2O_3 = 3.5, H_2O/Na_2O = 13 and Na_2O/Al_2O_3 = 1. They reported hardness and Young's modulus of 14 GPa and 0.5 GPa, respectively [76].

Although, properties of GPs processed form fly ash is not a topic of this thesis, it is worth mentioning that GPs processed using fly ash as an aluminosilicate sources have in general better mechanical properties that those processed from metakaolin. More details about mechanical properties of GPs processed from fly ash can be found in several recently published papers [35, 77-79].

CHAPTER III

EXPERIMENTAL METHODS

3.1. Materials

Although many precursors are available for the synthesis of geopolymers (GPs) Metakaolin (MK) is a model precursor because it usually contains smaller amount of impurities than other precursors. The chemical composition of MK can vary but is close to $2SiO_2 \cdot Al_2O_3$. Metakaolin is processed by calcining kaolinite at elevated temperatures to remove water. Since calcining temperatures can vary the structure of resulting MK [30] , selecting a high quality MK precursor is important for processing of GPs.

Three different MK precursors where considered for this project, namely: MetaMax® (BASF catalysts LLC, NJ), White Mud MK (Whitemud Resources INC, Calgar, AB), and Powerpozz^{tm} High Reachivity Metakaolin (Concrete Depot LLC, NC). The chemical compositions of different MKs provided by manufacturers are given in **Table 3-1**. Preliminary testing of selected MKs was performed using XRD and NMR in order to determine the best material for this project, i.e. material with the smallest amount of crystalline impurities and large amount of 4-coordinated Al.

Table 3 - 1: The detail chemical compositions of three different MKs

Properties	Weight (%)		
	MetaMax	WhiteMud MK	Powerpozz(HRM)
SiO_2	53	53	51
Al_2O_3	43.8	43.4	41.55
Impurities	3.2	3.6	7.45

The amorphous fumed silicon (IV) oxide (Alfa Aesar, MA) with surface area of 350-410 m^2/g was used to modify SiO_2/Al_2O_3 ratio of geopolymers in this study. A 87.8% pure KOH (Mallinckrodt Chemicals, NJ) and 99% pure NaOH pellets (Mallinckrodt Chemicals, NJ) were used to make alkali aqueous activators in this study.

3.2. Geopolymer Synthesis

Sodium and potassium silicate solutions were prepared by dissolving sodium-hydroxide (NaOH) or potassium-hydroxide (KOH) together with different amounts of SiO_2 in deionized water and mixing in a magnetic stirrer for 24 hours at room temperature. Alkali silicon solutions were mixed in sealed containers to minimize their possible reaction with atmospheric CO_2. The silicate solutions are then mixed with the selected MetaMax® metakaolin precursor in a vacuum mixer until homogenous mixtures were obtained. Since selected metakaolin precursors have fixed SiO_2/Al_2O_3 ratio, in order to increase the Si content and thus SiO_2/Al_2O_3 ratio in the final product, different amounts of SiO_2 are used to prepare activated alkali silicate solutions. SiO_2

amount in the activating solution is calculated as a difference between amount of SiO_2 needed for geopolymer samples with different SiO_2/Al_2O_3 ratios and amount of SiO_2 in metakaolin (0.53 wt %) that will be added to activating solutions to process samples. The molar ratios chosen for this investigation were SiO_2/Al_2O_3= 2.5, 3, 4, and 5, M_2O/Al_2O_3 =1, and H_2O/Al_2O_3 = 11 or 13. The weight percentages and molar and atomic ratios are summarized in **Table 3-2**. Mixing times were dependent on alkali metal solution and **Table 3-3** provides detail mixing methods for samples processed using NaOH and KOH alkali solutions. All processed samples were labeled as it is shown in **Table 3-4**.

Table 3 - 2: The chemical composition table for synthesis GPs (M: Na or K)

SiO_2/Al_2O_3	M_2O/Al_2O_3	H_2O/Al_2O_3	Si/Al	M/Al
Molar ratio	Molar ratio	Molar ratio	atomic	atomic
2.5	1.00	11.0	1.25	1.00
3.0	1.00	11.0	1.5	1.00
4.0	1.00	11.0	2.00	1.00
5.0	1.00	13.0	2.5	1.00

Table 3 - 3: Mixing time and vacuum time for different alkali solutions

Alkali solution	Stirring Time	Mixing time in vacuum	Outcome
K	275 seconds	1375 s	Liquid
Na	120 seconds	180 s	A viscous fluid

Table 3 - 4: Labeling of the different samples

Sample	SiO_2/Al_2O_3	Alkali activator	Curing in the oven	Ageing in air
K-2.5-24	2.5	KOH	24 h	1 day
K-2.5-48	2.5	KOH	48 h	2 days
K-2.5-24-10D	2.5	KOH	24 h	10 days
K-3-24	3.0	KOH	24 h	1 day
K-3-48	3.0	KOH	48 h	2 days
K-4-24	4.0	KOH	24 h	1 day
K-4-48	4.0	KOH	48 h	2 days
K-4-24-10D	4.0	KOH	24 h	10 days

Table 3 - 4 Continued

Sample	SiO_2/Al_2O_3	Alkali activator	Curing in the oven	Ageing in air
K-5-24	5.0	KOH	24 h	1 day
K-5-48	5.0	KOH	48 h	2 days
Na-2.5-24	2.5	NaOH	24 h	1 day
Na-2.5-48	2.5	NaOH	48 h	2 days
Na-3-24	3.0	NaOH	24 h	1 day
Na-3-48	3.0	NaOH	48 h	2 days
Na-4-24	4.0	NaOH	24 h	1 day
Na-4-48	4.0	NaOH	48 h	2 days
Na-4-24-10D	4.0	NaOH	24 h	10 days
Na-5-24	5.0	NaOH	24 h	1 day
Na-5-48	5.0	NaOH	48 h	2 days

3.3. XRD Analysis

X-ray Diffraction (XRD) of GP materials were collected by a Bruker-AXS D8 Advanced Bragg-Brentano X-ray Powder Diffractometer (Bruker AXS Inc, WI) using CuKα radiation generated at 40 mA and 40 kV, in 10-50° 2θ range and 2θ step of 0.02°. The EVA program was used for identification of peaks. The picture in **Figure 3-1** shows the XRD instrument used for this study.

Figure 3 - 1: Bruker-AXS D8 Advanced Bragg-Brentano XRD

3.4. FTIR Spectroscopy

Fourier Transform Intra-Red, FTIR, spectroscopy is commonly used technique to characterize the structure of geopolymers in conjunction to XRD because geopolymers are amorphous materials and thus cannot be fully characterized using XRD. FTIR was used to identify the chemical functional groups in GPs. This method is based on collecting infrared transmittances spectra that can be further related to the modes of vibration of different atomic bonds in the materials. FTIR spectra of GPs were acquired using a Thermo Scientific Nicolet 380 FT-IR Spectrometer (Thermo Fisher Scientific Inc, MA) in a transmission mode, **Figure 3-2.** About 1.0 g of GP powders was analyzed using the ATR-FTIR technique and spectra were collected at 8 cm^{-1} resolution at the rate of 48 scans per spectrum.

Figure 3 - 2: Thermo Scientific Nicolet 380 FT-IR Spectrometer

3.5. NMR Spectroscopy

The determination of the core molecular structure of GPs was done by solid-state Nuclear Magnetic Resonance, NMR spectroscopy using a WB Advance 400 Bruker (Bruker AXS Inc, WI). The ^{27}Al MAS NMR spectra were used to confirm presence of 4-coordinated Al that is crucial structural characteristic of geopolymers. NMR has be proven to be the most accurate technique to indentify coordination of Al and Si species in geopolymers and their surrounding, as it is described in more details in the previous chapter.

3.6. The Analysis of Microstructure

The Scanning Electron Microscope (SEM), Quantum Q600 FEG-SEM (FEI Corporate, OR), with Energy-Dispersive Spectrometer (EDS) was used to examine microstructure and chemical composition of the synthesized samples. Both fracture and polished surfaces of the samples were analyzed. Since GPs are non-conductive materials, samples were coated using a palladium/gold sputtering coater to enhance the quality of SEM images. A photograph of the instrumentation used in this study is shown in **Figure 3-3**.

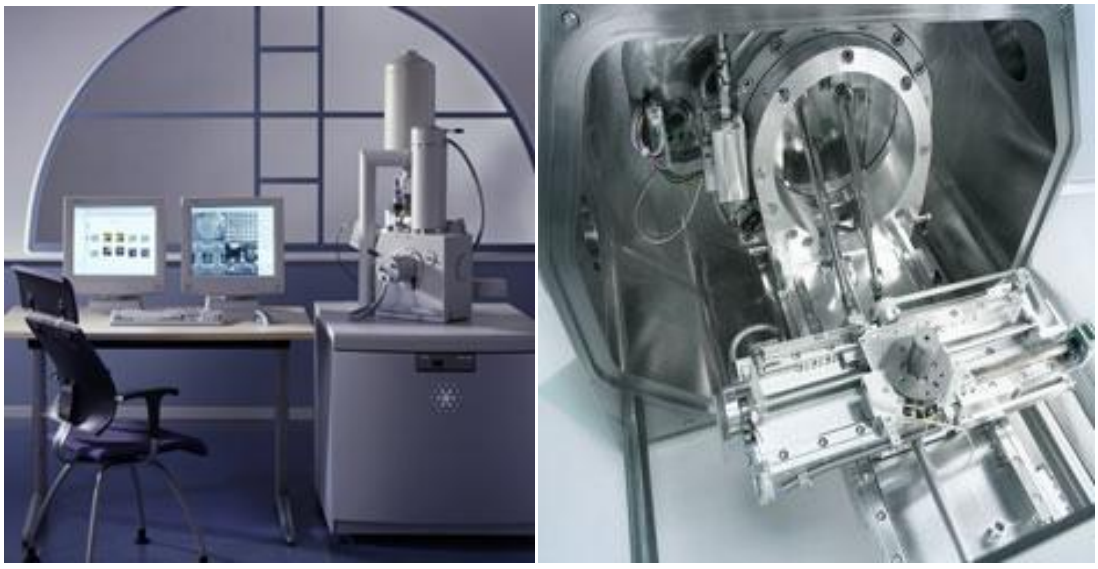

Figure 3 - 3: Quanta 600 FE-SEM devices

3.7. Apparent Density of Samples

For measuring density, samples with different SiO_2/Al_2O_3 ratio aged for 24 h were prepared. Apparent density of sample was calculated by the dividing the measured weight of sample by its volume.

3.8. Microindentation

Microindentation is widely used technique to determine the mechanical properties of materials such as hardness and Young's Modulus. Microindentation is based on the micromechanical measurements of the load and displacement during indentation of a diamond tip into the sample. Micromechanical measurements were performed on the polished GPs with SiO_2/Al_2O_3 ratio 2.5, 3, 4, and 5. Picodentor® HM500 (Helmut Fisher GMBH, Germany) micro-indenter with standard pyramidal Berkowich type indenter was

used for all experiments, **Figure 3-4**. Indentation was carried out in minimum 9 locations for each sample up to the depth of 0.1 μm and holding time of 20s. All of samples were polished using up to 0.25 μm diamond suspensions.

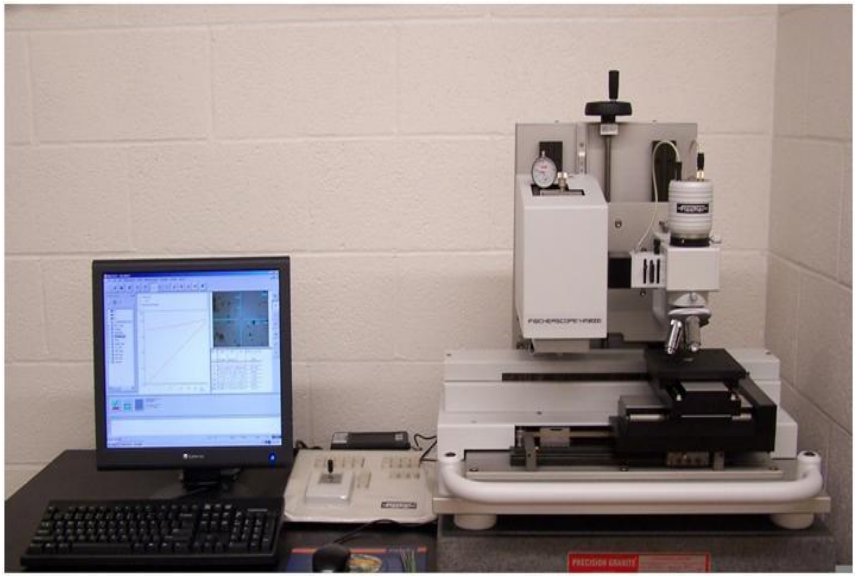

Figure 3 - 4: Microindenter

3.9. Vikers Hardness and Fracture Toughness Test

The Vickers hardness of materials was determined using a Micro-hardness Tester LM 300 AT (LECO, Michigan) at room temperature, **Figure 3-5**. The specimens were prepared in the form of 1.5" dia. discs from K or Na alkali-activated MK-based materials and cured for 24 h. Before testing, indentation surfaces were polished using sandpaper and diamond suspensions. The polished samples were placed on machine stage and loads

of 100 or 500 g were applied using a standard Vickers indentor. The following equation is used to calculate a Vickers hardness number (HV):

$$HV = 1.854\left(\frac{P}{d^2}\right) \quad \text{.....(3.1)}$$

where P is applied loads in kgf, and d is the average length of diagonals of indents in mm.

Figure 3 - 5: Micro-hardness Tester LM 300AT

The length of the corner cracks generated by indentations was measured using a Q600 FEG-SEM. It has been shown that those cracks can be used to estimate, the fracture toughness (K_{IC}) of the brittle materials and several different models have been

proposed in the literature:

- K.Nihara, et al. [80] calculated K_{IC} of brittle solids by the indentation method for a penny-shaped crack. They proposed following equation for the fracture toughness :

$$K_{IC} = \left(\frac{0.129H\sqrt{a}}{\phi}\right)\left(\frac{E\phi}{H}\right)^{0.4}\left(\frac{c}{a}\right)^{-1.5} \quad \text{.....(3.2)}$$

where H is hardness, a is the length of the indent diagonal, E is Young's modulus, ϕ is constant related to the sample's geometry and c is the length of surface crack.

- James Lankford [81] at Southwest Research Institute developed model for the Palmqvist-type cracks as:

$$K_{IC} = \left(\frac{0.142H\sqrt{a}}{\phi}\right)\left(\frac{E\phi}{H}\right)^{0.4}\left(\frac{c}{a}\right)^{-1.56} \quad \text{.....(3.3)}$$

where H is hardness, a is the length of the indent diagonal, E is Young's modulus, ϕ is constant related to the sample's geometry and c is the length of surface crack.

- B. R Lawn and A. G. Evans [82] at University of California and University of New South Wales developed method for elastic / plastic indentation damage in ceramics. For a point loading in a semi infinite solid, they proposed the following relationship between fracture toughness and length of indentation cracks:

$$K_{IC} = 0.028H\sqrt{a}\left(\frac{E}{H}\right)^{0.5}\left(\frac{c}{a}\right)^{-1.5} \quad \text{.....(3.4)}$$

where H is hardness, a is the length of the indent diagonal, E is Young's modulus, c

is the length of surface crack.

- G. R. Anstis, et al. [83] at University of New South Wales measured a fracture toughness using a critical evaluation of indentation. They measured radial cracks that correspond to the part of the indentation field and developed the following equation for the fracture toughness :

$$K_{IC} = 0.016\left(\frac{E}{H}\right)^{0.5}\left(\frac{P}{c^{3/2}}\right)^{-1.5} \quad \text{.....(3.6)}$$

where H is hardness, E is Young's modulus , P is applied loads in Kgf and c is the length of surface crack.

3.10. The Compressive Strength Testing

The compressive strength was determined using a 810 Material Testing System (MTS Corporation, MN), **Figure 3-6**, at the constant displacement rates of 0.60 mm/min at room temperature. Displacements (mm) and forces (lbs) were monitored during testing using a Flextest SE Ver. 5.0 program.

Figure 3 - 6: 810 Material Testing System

Compressive strength was calculated from the failure force, F, using following equation:

$$\sigma = \frac{F}{A} \quad \text{.....(3.7)}$$

where F is applied force and A is initial cross-section area of the samples. Specimens were cylindrical in shape - 1 inch in diameter and 1 inch height. Sample surfaces were polished flat to avoid non-uniform loading and eventual low compressive strength from an edge braking.

For each composition, more than 10 samples were tested at the same conditions and the results were analyzed using Weibull distribution. Weibull distribution is

commonly used to describe the probability of survival of brittle solids as a function of stress. The Weibull distribution [84] is described by:

$$f(x) = m(x)^{m-1}exp(-x^m) \quad \text{.....(3.8)}$$

where, x is a random variable, m is a shape factor (Weibull modulus) and $f(x)$ is the frequency distribution of variable x. Because distribution of compressive strength of geopolymers is considered in this work, a variable x is defined as σ/σ_o, where σ is the failure stress and σ_o is a normalizing parameter. **Figure 3-7** shows a plot of frequency distribution function vs. variable σ/σ_o as defined in Eq. 3.8 for different values of m. As it can be seen from **Figure 3-7**, large m results in a more narrow distribution of the strength of the brittle solid.

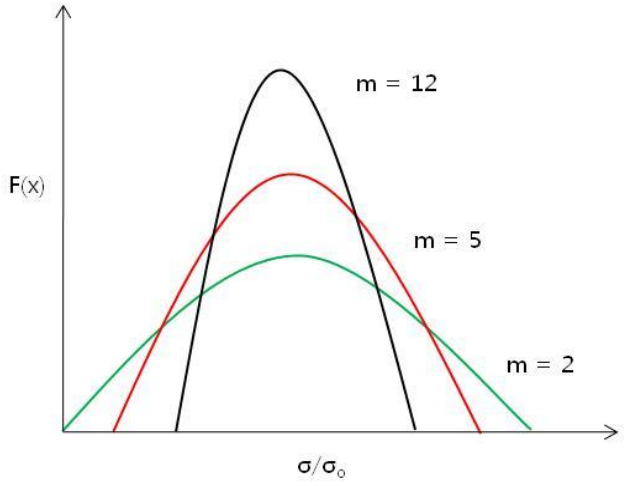

Figure 3 - 7: The effect of m on the shape of the weibull distribution [84]

Eq. 3.8 is usually represented as [84]:

$$S = exp\left[-\left(\frac{\sigma}{\sigma_o}\right)^m\right] \quad \text{(3.9)}$$

or

$$ln\, ln\frac{1}{S} = m\, ln\frac{\sigma}{\sigma_o} = m\, ln\,\sigma - m\, ln\,\sigma_o \quad \text{(3.10)}$$

where S is probability of survival of the sample. Equation 3.10, when plotted in ln(ln(1/S)) v.s lnσ plot, results in the straight line with slope equal to m. Thus, to determine m and σ_o, the Weibull distribution for the examined population of samples has to be plotted using following procedure [84]:

- All specimens should be ranked in order of increasing strength, 1, 2, 3, …, j, …, N, where N is total number of samples. Then, the survival probability for the j_{th} sample can be calculated as:

  $$S_j = 1 - \frac{j-0.3}{N+0.4} \quad \text{(3.11)}$$

  Where j is the rank of the j specimen and N is total number of specimens.

- –ln ln (1/S) should be plotted as a function of ln σ, where σ is compressive strength of the j sample.. The least-square fit to the resulting line is the Weibull modulus m.

- σ_o is calculated from the plot that is a value of an intercept divided by the slope of the fitted line and it represents stress at which probability of survival is 37%.

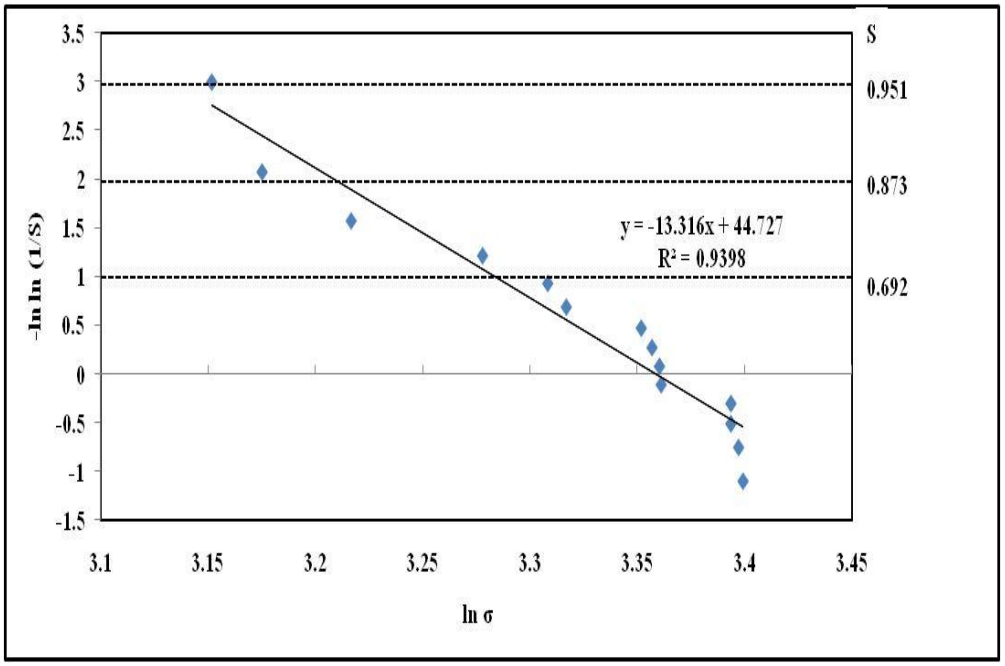

Figure 3 - 8: Weibull plot of data shown in Table 3-5

Table 3 - 5: Typical strengths of GP samples

Rank	Survival P	σ (MPa)	ln σ (Mpa)	-lnln1/S
1	0.951389	23.38361	3.152035	2.999090431
2	0.881944	23.93815	3.175473	2.074444344
3	0.8125	24.95132	3.216927	1.571952527
4	0.743056	26.52346	3.27803	1.214075448
5	0.673611	27.33964	3.308338	0.928610507
6	0.604167	27.57673	3.316972	0.685367162
7	0.534722	28.55571	3.351857	0.468392324
8	0.465278	28.69878	3.356855	0.267721706
9	0.395833	28.79769	3.360295	0.076058454
10	0.326389	28.82117	3.36111	-0.113030157
11	0.256944	29.77115	3.39354	-0.306672154
12	0.1875	29.77159	3.393554	-0.515201894
13	0.118056	29.87763	3.39711	-0.75921576
14	0.048611	29.93963	3.399183	-1.106548431

Table 3-5 and **Figure 3-8** illustrates above described procedure for the typical set of geopolymers samples (K-2.5-48h). From the **Figure 3-8**, Weibull modulus of 13.316 can be calculated as a negative value of slope of the fitted straight line, while the average strength σ_o of 28.785 MPa can be calculated by setting -lnln1/S = 0.

CHAPTER IV

RESULTS

4.1. Selection of Metakaolin Precursor

Three different MK where considered as geopolymer precursor in this work, namely: MetaMax®, White Mud MK, and Powerpozz (HRM) and their chemical compositions provided by manufacturer are given in Chapter II of this thesis. Preliminary characterization using XRD was performed in order to determine the best material for this project. **Figure 4-1** shows the XRD results for all examined MK precursors.

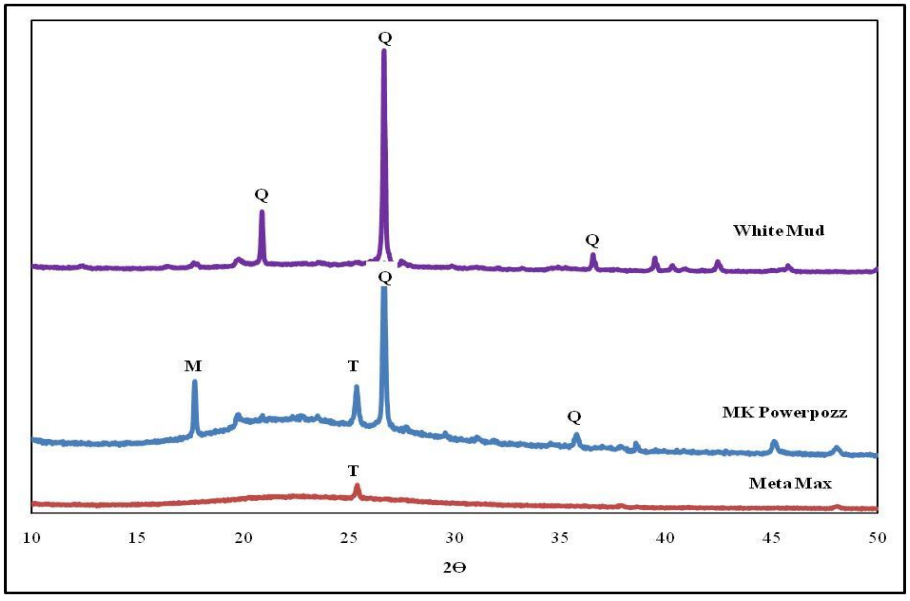

Figure 4 - 1: The XRD of Metakaolin precursors. T, M and Q denontes peaks for TiO_2, Mullite, and Qualtz, respectively

MetaMax® was selected as a precursor for processing of geopolymer samples because it contains smallest amount of crystalline TiO_2 impurities as detected by XRD, **Figure 4-1**. In addition, selected MetaMax® MK precursor contains smallest overall amount of impurities (mostly TiO_2) according to manufacturer's specification, **Table 3-1**.

4.2. X-Ray Diffraction, XRD

The XRD patterns of MK precursor and processed GPs are compared in **Figures 4-2 and 4-3**. The figures show XRD of the virgin Metakaolin, as well as of potassium and sodium activated GPs with molar ratios SiO_2/Al_2O_3 =2.5 to 5 after curing for 24 hours at 80 ^oC. For the unprocessed MK, a strong amorphous hump is seen for 2θ ranging from 15 to 30° with maximum at $2\theta_{max}$ = 23°, which is typical of an amorphous aluminosilicate phases [31]. The K and Na based GPs shows a shift in the hump to 2θ =25-35°. In both the K-GPs and Na-GPs with SiO_2/Al_2O_3 =2.5, 3 displayed $2\theta_{max}$ at 30° while the samples with SiO_2/Al_2O_3 = 4, 5 had a $2\theta_{max}$ at 28°. A sharp peak 2θ =25.5 ° is crystalline peak in both MK and GPs due to presence of unreacted TiO_2 impurity from MK precursor [85].

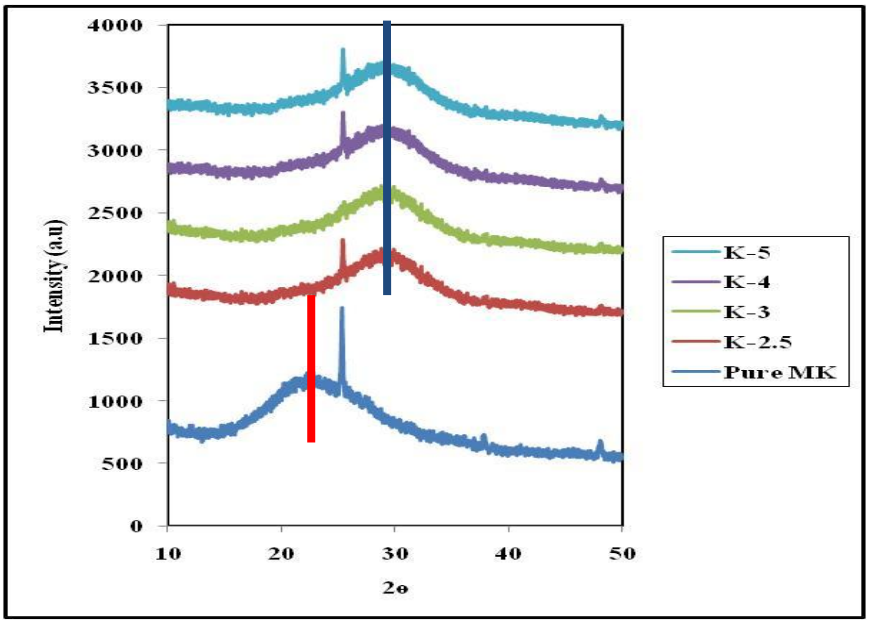

Figure 4 - 2: XRD of K Geopolymers

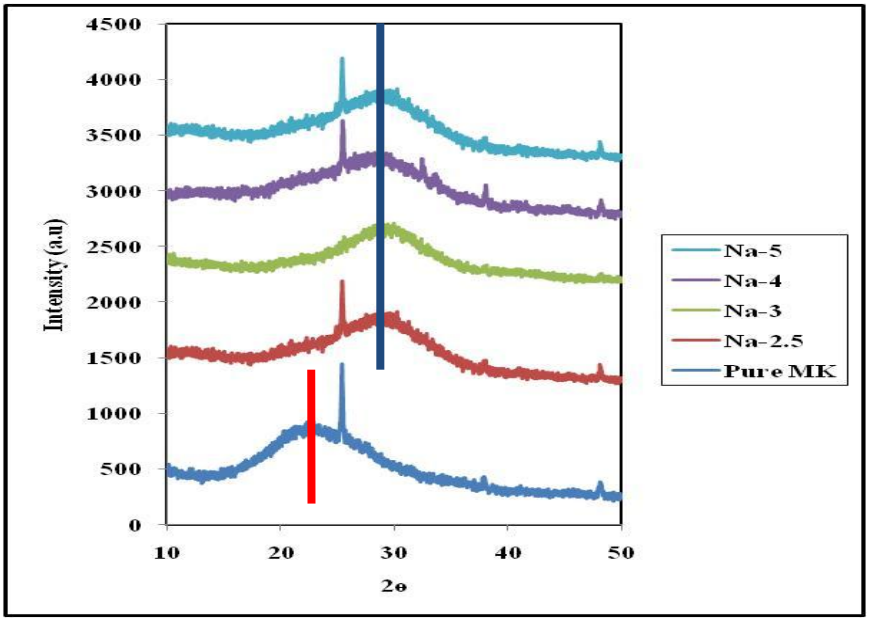

Figure 4 - 3: XRD of Na Geopolymers

The shifts of amorphous hump in GPs is attributed to the hydrolytic attack of alkali metal cations such as K and Na during de-polymerization process of alumino-silicate [86]. Although the X-ray data show typical hump shift for geopolymerisation, they do not provide detailed information on the atomic ordering of Al and Si monomeric units in geopolymers [31]. Thus, FTIR and NMR spectroscopy have to be carried out in addition to XRD to verify presence of GPs in the processed samples.

4.3. Fourier Transform Infrared, FTIR Spectroscopy

Figure 4-4 shows the transmission mode of ATR-FTIR spectra for the MK and selected GP samples, while **Table 4-1** lists the position of wave numbers for molecular vibrations of different bonds that are usually present in GPs [87].

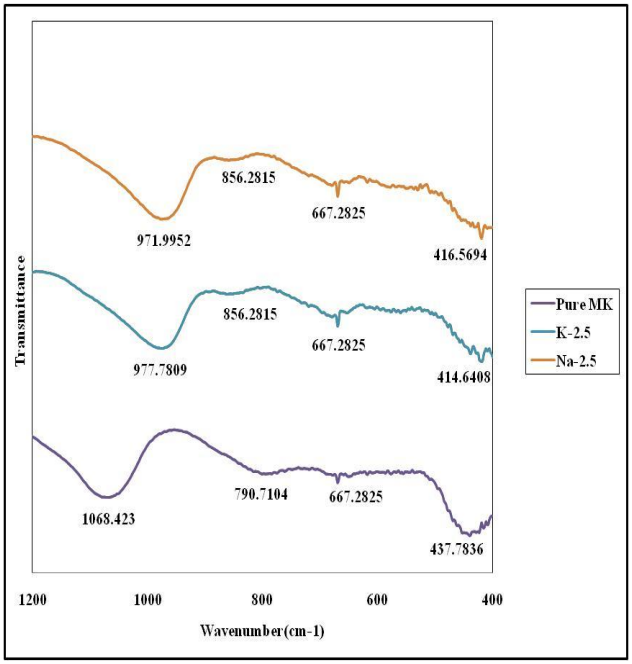

Figure 4 - 4: The FTIR Plots for GPs

Table 4 - 1: FTIR Wave numbers of the atomic bonds in geopolymers

Ranges	Bands
950-1250 cm^{-1}	Asymmetric Si-O-Si and/or Al-O-Si Stretching
856 cm^{-1}	Al-O / Si-O bending
790 cm^{-1}	Al-O Bending
667 cm^{-1}	Al-O bending
414-450 cm^{-1}	Network Al-O-Si bending

In **Figure 4-4**, a Si-O-Al (or Si) bending band is present at 410-450 cm^{-1} in both, MK and GPs [88]. In XRD amorphous MK, alumino-silicates are arranged in long-distance ordered structures, while GPs exhibit short-range ordering of alumino-silicate units with weak network bands. Therefore, FTIR spectra of GPs exhibited in general weaker transmittance than pure MK at 410-450 cm^{-1}.

A strong shoulder peak for the pure MK can seen in **Figure 4-4** located at 790 cm^{-1} that corresponds Al-O, Si-O bending. However, this peak moves to a higher frequency at 856 cm^{-1} after geopolymerization which is an evidence for presence of the larger amount of tetrahedral coordinated AlO_4, formed by dissolution of MK [89]. The shift of the peak related to asymmetric Si-O-Si and/or Al-O-Si stretching from 1068 cm^{-1} for MK to 970 $cm^{-1}$for the GPs is also additional evidence of geopolymersiation of Al and Si species from MK [5].

4.4. ^{27}Al Nuclear Magnetic Resonance, NMR Spectroscopy

The ^{27} Al MAS NMR spectra for the unreacted MK and both K and Na GP samples are shown in the **Figures 4-5**, **4-6** and **4-7**. The ^{27}Al spectra in **Figure 4-5** indicates IV, V and VI- coordinated Al in the virgin MK with about equal amounts of IV coordinated Al with the peak at 50 ppm and VI-coordinated Al with the peak at 0 ppm of chemical shift. Additionally it appears that there is a higher concentration of V-coordinated Al with the chemical shift of 23.3 ppm. The ^{27} Al MAS NMR spectra of K and Na based samples are shown in **Figures 4-6 and 4-7** for SiO_2/Al_2O_3 = 2.5, 3, and 4 respectively. They all show that only IV coordinated aluminum is present in processed GPs because only peak with at 50 ppm can be observed. The presence of only IV coordinated Al species in GPs is consider to be crucial evidence for indentifying processed materials as GPs [5].

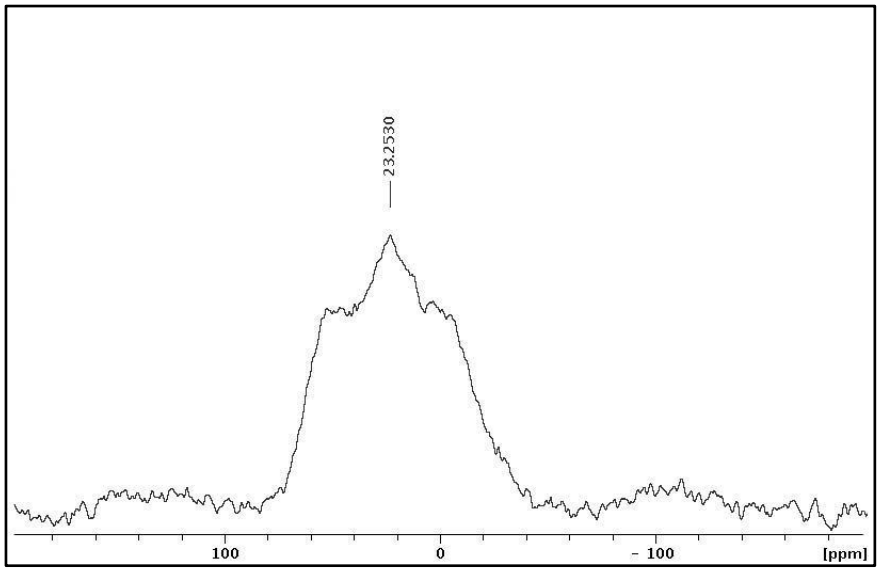

Figure 4 - 5: ^{27} Al MAS-NMR of MK

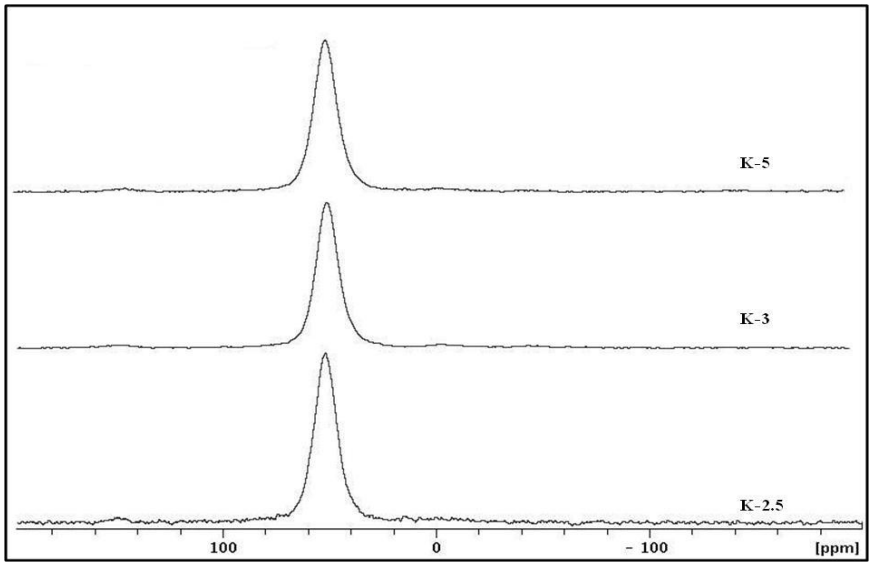

Figure 4 - 6: ^{27} Al MAS-NMR of K based geopolymers

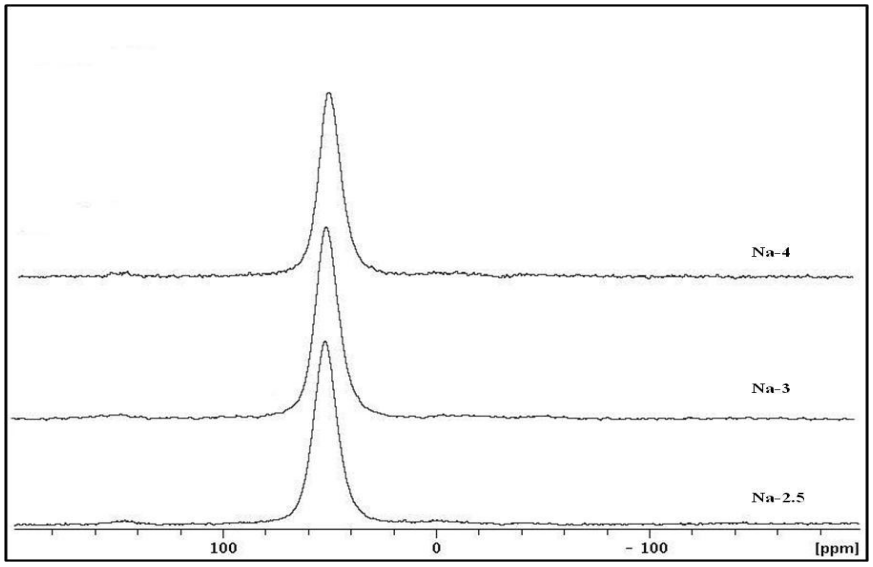

Figure 4 - 7: ^{27} Al MAS-NMR of Na based geopolymers

4.5. SEM and EDS Compositional Analysis of the Samples

The **Figures 4-8 and 4-9** show the microstructure of K-GPs and Na-GPs specimens. The SEM images are taken at cross-sections of the reacted product with molar ratios SiO_2/Al_2O_3 = 2.5, 3, 4, 5.

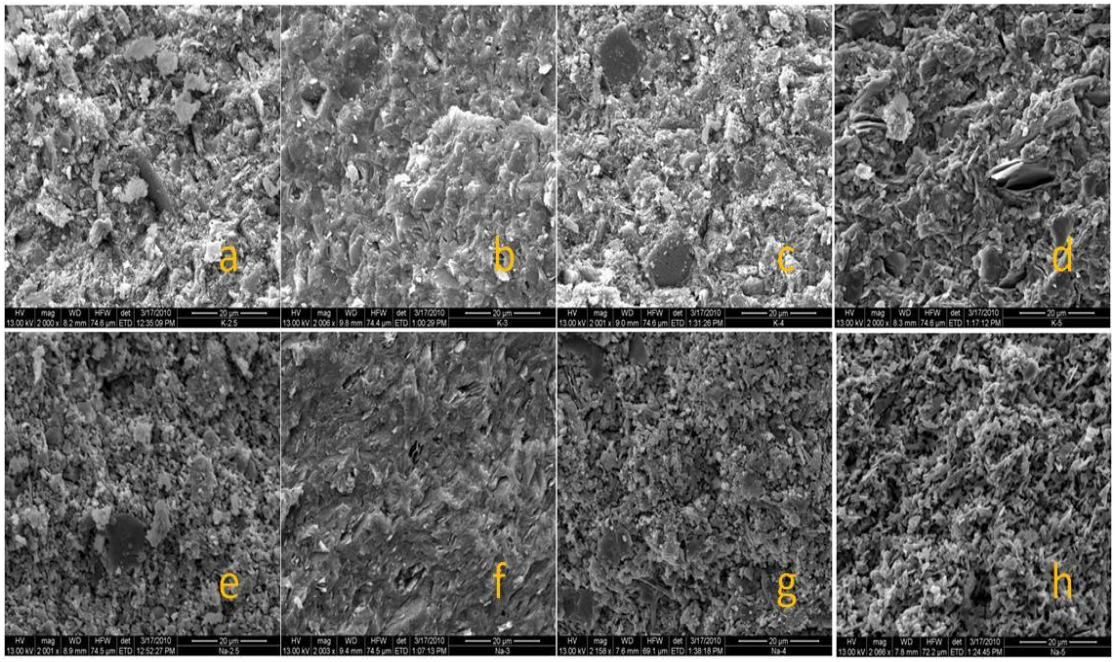

Figure 4 - 8: Secondary electron SEM images of GPs at magnification of 2,000 X. (a-d) K-2.5, 3, 4, 5 for ageing 24h, (e-h) Na-2.5, 3, 4, 5 for ageing 24h

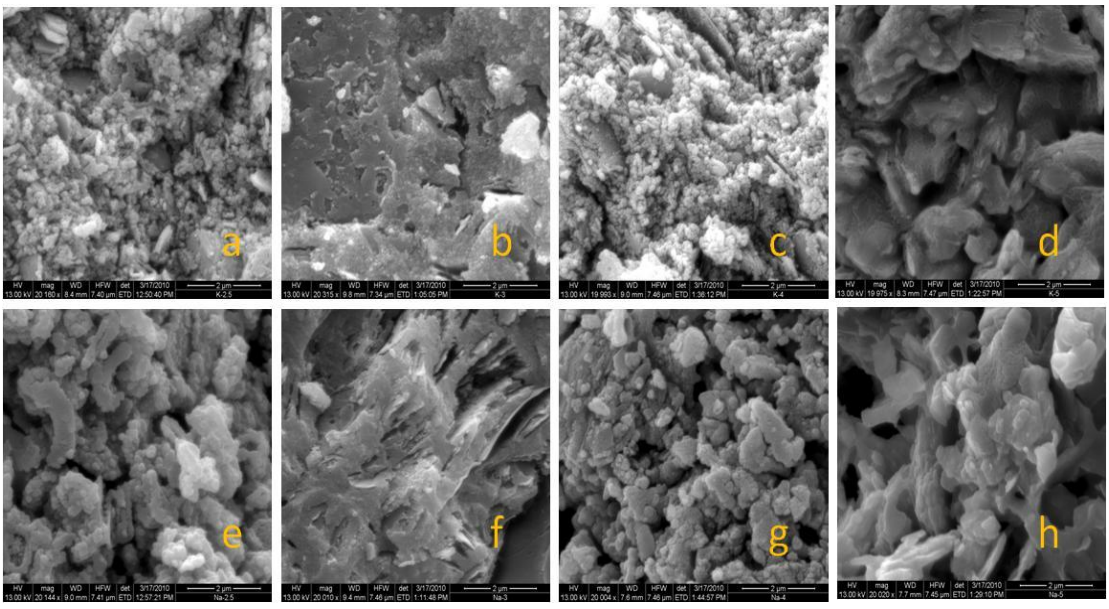

Figure 4 - 9: Secondary electron SEM images of GPs at magnification of 20,000 X. (a-d) K-2.5, 3, 4, 5 for ageing 24h, (e-h) Na-2.5, 3, 4, 5 for ageing 24h

In general, **Figures 4-8 and 4-9** show that microstructure of GPs consist of more or less loosely packed GP particles with high porosity and some grains of unreached material having layered structure. K-based GPs have more dense and homogeneous structure than Na-based GPs at SiO_2/Al_2O_3=2.5. This is most likely result of a greater degree of reaction of metakaolin and a higher degree of aluminum incorporation, when K is used as alkali activator [26]. Also, when compared Na- and K-based GPs with different SiO_2/Al_2O_3 ratio, it can be concluded that GPs with SiO_2/Al_2O_3 = 3 and 4 appears to have more dense microstructures than samples with other compositions, **Figures 4-8 and 4-9**. Further increase of SiO_2/Al_2O_3 ratio leads to more loosely packed

structure again.

The main microstructural differences between K-based and Na-based GPs are also illustrated in **Figures 4-10 and 4-11**. While microstructure of K-based GPs consist of closely packed, interconnected spherical GPs particles that are usually called micelles, microstructure of Na-based GPs consist of more or less plate-like particles that are loosely packed. **Figure 4.12** shows unreacted aluminosilicate particles with layer structure that can be found in both K- and Na- based GPs.

This finding is in good agreement with prevous microstructural studies that show that lower ratio of Si/Al results in less cohesive structure with separated particles of GPs phase [69]. However, presence of the large amount of the large pores in sample with Si/Al=5 can be attributed to the larger amount of the water that was used to prepare those samples. Previous studies also reported on presence of layered, uncreated aluminosilicate source in GPs [31] like that in **Figure 4-12**. Since, the mixing process is the solid-liquid reaction system, some parts of material have a less water available than other parts, and thus do not react compatibly [90].

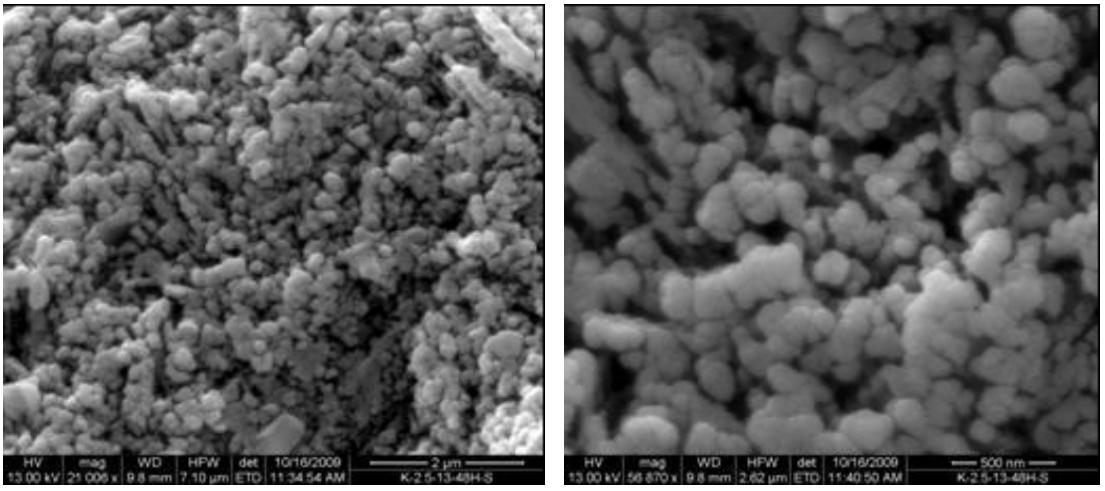

Figure 4 - 10: FEG-SEM images for K-2.5 GPs

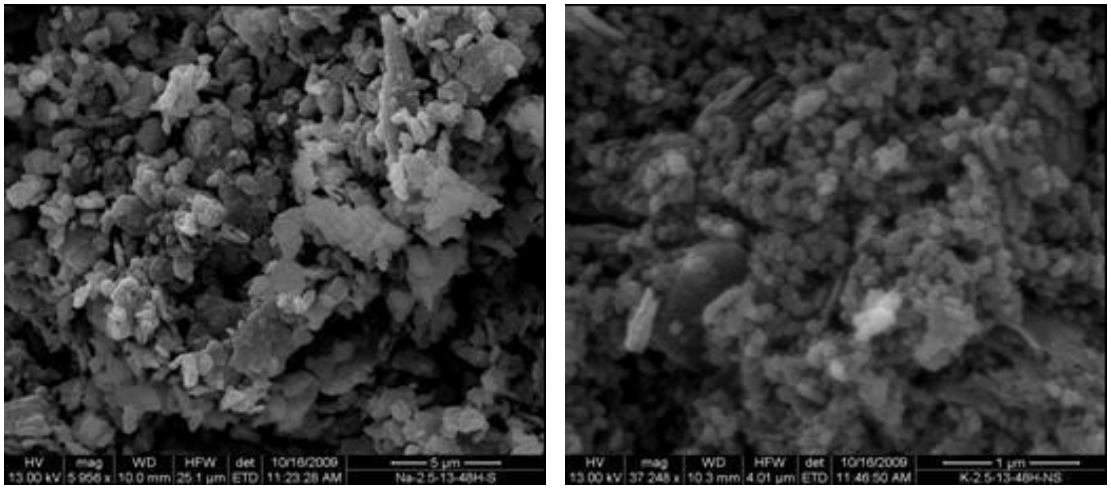

Figure 4 - 11: FEG-SEM images for Na-2.5 GPs

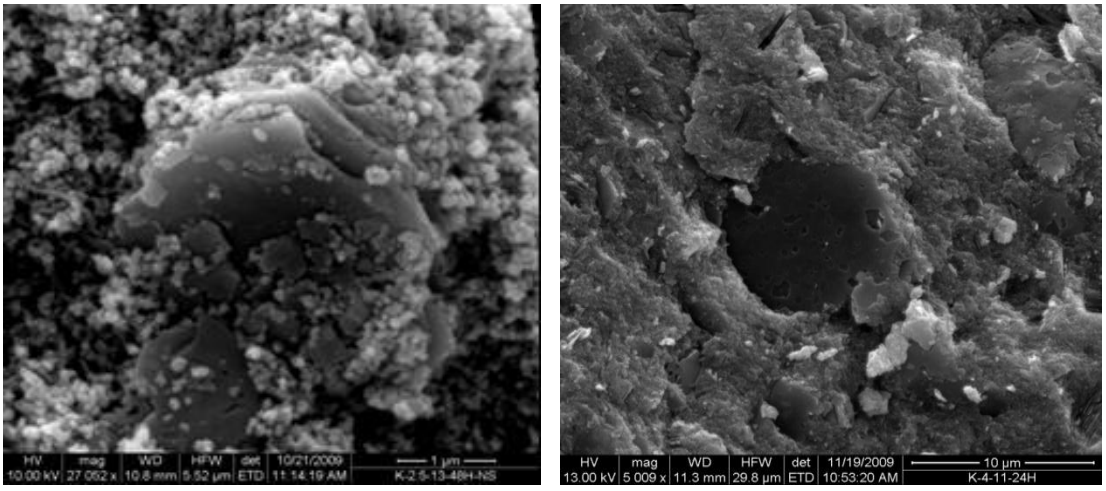

Figure 4 - 12: SEM images of unreacted aluminosilicate particles in K-2.5 and K-4

The chemical composition of processed GPs analyzed using qualitative and quantitative. Qualitative EDS analysis confirmed presence of only Al, Si, O and K or Na in all processed samples. The chemical composition of different samples of the produced GPs obtained from large area quantitative EDS analysis are listed in **Table 4-2**. As it can be seen from the two most right columns in that table, overall Si/Al and Na (or K)/Al ratios calculated from EDS analysis are close to that of the initial precursor mixture.

Table 4 - 2: EDS results for K and Na based GPs

Sample	Elements of GPs (atomic wt %)				Si/Al atomic ratio	Na(K)/Al atomic ratio
	O	Al	Si	K (or Na)		
K-2.5-11	69.2	10.6	14.1	6.1	1.45	0.86
K-3-11	60.7	13.8	16.6	9.0	1.31	0.64
K-4-11	63.9	11.9	17.8	6.4	1.63	0.72
K-5-11	65.8	9.0	15.5	9.8	1.87	1.09
Na-2.5-11	45.4	13.5	21.3	19.8	1.58	1.47
Na-3-11	66.1	9.0	13.0	11.7	1.58	1.30
Na-4-11	47.5	9.0	21.9	21.4	2.64	1.16
Na-5-11	71.0	8.3	16.6	4.1	1.99	0.49

However, some compositional inhomogeneity can be observed in all processed samples. For example, **Figures 4-13 and 4-14** shows microstructure of K- and Na-based GPs, respectively, and their chemical compositions as determined in several points by quantitative EDS.

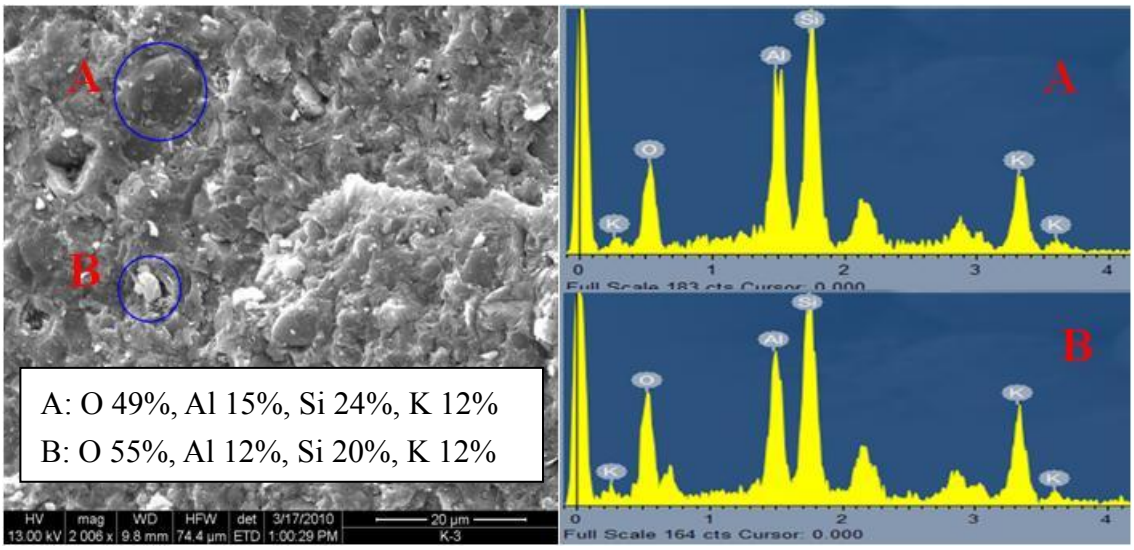

Figure 4 - 13: Qualitative EDS analysis of K-3-24h

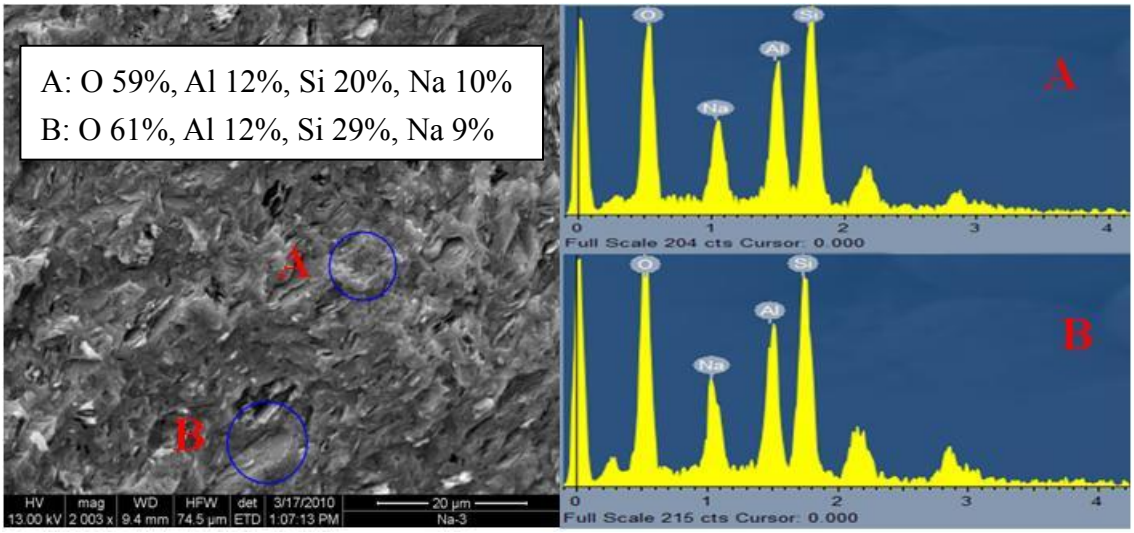

Figure 4 - 14: Qualitative EDS analysis of Na-3-24h

4.6. Apparent Density of Samples

Apparent density of both K and Na activated MK-based samples increases with SiO_2/Al_2O_3 ratio increasing, **Figure 4-15**. These results indicate that samples with SiO_2/Al_2O_3 ratio of 5 have a higher apparent density than other samples with different SiO_2/Al_2O_3 ratios. In addition, Base on those results we can conclude that GPs with K-GPs with SiO_2/Al_2O_3=5 ratio have 1.82 g/cm^3 of maximum apparent density. This result gives evidence to the high dissolution of the MK monomers and quickly condensation of the structure unit with high SiO_2/Al_2O_3 ratio [73].

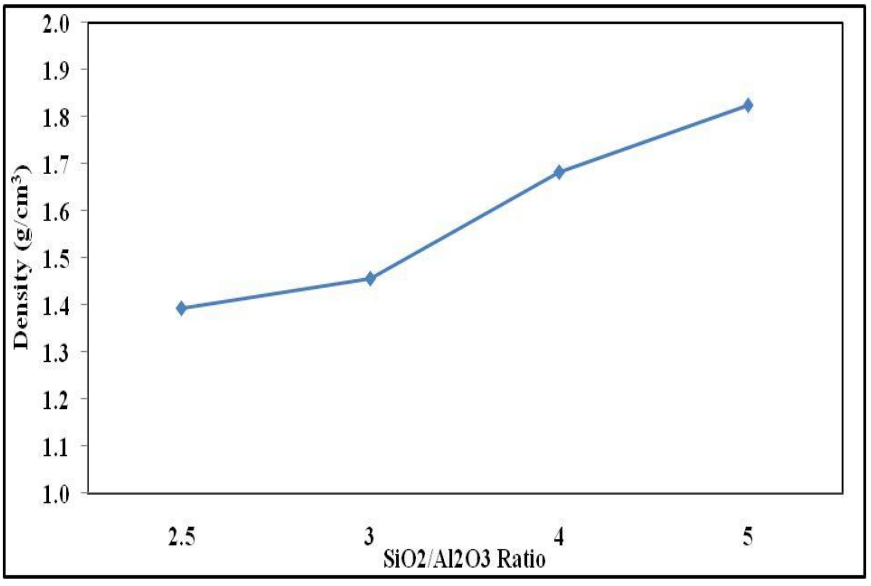

(a)

Figure 4 - 15: Apparent density of GPs: (a) K-GPs, (b) Na-GPs

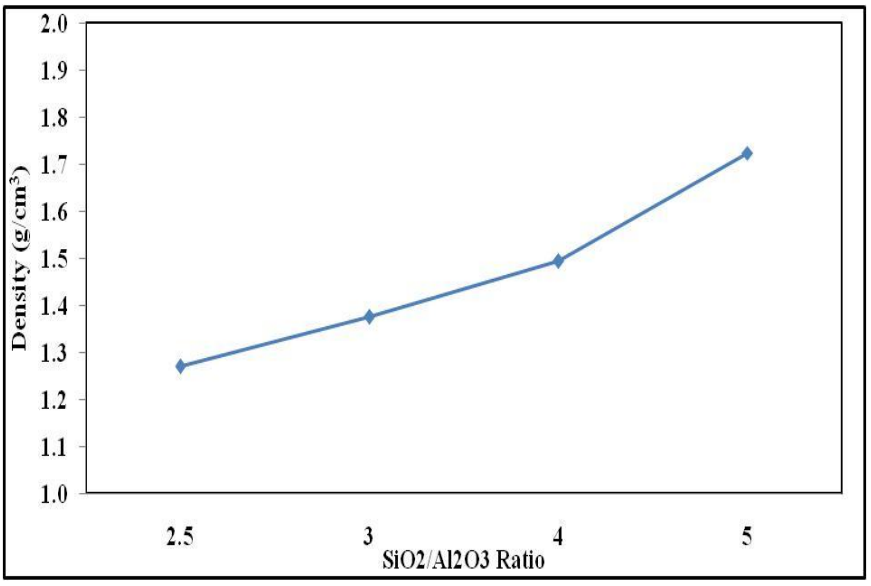

(b)

Figure 4 – 15 Continued

4.7. Microindentation

Table 4-3 and Figure 4-17 show Young's moduli, hardness of different samples that were determined using micro-indentation. **Figure 4-16** shows examples of experimental indentation curve and indentation creep during 20 s dwell time. The Young's modulus and hardness of both Na- and K-based GPs increase as SiO_2/Al_2O_3 ratio increases, reaching maximum value of about 8 GPa and 160.4 MPa for Na-based GP with SiO_2/Al_2O_3 =3 and 5.3 GPa and 98.6 MPa for K-based GP with SiO_2/Al_2O_3 =4, after which it decreases again with increasing SiO_2/Al_2O_3 ratio.

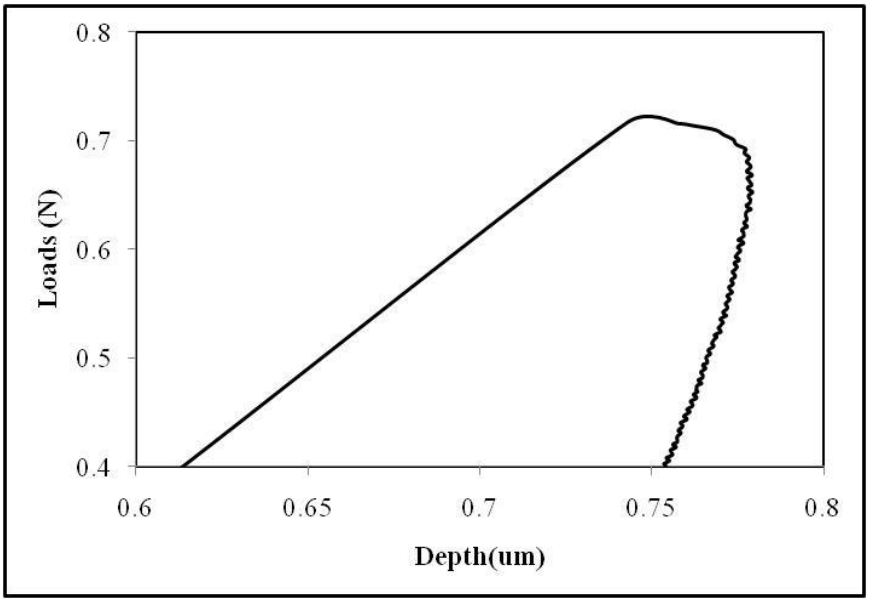

(a) K-2.5-11-24h

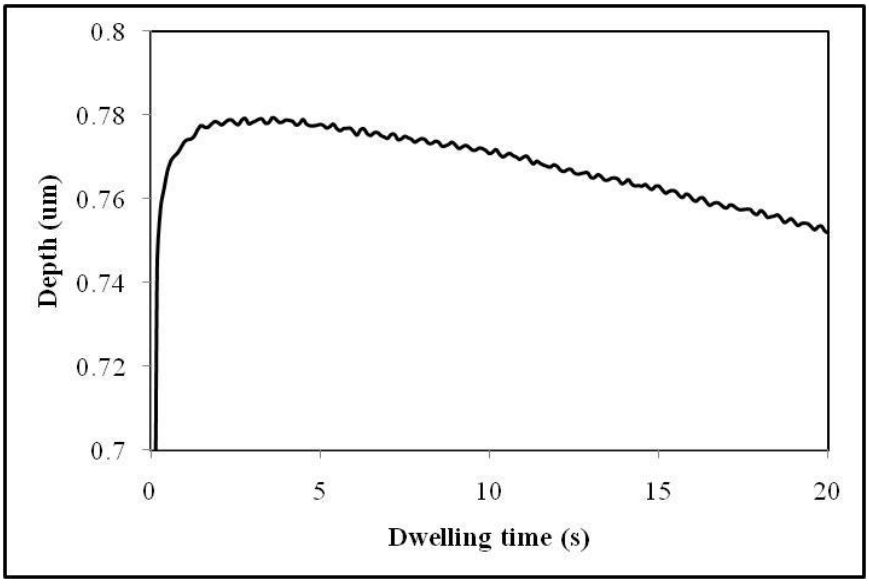

(b) K-2.5-11-24h

Figure 4 - 16: Examples of experimental (a) indentation curve and (b) indentation creep

Table 4 - 3: The Young's Modulus, hardness of GPs

SiO_2/Al_2O_3 / CuringTime	K specimens				Na specimens			
	2.5	3	4	5	2.5	3	4	5
Average Young's Modulus (GPa)	3.53	3.74	5.35	3.58	2.72	7.90	4.86	3.50
Standard Deviation of Young's Modulus (GPa)	0.27	0.38	1.44	0.26	0.53	1.35	0.41	0.52
Average Hardness (MPa)	25.4	68.9	98.6	25.4	22.0	160.4	80.6	29.9
Standard Deviation of Hardness (MPa)	3.7	17.7	20.5	3.8	1.7	40.5	14.7	8.6

Results of this work show increase of Young's modulus and hardness with increasing SiO_2/Al_2O_3 ratio until it reaches value of 3, after which it decreases again. This trends as well as measured values of Young's modulus are in good agreement with previously published work by P. Duxson [69]. Hardness also increased as SiO_2/Al_2O_3 ratio increases up to SiO_2/Al_2O_3 of 3 or 4. These results are different than those published by Lecomte et al [37] that suggests that hardness does not change with SiO_2/Al_2O_3 ratio.

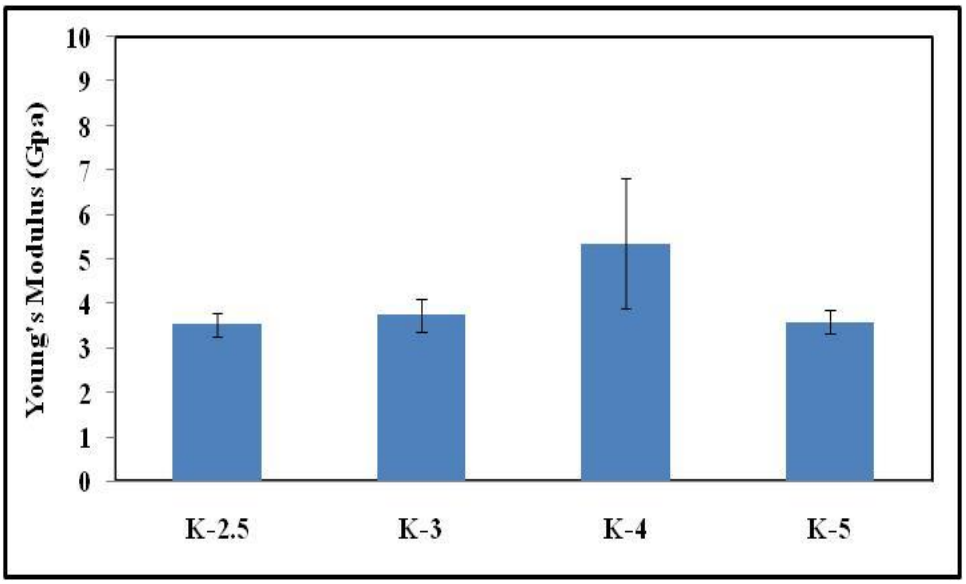

(a)

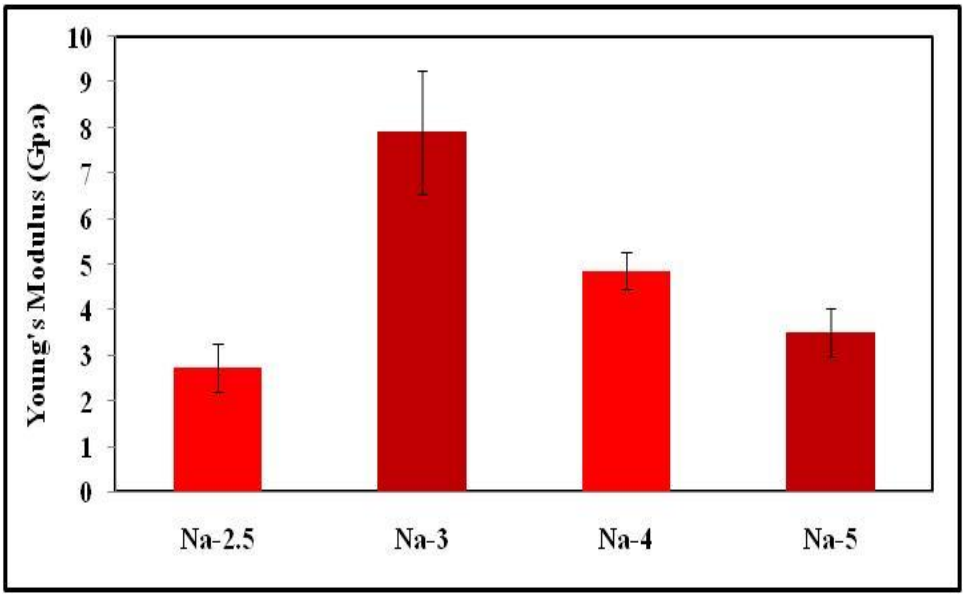

(b)

Figure 4 - 17: Young's modulus and Hardness of (a) K-based GPs, (b) Na-based GPs, and (c) K-based GPs, (d) Na-based GPs

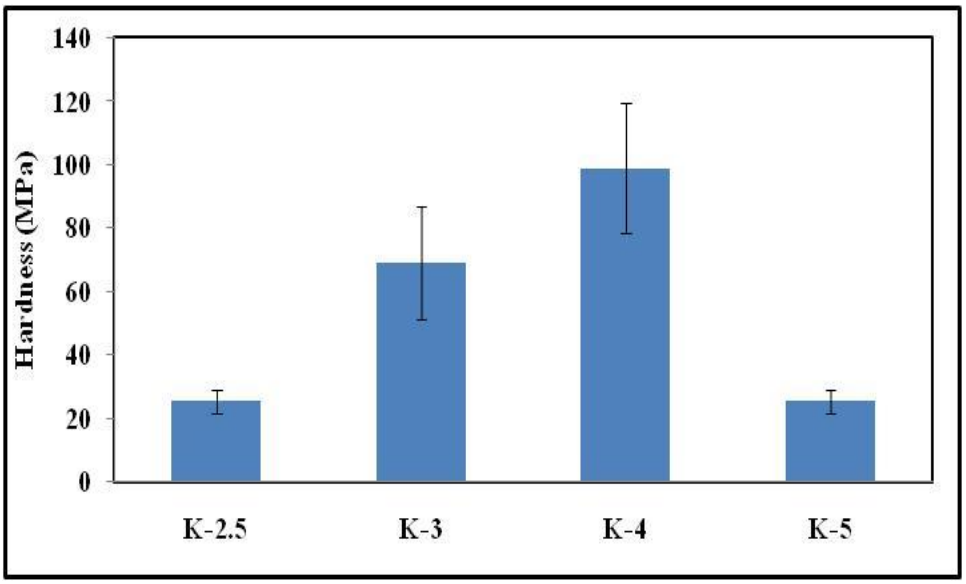

(c)

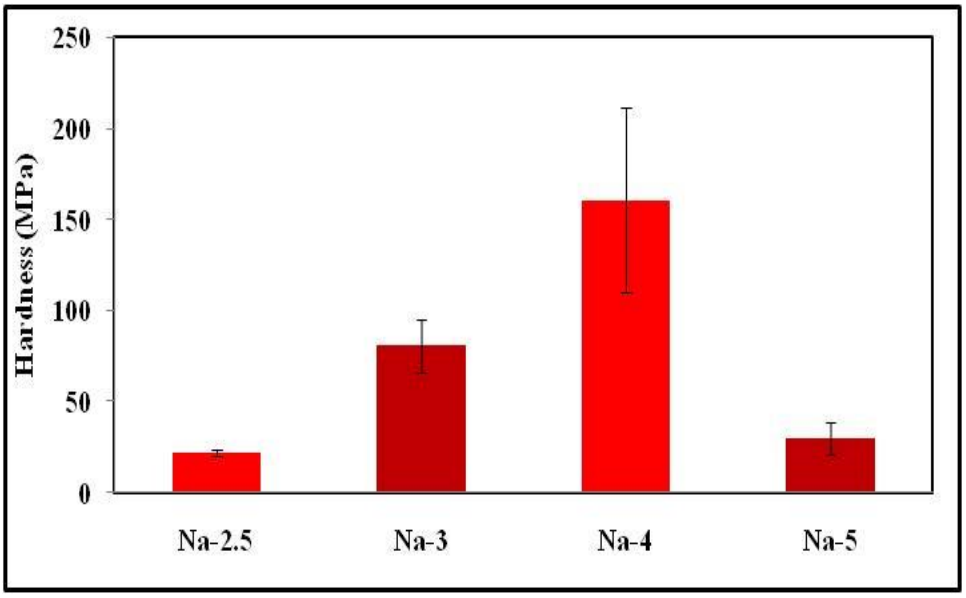

(d)

Figure 4 – 17 Continued

4.8. Vickers Indentation

The Vickes indentation was performed to characterize hardness and fracture toughness of different GPs. **Figure 4-18** shows typical SEM images of Vickers indent and surface corner cracks that form after indentation test. Indentation tests were performed using 100 and 500 gf and average values from at least 5 measurements are shown in **Figure 4-19** and listed in **Table 4-4**. These results shows that both, K-based with $SiO_2/Al_2O_3 = 4$ and Na-based GPs with $SiO_2/Al_2O_3 = 3$ exhibit the highest hardness.

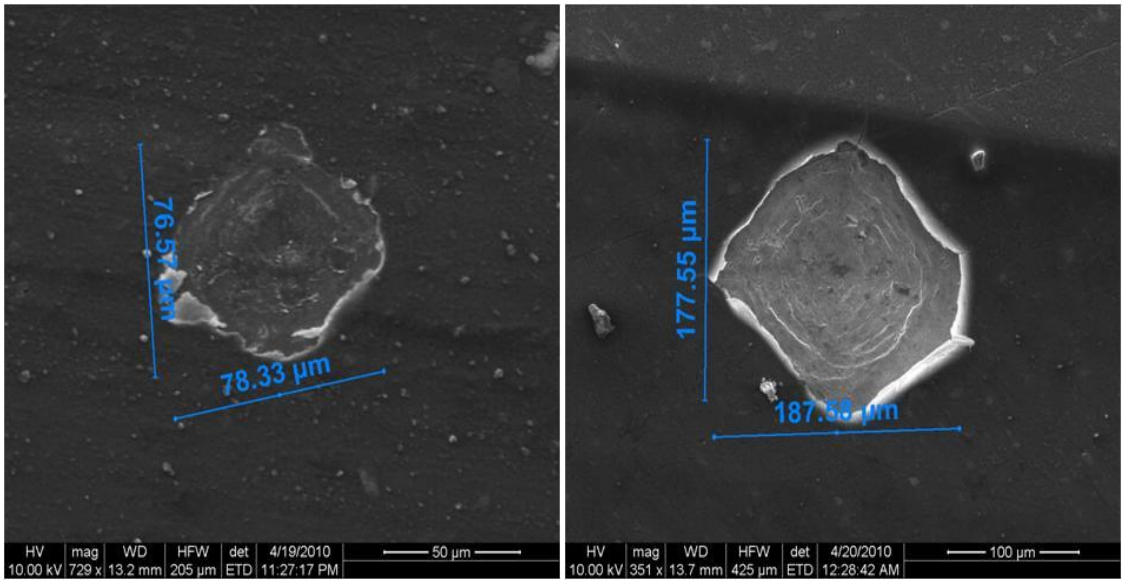

(a) K-4-24h (b) K-3-24h

Figure 4 - 18: Vickers indents made in GPs using (a) 100 gf, (b-d) 500 gf test forces

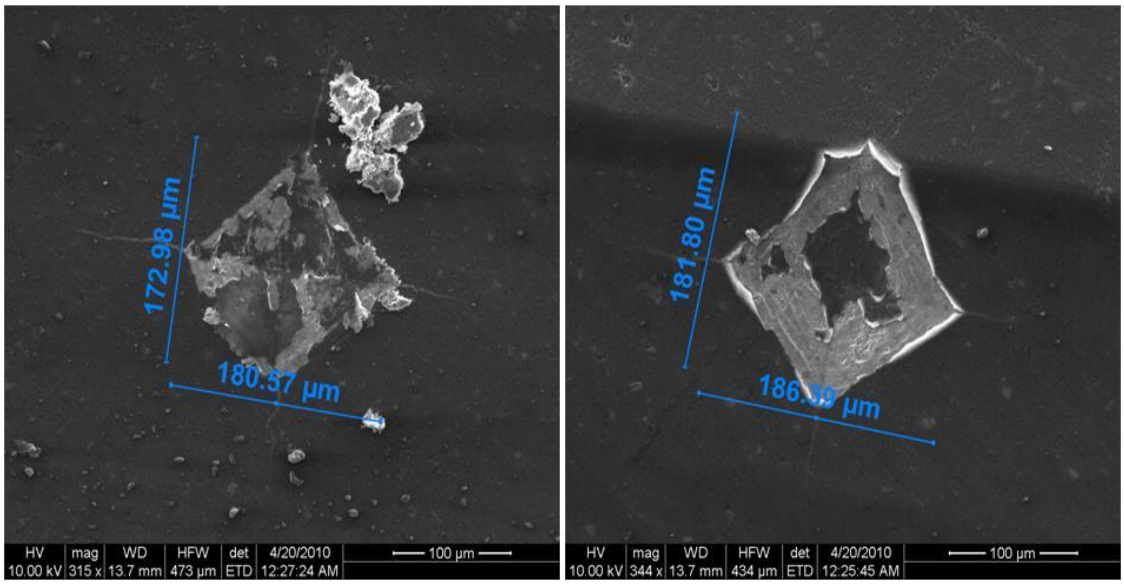

(c) K-2.5-24h (d) K-2,5-24h

Figure 4 – 18 Continued

Table 4 - 4: The hardness of GPs

SiO_2/Al_2O_3 / CuringTime	K specimens				Na specimens			
	2.5	3	4	5	2.5	3	4	5
Average Hardness (MPa)	287.5	313.4	326.6	272.8	270.5	366.8	345.7	255.8
Standard Deviation of Hardness (MPa)	22.0	79.9	61.0	31.2	135.8	167.3	54.7	21.2

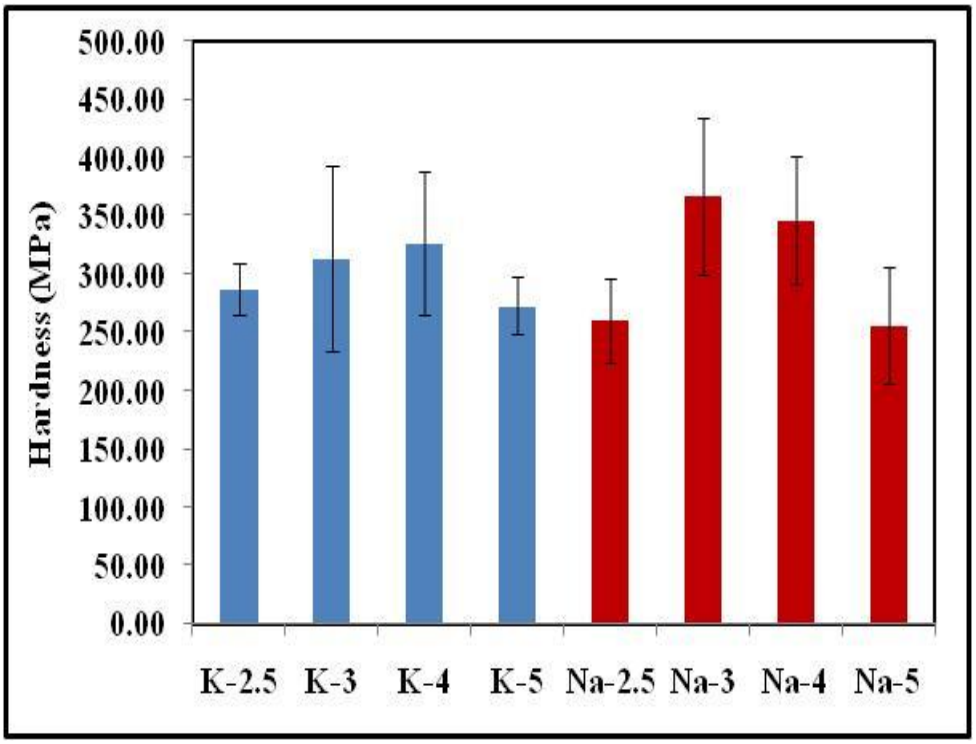

Figure 4 - 19: The Hardness values of GPs

Loading Force of 100 gf resulted in formation of indents without any observable corner cracks, as it is shown in **Figure 4-18**. Even, when using loads of 500 gf, corner cracks were observed only on some indents in GPs with SiO_2/Al_2O_3 equal to 2.5, 3 and 4 while no corner cracks were observed on GPs with ratio $SiO_2/Al_2O_3 = 5$. For the samples where corner cracks can be observed, fracture toughness was calculated using four different methods [80, 83] and the results are shown in **Table 4-5 and Figure 4-20.** Base on those results we can conclude that GPs with K-GPs with SiO_2/Al_2O_3=4 ratio have 0.60 MPa-$m^{1/2}$ of maximum fracture toughness.

Results shown here are slightly different than previously published results by Lecomte et al. [37] who showed that hardness doesn't depend on Si/Al ratio. However, the fracture toughness reported here are very close to the values by B. A. Latella et al. [29].

Table 4 – 5: The fracture toughness of GPs (Unit: Mpa-$m^{1/2}$)

	Niihara et al.[80]		Lankford [81]		Lawn et al. [82]		Anstis et al. [83]	
	average	standard deviation	average	standard deviation	average	standard deviation	average	standard deviation
K-2.5	0.32	0.12	0.35	0.13	0.18	0.06	0.22	0.07
K-3	0.30	-	0.32	-	0.17	-	0.21	-
K-4	0.54	-	0.60	-	0.30	-	0.37	-
Na-2.5	0.32	-	0.34	-	0.18	-	0.22	-
Na-3	0.18	0.05	0.19	0.05	0.10	0.03	0.13	0.03
Na-4	0.45	-	0.49	-	0.25	-	0.31	-

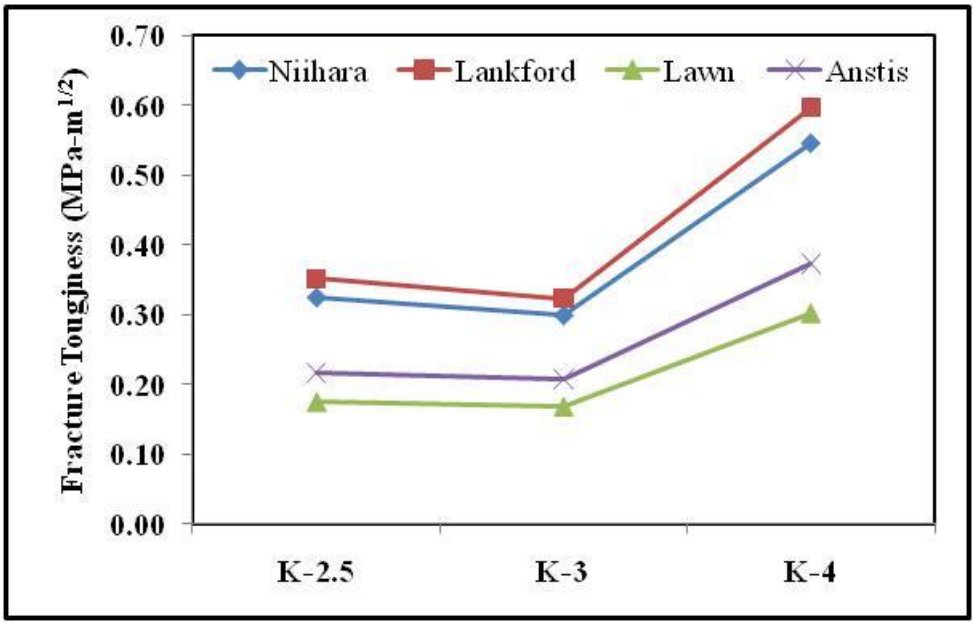

(a)

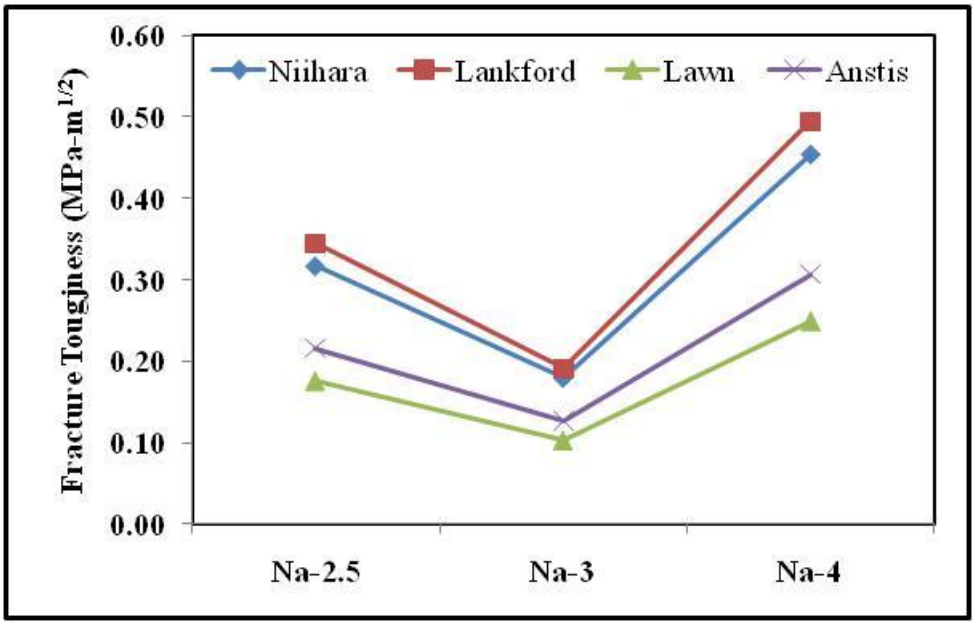

(b)

Figure 4 - 20: The results of fracture toughness: (a) K-GPs, (b) Na-GPs

4.9. The Compressive Strength Testing Results

For calculating a compressive strength, the load at which the first cracking in the GP samples occurred were determined from load-displacement curves recorded during compressive testing. Typical load displacement curves are shown in **Figure 4-21**. Compressive strengths were calculated and analyzed using Weibull statistic as it is explained in more detail in Chapter III of this thesis.

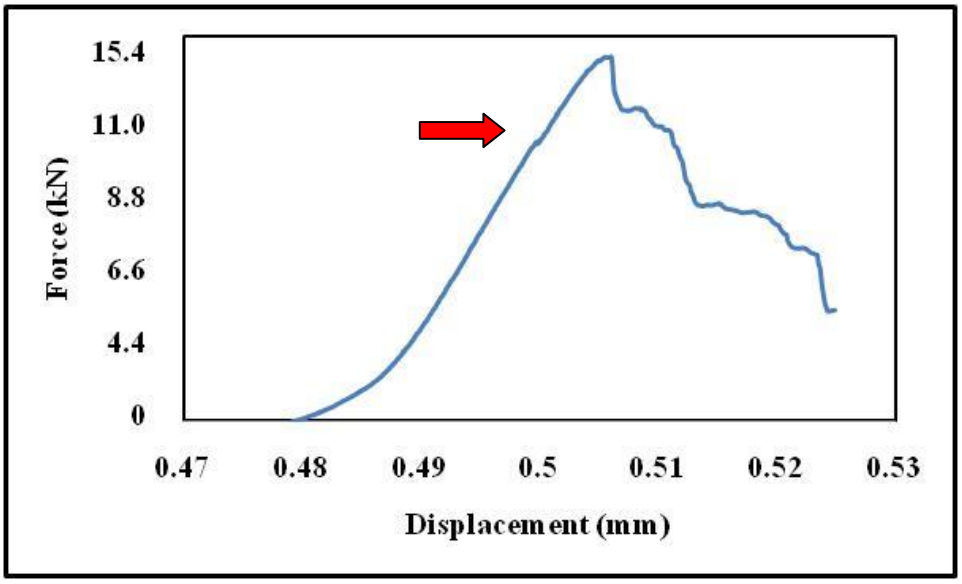

(a) K-2.5-24h

Figure 4 - 21: The typical load-displacement curves for examined GPs

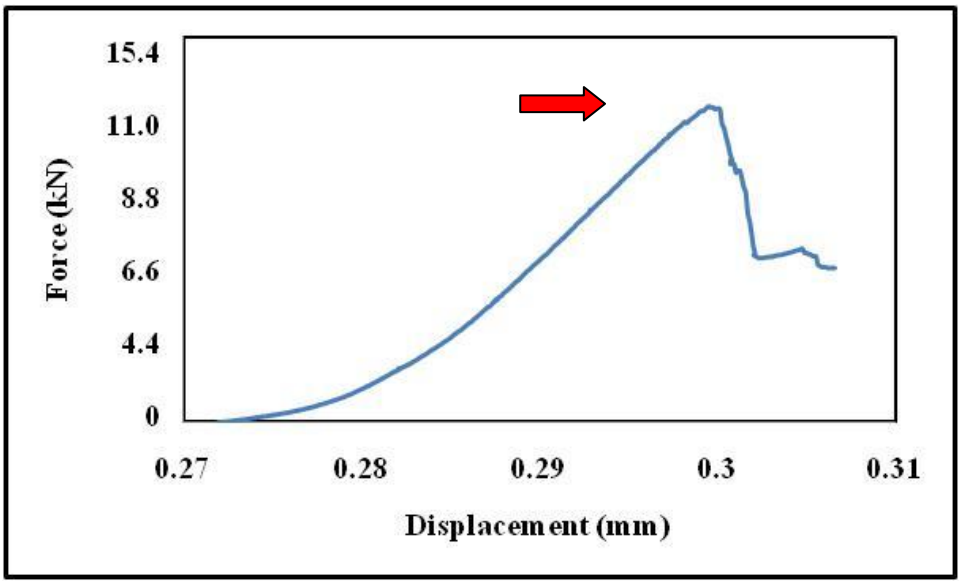

(b) Na-3-24h

Figure 4 – 21 Continued

Table 4-6 and Figure 4-22 show the average compressive strengths of GPs with different SiO_2/Al_2O_3 and cured for 24 or 48 hours. These results indicate that samples with SiO_2/Al_2O_3 ratio of 3 have a higher compressive strength than other samples with different SiO_2/Al_2O_3 ratios. A decrease in compressive strength with SiO_2/Al_2O_3 ratios can be observed in all of samples beyond SiO_2/Al_2O_3 ratio 3. In addition, K specimens were notably stronger than Na specimens for all SiO_2/Al_2O_3 ratios, with exception of SiO_2/Al_2O_3= 3. For most of the compositions, the compressive strength is slightly increased by extending curing time from 24H to 48H.

The changes of compressive strength with Si/Al ratio have the same trend as that published by P. Duxson et al. [69]. Compressive strengths of GPs examined in this study

is lower for about 10 MPa than for samples with SiO_2/Al_2O_3 ratio = 3, but higher for about 5 MPa for samples with SiO_2/Al_2O_3 ratio = 2.5 when compared to results published by P. Duxson et al. [69].

Table 4 - 6: Average compressive strengths of GPs with different composition after 24 and 48 hours of curing

CuringTime	Average compressive strength of K specimens (MPa)				Average compressive strength of Na specimens (MPa)			
	SiO_2/Al_2O_3 ratio				SiO_2/Al_2O_3 ratio			
	2.5	3	4	5	2.5	3	4	5
24 hours	24.5	31.0	24.4	23.3	16.3	31.1	24.6	23.3
48 hours	27.7	32.3	29.0	24.0	16.8	35.9	25.2	23.1

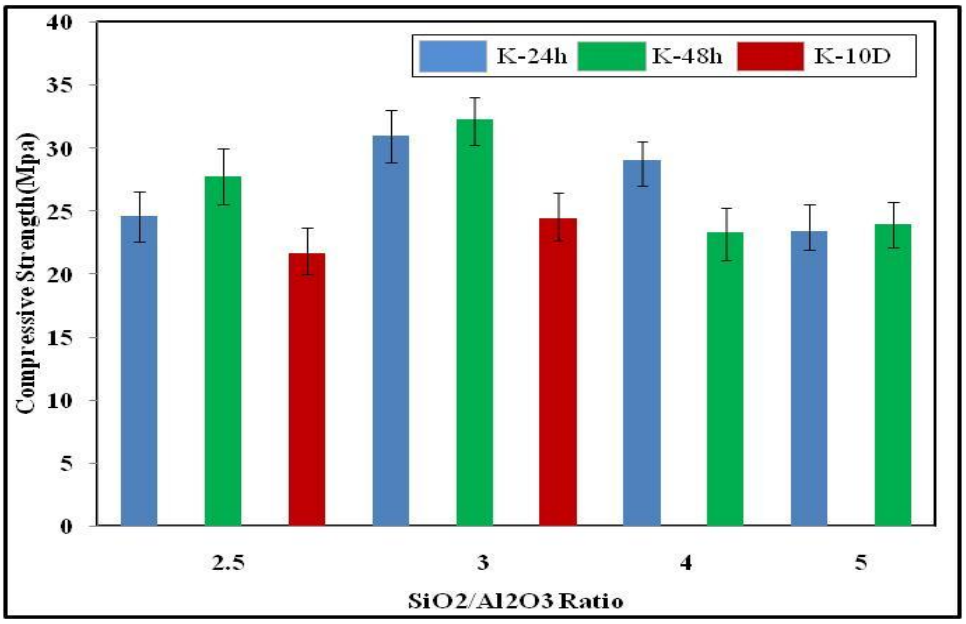

(a)

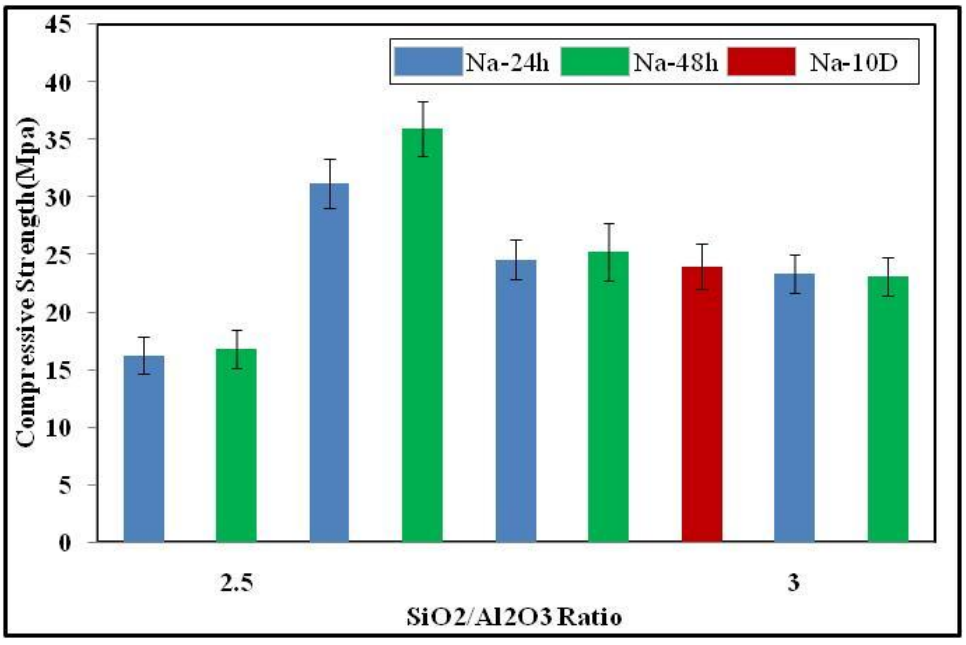

(b)

Figure 4 - 22: The average strength of GPs: (a) K-GPs, (b) Na-GPs

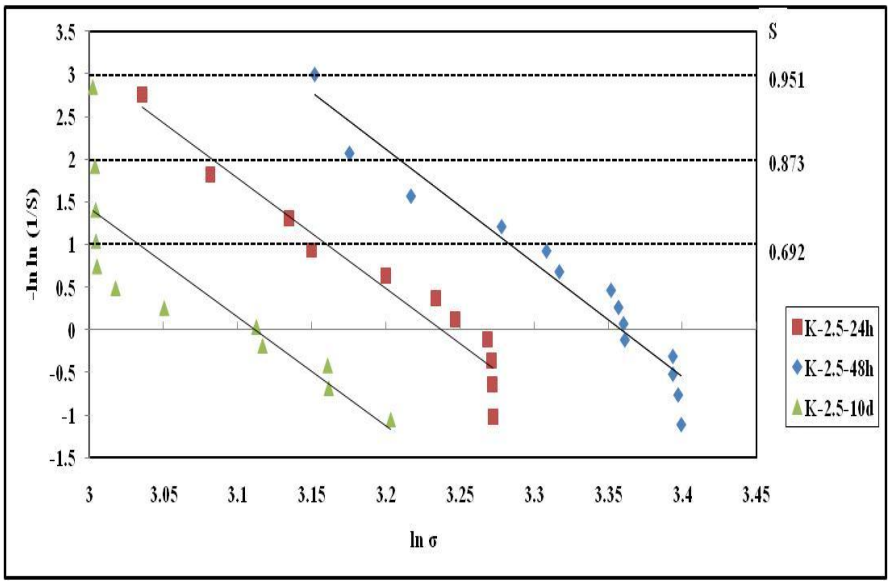

(a)

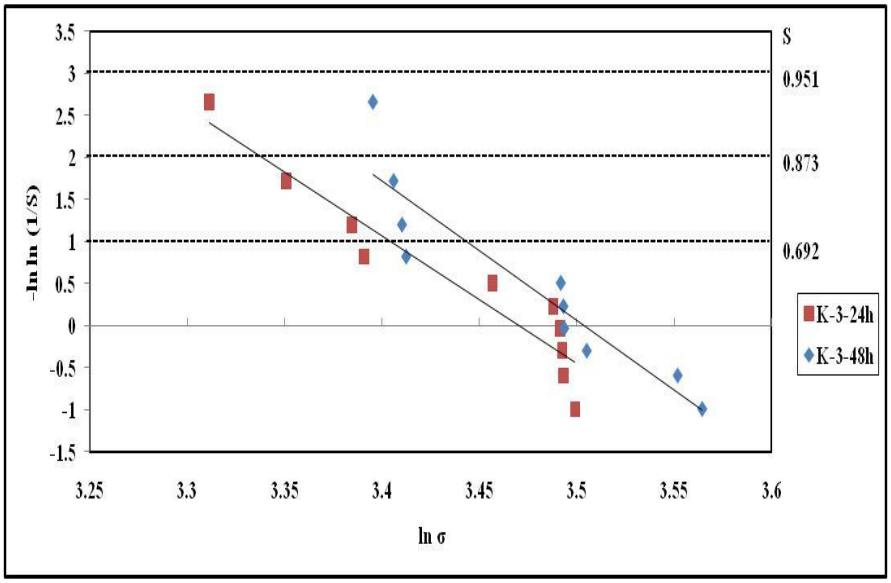

(b)

Figure 4 - 23: Weibull plots for (a-d) K-2.5, 3, 4 and 5 (e-h) Na-2.5, 3, 4 and 5

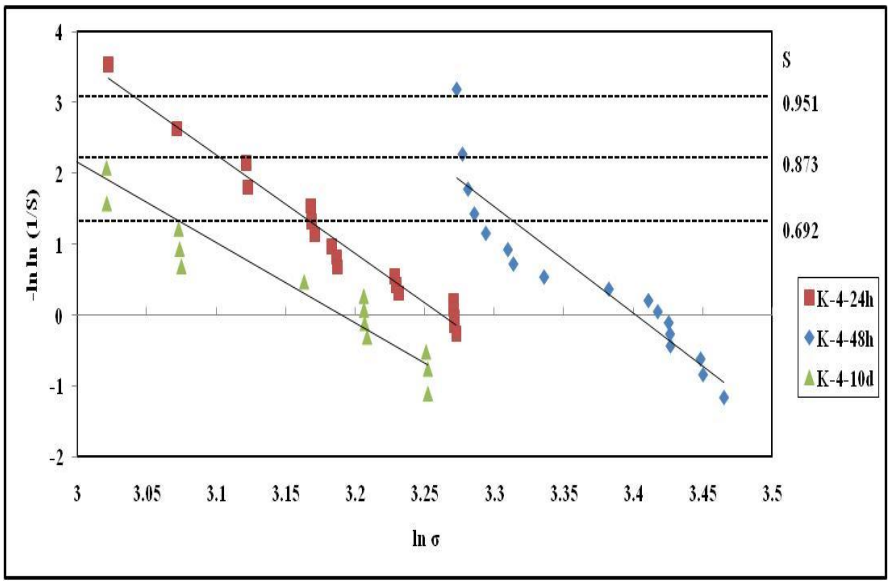

(c)

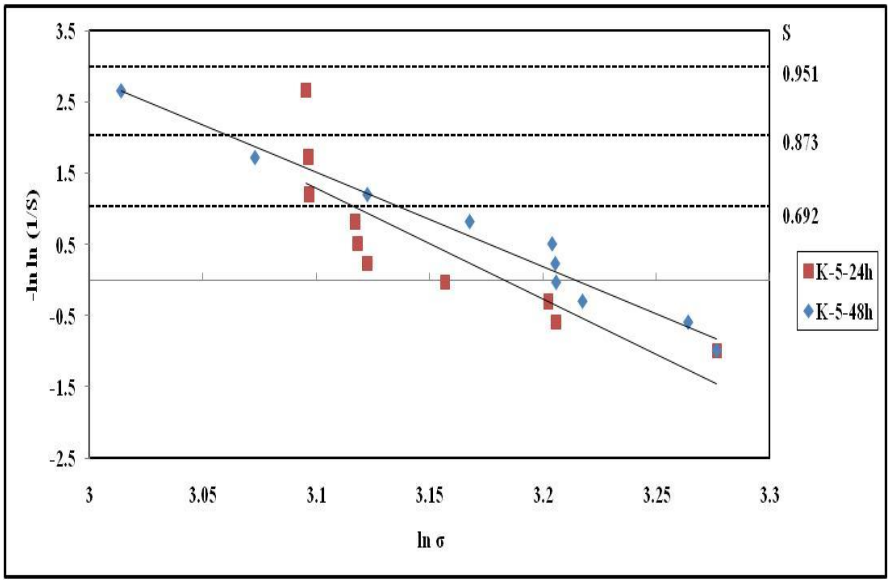

(d)

Figure 4 – 23 Continued

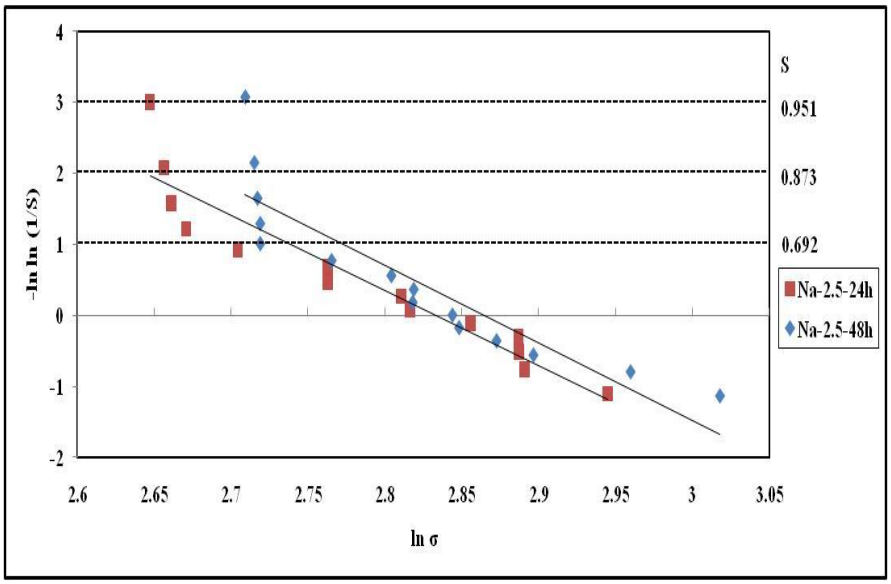

(e)

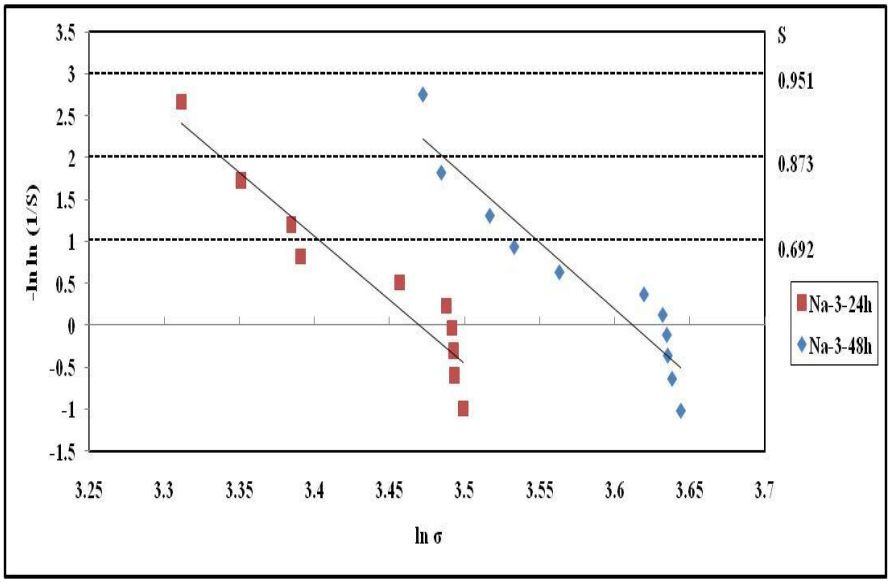

(f)

Figure 4 – 23 Continued

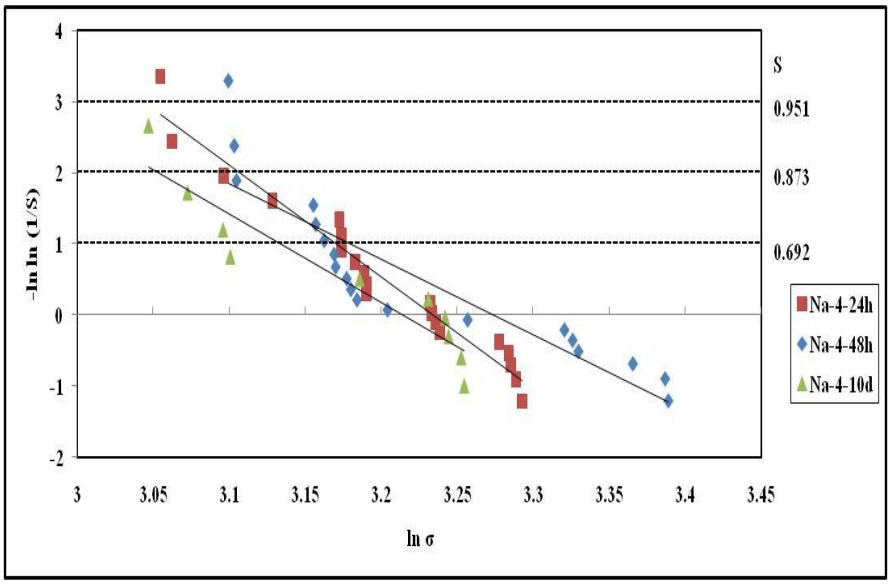

(g)

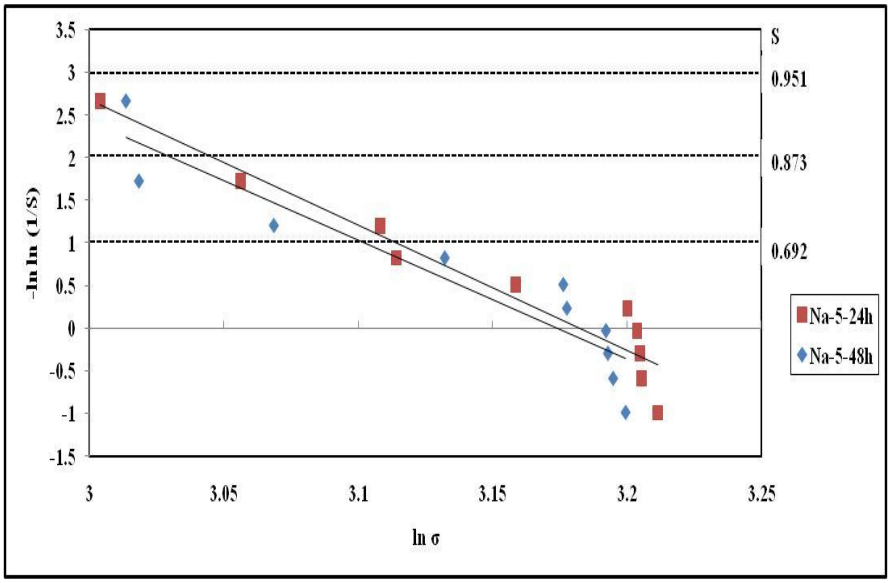

(h)

Figure 4 – 23 Continued

The results of Weibull analysis are shown in **Figures 4-22** and **4-23**, while parameters of Weibull distribution are listed in **Tables 4-7** and **4-8**. The Weibull modulus of GPs samples with SiO_2/Al_2O_3 ratio 3 to 4 is slightly higher that of samples with SiO_2/Al_2O_3 ratios of 5 or 2.5. However, the characteristic (Weibull) strength changes in the same way with SiO_2/Al_2O_3 as it is the case with average strength, **Figure 4-24**.

Table 4 - 7: Weibull moduli of characterized GPs

Curing Time / SiO_2/Al_2O_3	K-specimens		Na-specimens	
	24 h	48 h	24 h	48 h
2.5	12.9	13.3	10.6	10.9
3	15.4	16.6	15.2	15.9
4	13.9	15.0	15.7	10.6
5	15.5	13.9	14.7	13.2

Table 4 - 8: The strengths of characterized GPs

CuringTime	Characterized compressive strength of K specimens (MPa)				Characterized compressive strength of Na specimens (MPa)			
	SiO_2/Al_2O_3 ratio				SiO_2/Al_2O_3 ratio			
	2.5	3	4	5	2.5	3	4	5
24 hours	25.5	32.0	26.1	24.1	17.0	32.1	26.6	24.1
48 hours	28.7	33.3	30.1	25.0	17.5	37.1	26.4	24.0

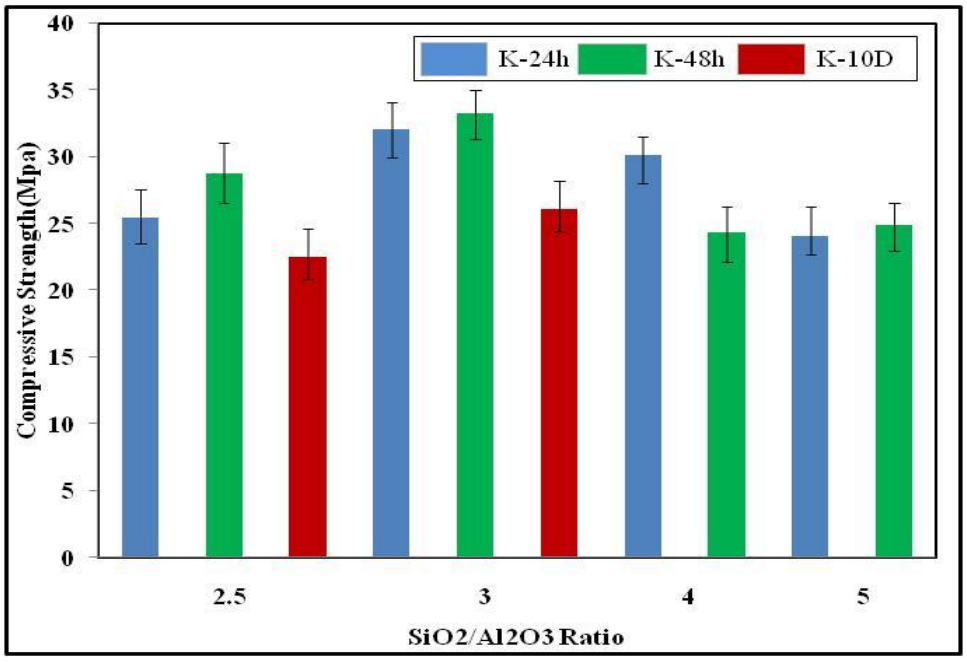

(a)

Figure 4 - 24: Characteristic (Weibull) strength of characterized GPs: (a) K-, (b) Na-GPs

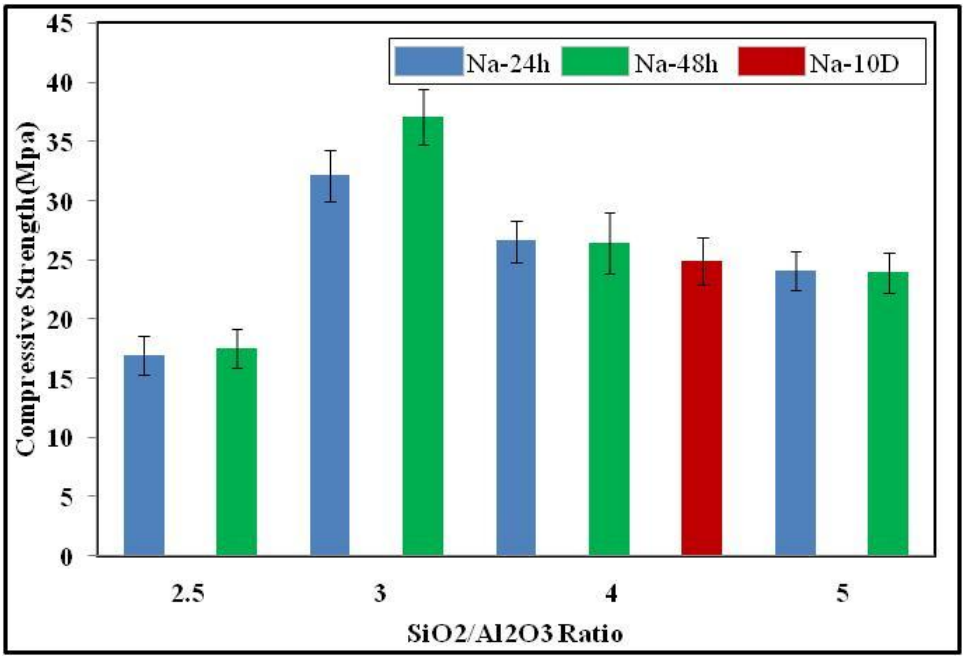

(b)

Figure 4 – 24 Continued

CHAPTER V

CONCLUSIONS AND FUTURE WORK

Geopolymers have been proven to have potential for many applications in different industries and are currently utilized in low tech applications due to their properties such as low processing temperatures, thermal stability at elevated temperatures, chemically inert, and fast curing times, just to name a few. Yet, there is a significant amount of information lacking that may take them to the forefront of many industrial applications. The expected outcome of this research was to bring forth a significant contribution in understanding geopolymer technology so as to aid in bringing this technology full circle from conception to utilization. The conclusions of this research project are presented below.

The purpose of this research was to obtain an understanding of the effects of various parameters on the mechanical properties of metakaolin-based geopolymers. Investigations were performed on the effect of alkali cations (K^+, Na^+), SiO_2/Al_2O_3 molar ratios, and curing times. The study focused on characteristic features and mechanical properties of geopolymers.

In order to verify that the materials were geopolymers, material characterization studies were carried out using X-ray diffraction (XRD), Fourier Transform Infrared spectroscopy (FTIR), Nuclear Magnetic-Resonance spectroscopy (NMR), Scanning Electron Microscopy (SEM) with Energy Dispersive Spectroscopy (EDS). These methods showed that samples have characteristic features of GP structure. X-ray

diffraction, XRD, shows that samples have 2Θ max at about 30° and amorphous hump between 25 and 35° 2Θ angle. Fourier Transform Infra-Red, FTIR spectroscopy, indicated that samples have Al-O-Al (or Si) linkages that are typical in GP structure. Nuclear Magnetic Resonance, NMR Spectroscopy, showed that virgin MK contained 4, 5, and 6 coordinated Al. After geopolymerization only 4 coordinated Al was detected at 55 ppm. **Figure 5-1** summarizes results of NMR spectroscopy and compare them to previously published data.

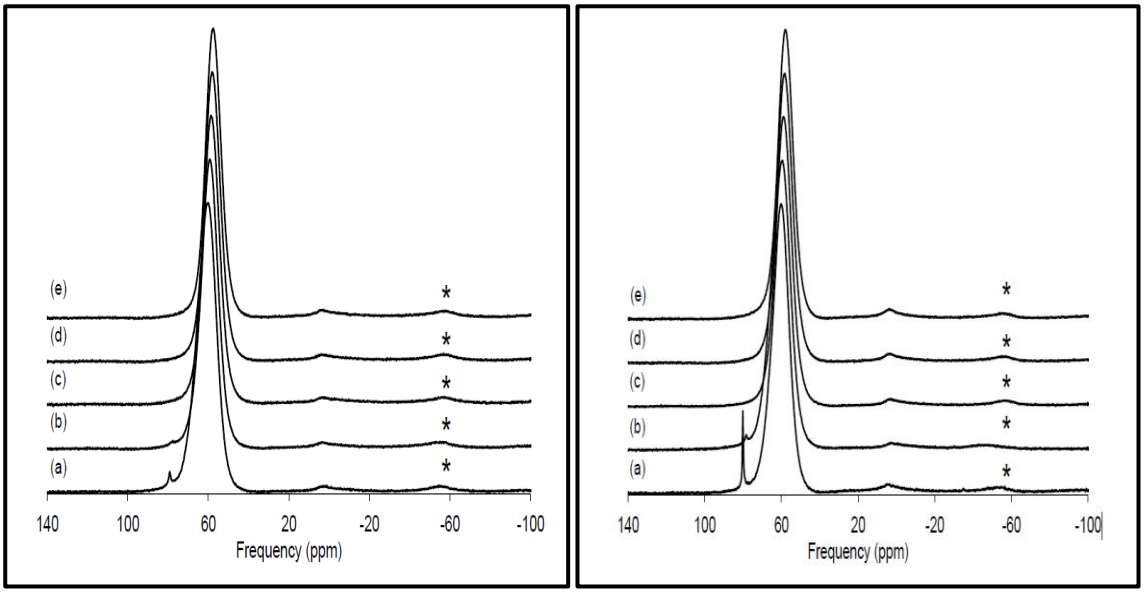

(a) K-GPs (b) Na-GPs

Figure 5 - 1: The comparison of NMR spectroscopy: (a-b) P. Duxson's work [30], (c-d) this thesis works

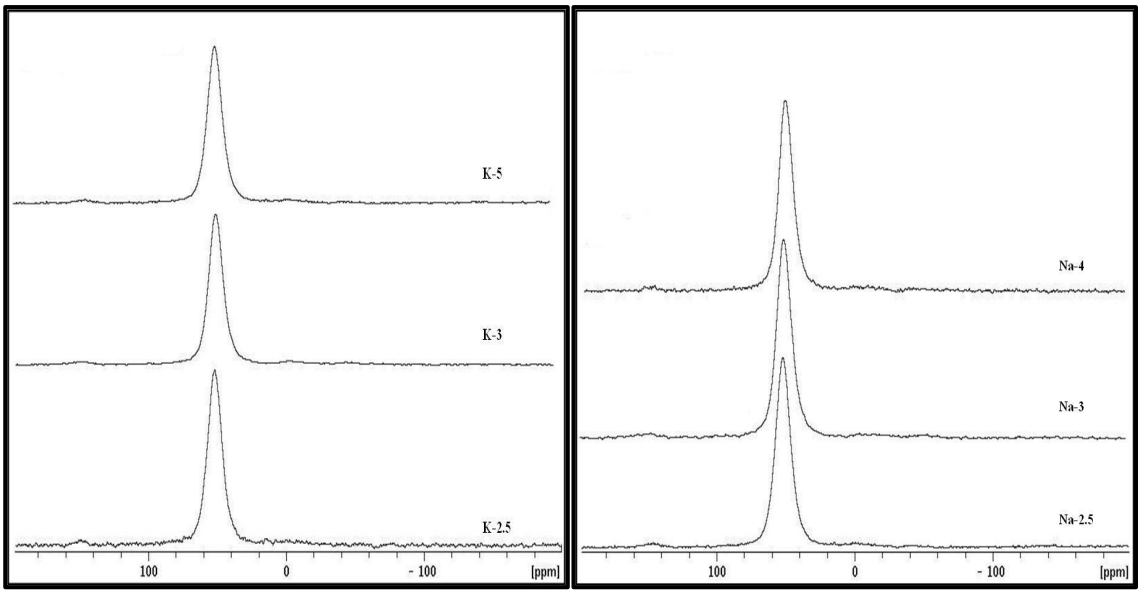

(c) K-GPs (d) Na-GPs

Figure 5 – 1 Continued

The importance of this conclusion cannot be underestimated, since it was postulated earlier that only MK with most of the Al in 4-fold coordination could result in full geopolymerization. Our work shows that this is not necessary. Even more, structural characterization showed that geopolymerization was successful for SiO_2/Al_2O_3 ratios of 2.5, 3, 4 and 5 for both metal activators K and Na, resulting in products with no 6-coordinated alumina (with chemical shift of 0 ppm in ^{27}AlNMR spectra) unlike in the case of previously published data that always showed presence of small amount of 6-coordinated Al in final products [30].

The SEM results proved that the different alkali and SiO_2/Al_2O_3 molar ratio of GPs

affected on the microstructure. The results showed that higher SiO_2/Al_2O_3 molar ratio have a more morphological dense microstructure until molar ratio 4. In addition, SEM analysis revealed a certain level of chemical in-homogeneity of the samples on the micro level, as well as presence of small amount of un-reacted precursor phase with layered structure. However, molar ratio 2.5, 5 has porous structure, which resulted in lower mechanical properties.

Mechanical properties of examined GPs are measured by different methods and results are summarized on **Figures 5-2, 5-3 and 5-4**. In general, both Na- and K-based GPs with SiO_2/Al_2O_3 =3~4 have the highest Young's modulus, strength, hardness and fracture toughness. The Young's modulus and hardness, **Figure 5-3**, and of samples increases up to SiO_2/Al_2O_3 molar ratio 4 after which it decreases with increasing SiO_2/Al_2O_3 molar ratio, with exception of Young's modulus of Na-based GPs. The fracture toughness, **Figure 5-4**, changes with SiO_2/Al_2O_3 in similar way, i.e. it increases with increasing SiO_2/Al_2O_3 molar ratios. Unfortunately, in samples with SiO_2/Al_2O_3=5 corner crack did not form during Vickers indentation and thus we were unable to determine fracture toughness of those samples. More work is needed to understand fracture behavior of GPs in indentation tests since it is very untypical for brittle solids.

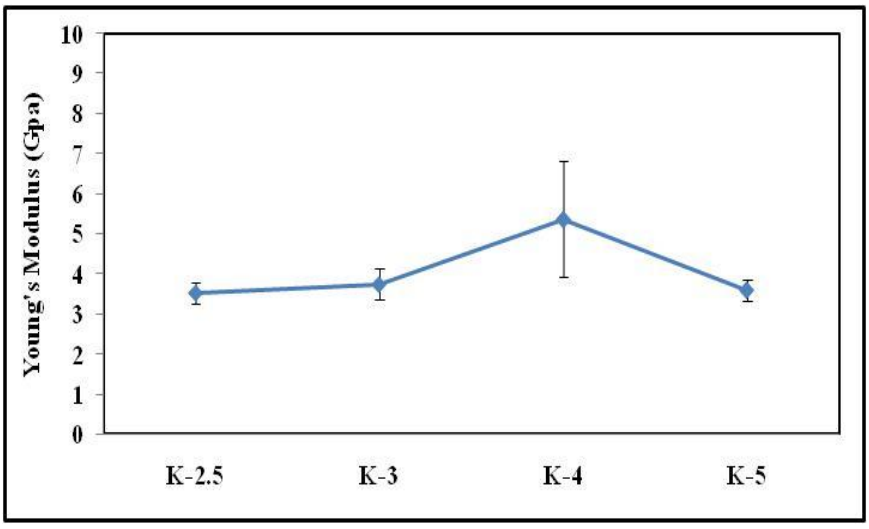

(a)

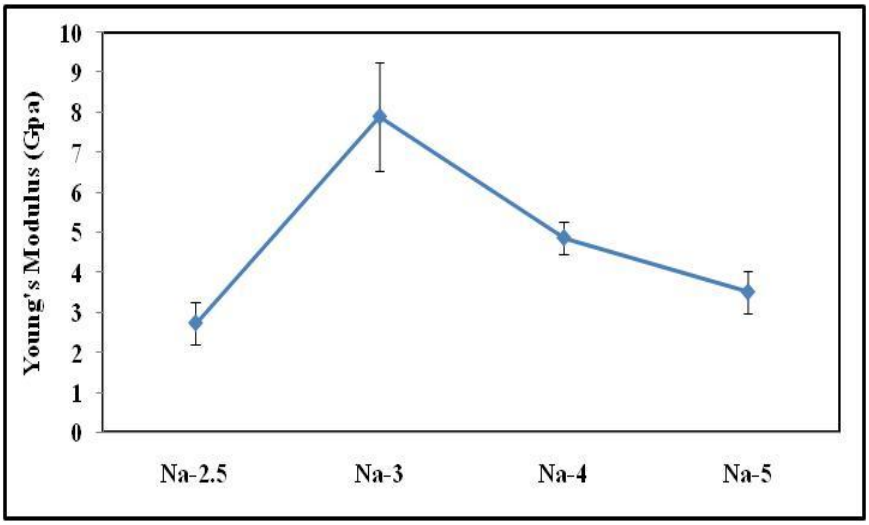

(b)

Figure 5 - 2: Young's modulus and Hardness of (a, c) K-, (b, d) Na-GPs cured for 24 h

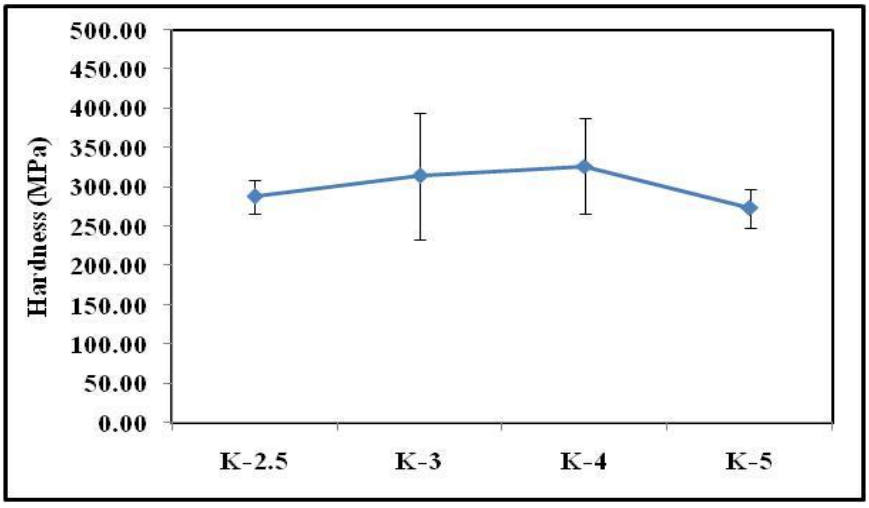

(c)

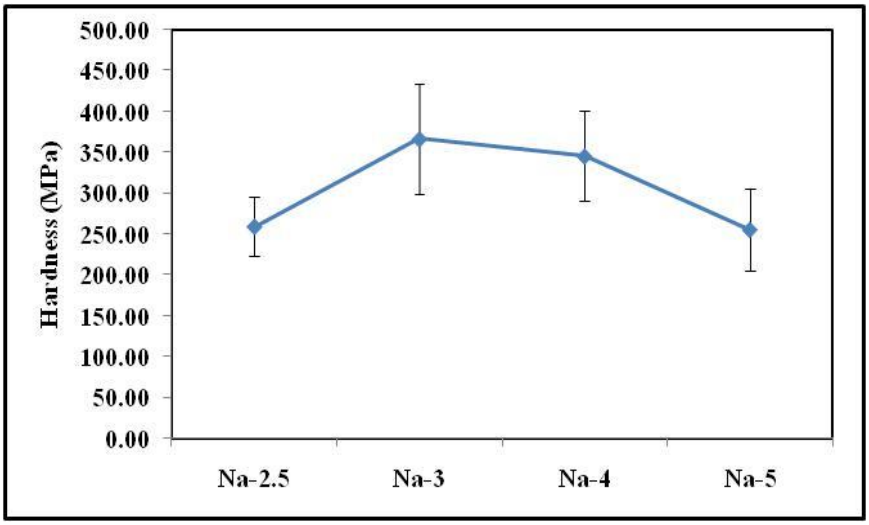

(d)

Figure 5 – 2 Continued

The observed trend in changes of mechanical properties with increasing SiO_2/Al_2O_3 ratio can be partially explained by observed microstructural features/morphology and change in apparent density of the samples. For both, K- and Na-based geopolymers, apparent density increases with increasing SiO_2/Al_2O_3 ratio. However, the microstructure of the samples appears to be more homogenous and with smaller number of large pores as SiO_2/Al_2O_3 increases from 2.5 only up to 4. Samples with SiO_2/Al_2O_3=5, although they have the highest appernant density, contains larger amount of large pores than those with SiO_2/Al_2O_3=4. Thus, decrease in mechanical properties for the samples with $SiO_2/Al_2O_3 > 4$ is most likely caused by larger amount of the large pores that can be observed in the microstructure of the processed samples. Although, the reason for appearance of large pores in the samples with SiO_2/Al_2O_3=5 is not clear at this point, we can speculate that it is result of incomplete reaction even after curing for 24 and 48 hours and larger amount of water used to process those samples. In addition, samples with SiO_2/Al_2O_3=5 were much softer than samples with lower SiO_2/Al_2O_3 after curing for 24 or 48 hour indicating that in samples with this composition geopolymerization was incomplete, resulting in less rigid 3-D network.

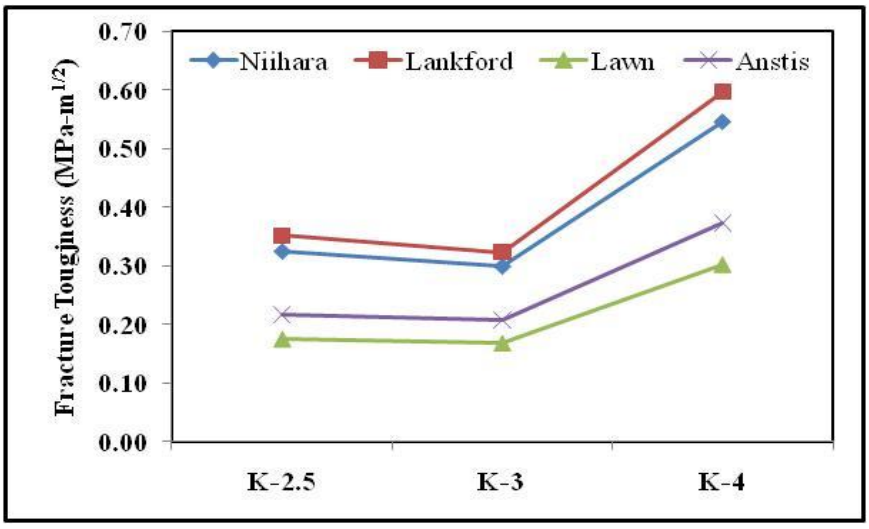

(a)

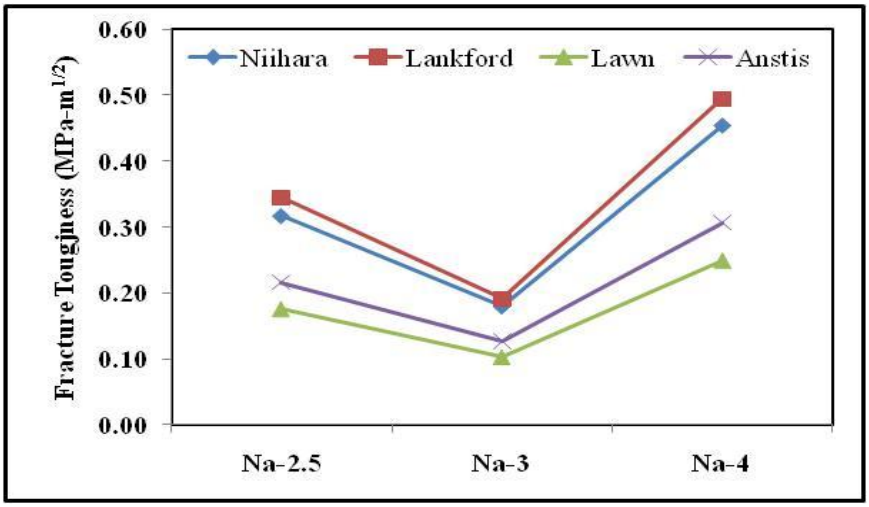

(b)

Figure 5 - 3: Fracture toughness of (a) K-GPs, (b) Na-GPs cured for 24 hours

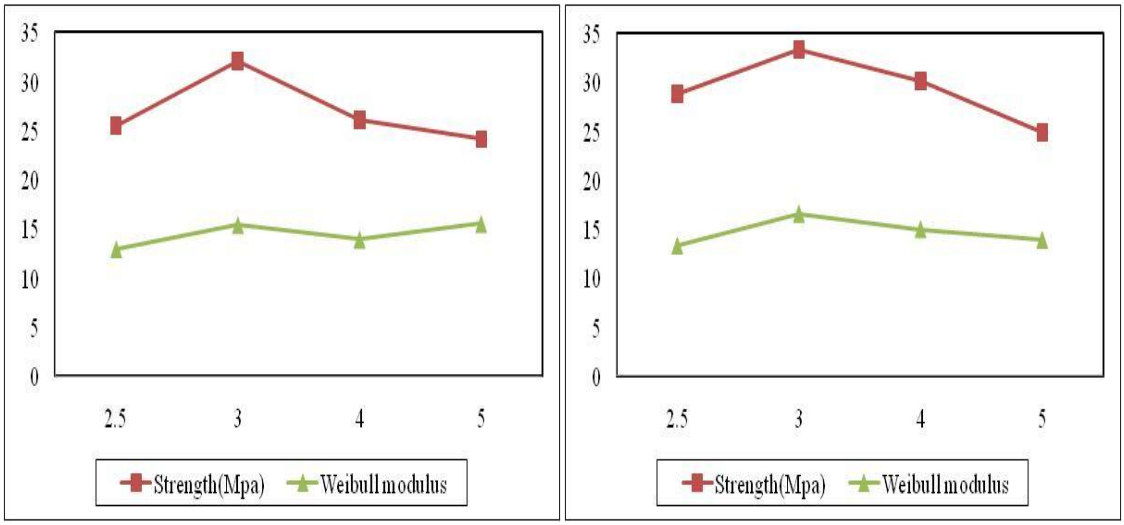

(a) (b)

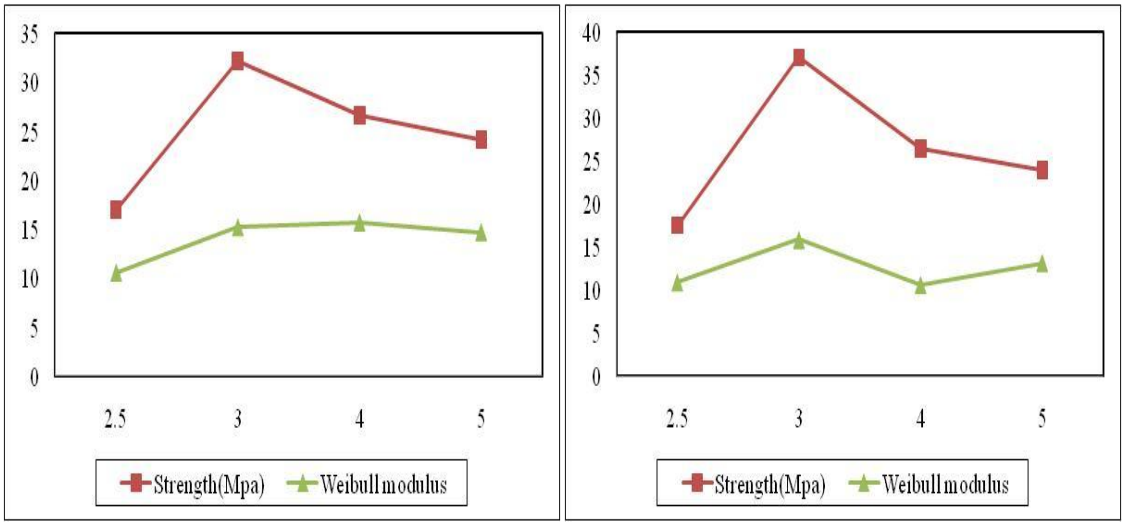

(c) (d)

Figure 5 - 4: The results of compressive strength and the Weibull modulus: (a) K-24h, (b) K-48h, (c) Na-24h, Na-48h (curing time)

This research also shows that the compressive strength of K- and Na-based GPs increases as SiO_2/Al_2O_3 molar ratio increases from 2.5 to 4, **Figure 5-4**. A decrease in strength was noticeable for samples with SiO_2/Al_2O_3 molar ratio 5. This decrease came from incomplete curing and structures with larger number of large pores than in samples with lower SiO_2/Al_2O_3 molar ratio, as it was discussed in more details previously. For solving problems and eventually increase strength of GPs with higher SiO_2/Al_2O_3 ratios, the more detailed research is needed that will result in better curing condition and improved structural properties of GPs with high SiO_2/Al_2O_3 ratios. Since extended curing time (up to 48 h) and ageing time (up to 10 days) do not results in significant increase of mechanical properties, effect of other curing parameters, such as curing temperature, humidity, etc. on mechanical properties has to be investigated in order to increase mechanical properties of GPs, especially those with higher SiO_2/Al_2O_3 ratios.

The Weilbull analysis, **Figure 5-4**, indicates the tendencies in compressive strength of GPs with different alkali cations and SiO_2/Al_2O_3 molar ratio. The Weibull modulus varies slightly between 10 and 15 for all the samples. It is worth noting that such a high value of Weibull modulus is untypical for brittle solid with such low fracture toughness as GPs. Thus, relatively high Weibull moduli indicate that the distribution of the strength controlling critical flaws is uniform in all processed samples.

REFERENCES

[1] A. O. Purdon, "The action of alkalis on blast furnace slag," *Journal of the Society of Chemical Industry,* vol. 59, pp. 191-202, 1940.

[2] V. D. Glukhovsky, G.S. Rostovskaja, and G.V. Rumyna, "High strength slag-alkaline cements," *Communications of the 7th International Congress on the Chemistry of Cement,* vol. 3, pp. 164-168, 1980.

[3] J. Davidovits, "Geopolymers - inorganic polymeric new materials," *Journal of Thermal Analysis,* vol. 37, pp. 1633-1656, Aug 1991.

[4] F. Pacheco-Torgal, J. Castro-Goines, and S. Jalali, "Alkali-activated binders: A review Part 1. Historical background, terminology, reaction mechanisms and hydration products," *Construction and Binding Materials,* vol. 22, pp. 1305–1314, 2008.

[5] J. Davidovits, *Geopolymer Chemistry and Applications*, 2nd ed. Saint-Quentin, France: Institut Geopolymer, 2008.

[6] L. Weng and K. Sagoe-Crentsil, "Dissolution processes, hydrolysis and condensation reactions during geopolymer synthesis: Part I—Low Si /Al ratio systems," *Journal of Materials Science,* vol. 42, pp. 2997-3006, 2007.

[7] K. Sagoe-Crentsil and L. Weng, "Dissolution processes, hydrolysis and condensation reactions during geopolymer synthesis: Part II. High Si/Al ratio systems," *Journal of Materials Science,* vol. 42, pp. 3007-3014, 2007.

[8] P. Duxson, "Geopolymer technology: The current state of the art," *Journal of Materials Science,* vol. 42, pp. 2917-2933, 2007.

[9] K. Komnitsas and D. Zaharaki, "Geopolymerisation: A review and prospects for the minerals industry," *Minerals Engineering,* vol. 20, pp. 1261-1277, 2007.

[10] J. L. Provis and J. S. J. van Deventer, "Geopolymerisation kinetics. 1. In situ energy-dispersive X-ray diffractometry," *Chemical Engineering Science,* vol. 62, pp. 2309-2317, 2007.

[11] P. Duxson, J. L. Provis, G. C. Lukey, and J. S. J. Van Deventer, "The role of inorganic polymer technology in the development of 'green concrete'," *Cement and Concrete Research,* vol. 37, pp. 1590-1597, 2007.

[12] J. L. Provis, *Modelling the Formation of Geopolymers*, Ph.D. dissertation, The University of Melbourne, Australia, 2006.

[13] M. G. Blackford, J. V. Hanna, K. J. Pike, E. R. Vance, and D. S. Perera, "Transmission electron microscopy and nuclear magnetic resonance studies of geopolymers for radioactive waste immobilization," *Journal of the American Ceramic Society,* vol. 90, pp. 1193-1199, 2007.

[14] J. G. S. van Jaarsveld, J. S. J. Van Deventer, and G. C. Lukey, "A comparative study of kaolinite versus metakaolinite in fly ash based geopolymers containing immobilized metals," *Chemical Engineering Communications,* vol. 191, pp. 531-549, 2004.

[15] Z. Yunsheng, S. Wei, C. Qianli, and C. Lin, "Synthesis and heavy metal immobilization behaviors of slag based geopolymer," *Journal of Hazardous Materials,* vol. 143, pp. 206-213, 2007.

[16] W. K. W. Lee and J. S. J. van Deventer, "The effects of inorganic salt

contamination on the strength and durability of geopolymers," *Colloids and Surfaces a-Physicochemical and Engineering Aspects,* vol. 211, pp. 115-126, 2002.

[17] H. Oudadesse, A. C. Derrien, M. Lefloch, and J. Davidovits, "MAS-NMR studies of geopolymers heat-treated for applications in biomaterials field," *Journal of Materials Science,* vol. 42, pp. 3092-3098, 2007.

[18] M. Sofi, J. S. J. Van Deventer, P. A. Mendis, and G. C. Lukey, "Bond performance of reinforcing bars in inorganic polymer concrete (IPC)," *Journal of Materials Science,* vol. 42, pp. 3107-3116, 2007.

[19] J. Bell, M. Gordon, and W. M. Kriven, "Use of geopolymeric cements as a refractory adhesive for metal and ceramic joints," *Ceramic Engineering and Science Proceedings,* vol. 26, pp. 407-413, 2005.

[20] S. L. Yong, "Chemical characterisation of the steel-geopolymeric gel interface," *Colloids and Surfaces a-Physicochemical and Engineering Aspects,* vol. 302, pp. 411-423, 2007.

[21] E. Gartner, "Industrially interesting approaches to 'low-CO_2' cements," *Cement and Concrete Research,* vol. 34, pp. 1489–1498, 2004.

[22] S. G. Hu, H, Wang, G. Zhang, and Q. Ding, "Bonding and abrasion resistance of geopolymeric repair material made with steel slag," *Cement & Concrete Composites,* vol. 30, pp. 239-244, Mar 2008.

[23] S. Andini, R. Cioffi, F. Colangelo, T. Grieco, F. Montagnaro, and L. Santoro, "Coal fly ash as raw material for the manufacture of geopolymer-based

products," *Waste Management,* vol. 28, pp. 416-423, 2008.

[24] A. Fernandez-Jimenez and A. Palomo, "Factors affecting early compressive strength of alkali activated fly ash (OPC-free) concrete," *Materiales De Construccion,* vol. 57, pp. 7-22, 2007.

[25] A. M. Fernandez-Jimenez, A. Palomo, and C. Lopez-Hombrados, "Engineering properties of alkali-activated fly ash concrete," *Aci Materials Journal,* vol. 103, pp. 106-112, 2006.

[26] C. D. Lawrence, "The production of low-energy cements," in *Lea's Chemistry of Cement and Concrete*, Butterworth-Heinemann, 4th ed, 2003.

[27] E. Rodriguez, R. Mejia De Gutierrez, and S. Bernal, "Effect of the SiO2/Al2O3 and Na2O/SiO2 ratios on the properties of geopolymers based on MK," *Revista Facultad De Ingenieria-Universidad De Antioquia,* pp. 30-41, Sep 2009.

[28] P. Duxson, S. W. Mallicoat, G. C. Lukey, W. M. Kriven and J. S. J. Van Deventer, "The effect of alkali and Si/Al ratio on the development of mechanical properties of metakaolin-based geopolymers," *Colloids and Surfaces a-Physicochemical and Engineering Aspects,* vol. 292, pp. 8-20, Jan 2007.

[29] B. A. Latella, D. S. Perera, D. Durce, E. G. Mehrtens, and J. Davis, "Mechanical properties of metakaolin-based geopolymers with molar ratios of Si/Al approximate to 2 and Na/Al approximate to 1," *Journal of Materials Science,* vol. 43, pp. 2693-2699, Apr 2008.

[30] P. Duxson, *The Structure and Thermal Evolution of Metakaolin Geopolymers*, Ph.D. dissertation, The University of Melbourne, Australia, 2006.

[31] V. F. F. Barbosa, K. J. D. Mackenzie, and C. Thaumaturgo, "Synthesis and characterisation of materials based on inorganic polymers of alumina and silica: sodium polysialate polymers," *International Journal of Inorganic Materials,* vol. 2, pp. 309-317, Sep 2000.

[32] P. Duxson, J. L. Provis, G. C. Lukey, and J. S. J. Van Deventer, "The role of inorganic polymer technology in the development of 'green concrete'," *Cement and Concrete Research,* vol. 37, pp. 1590-1597, Dec 2007.

[33] J. L. Provis, P. Duxson, and J. S. J. Van Deventer, "The role of particle technology in developing sustainable construction materials," *Advanced Powder Technology,* vol. 21, pp. 2-7, Jan 2010.

[34] K. Komnitsas, D. Zaharaki, and V. Perdikatsis, "Geopolymerisation of low calcium ferronickel slags," *Journal of Materials Science,* vol. 42, pp. 3073-3082, May 2007.

[35] J. G. S. van Jaarsveld and J. S. J. van Deventer, "Effect of the alkali metal activator on the properties of fly ash-based geopolymers," *Industrial & Engineering Chemistry Research,* vol. 38, pp. 3932-3941, Oct 1999.

[36] R. D. Hart, J. L. Lowe, D. C. Southam, D. S. Perera, and P. Wal, "Aluminosilicate inorganic polymers from waste materials," *Green Processing 2006,* vol. 2006, pp. 93-103, 198, 2006.

[37] I. Lecomte, M. Liegeois, A, Rulmont, R. Cloots, and F. Maseri, "Synthesis and characterization of new inorganic polymeric composites based on kaolin or white clay and on ground-granulated blast furnace slag," *Journal of Materials Research,*

vol. 18, pp. 2571-2579, Nov 2003.

[38] S. Alonso and A. Palomo, "Alkaline activation of metakaolin and calcium hydroxide mixtures: Influence of temperature, activator concentration and solids ratio," *Materials Letters,* vol. 47, pp. 55-62, Jan 2001.

[39] Z. H. Zhang, X. Yao, H. Zhu, S. Hua, and Y. Chen, "Activating process of geopolymer source material: Kaolinite," *Journal of Wuhan University of Technology-Materials Science Edition,* vol. 24, pp. 132-136, Feb 2009.

[40] X. Yao, Z. Zhang, H. Zhu, and Y. Chen, "Geopolymerization process of alkali-metakaolinite characterized by isothermal calorimetry," *Thermochimica Acta,* vol. 493, pp. 49-54, Sep 10 2009.

[41] F. Zibouche, H. Kerdjoudj, J. D. Lacaillerie, and H. V. Damme, "Geopolymers from Algerian metakaolin. Influence of secondary minerals," *Applied Clay Science,* vol. 43, pp. 453-458, Mar 2009.

[42] H. Xu and J. S. J. van Deventer, "Effect of source materials on geopolymerization," *Industrial & Engineering Chemistry Research,* vol. 42, pp. 1698-1706, 2003.

[43] E. Kamseu, A. Rizzuti, C. Leonelli, and D. Perera, "Enhanced thermal stability in K2O-metakaolin-based geopolymer concretes by Al2O3 and SiO2 fillers addition," *Journal of Materials Science,* vol. 45, pp. 1715-1724, Apr 2006.

[44] J. L. Provis, C. Z. Yong, P. Duxson, and J. S. J. Van Deventer, "Correlating mechanical and thermal properties of sodium silicate-fly ash geopolymers," *Colloids and Surfaces a-Physicochemical and Engineering Aspects,* vol. 336, pp.

57-63, Mar 2009.

[45] J. L. Bell, P. E. Driemeyer, and W. M. Kriven, "Formation of ceramics from metakaolin-based geopolymers. Part II: K-based geopolymer," *Journal of the American Ceramic Society,* vol. 92, pp. 607-615, Mar 2009.

[46] D. L. Y. Kong, J. G. Sanjayan, and K. S. Crentsil, "Factors affecting the performance of metakaolin geopolymers exposed to elevated temperatures," *Journal of Materials Science,* vol. 43, pp. 824-831, Feb 2008.

[47] C. Panagiotopoulou, E. Kontori, T. Perraki, and G. Kakali, "Dissolution of aluminosilicate minerals and by-products in alkaline media," *Journal of Materials Science,* vol. 42, pp. 2967-2973, May 2007.

[48] J. Davidovits, "Structural characterization of goepolymeric materials with X-Ray diffractometry and MAS-NMR spectroscopy," in Proc. *Geopolymer '88,* pp. 149-166, 1988.

[49] J. Sauer and G. Engelhardt, "Relative stability of (Al-O-Al) linkages in zeolites - a non-empirical molecular-orbital study," *Zeitschrift Fur Naturforschung Section a-a Journal of Physical Sciences,* vol. 37, pp. 277-279, 1982.

[50] J. Faimon, "Oscillatory silicon and aluminum aqueous concentrations during experimental aluminosilicate weathering," *Geochimica Et Cosmochimica Acta,* vol. 60, pp. 2901-2907, Aug 1996.

[51] N. Kasai and M. Kakudo. *Springer Series in Chemical Physics* [Electronic Book]. pp. 80, Apr 2005.

[52] H. Stanjek and W. Hausler, "Basics of X-ray diffraction," *Hyperfine Interactions,*

vol. 154, pp. 107-119, 2004.

[53] D. Khale and R. Chaudhary, "Mechanism of geopolymerization and factors influencing its development: A review," *Journal of Materials Science,* vol. 42, pp. 729-746, 2007.

[54] J. Davidovits, "Geopolymers: Inorganic polymeric new materials," *Journal of Thermal Analysis,* vol. 37, pp. 1633-1656, Aug 1991.

[55] E. Hemmings, "The role of non-crystalline phases in the activation of metallurgical slags," in *International Workshop on Granulated Blast-Furnace Slag in Concrete*, Toronto, Canada, 1987, pp. 441-458.

[56] W. K. W. Lee and J. S. J. van Deventer, "Use of infrared spectroscopy to study geopolymerization of heterogeneous amorphous aluminosificates," *Langmuir,* vol. 19, pp. 8726-8734, 2003.

[57] J. Davidovits, *Geopolymer Chemistry and Applications*, 2nd ed. Saint-Quentin, France: Insiritut Geopolymere, 2008.

[58] C. A. Rees, J. L. Provis, G. C. Lukey, and J. S. J. Van Deventer, "The mechanism of geopolymer gel formation investigated through seeded nucleation," *Colloids and Surfaces a-Physicochemical and Engineering Aspects,* vol. 318, pp. 97-105, Apr 2008.

[59] P. Duxson, G. C. Lukey, and J. S. J Van Deventer, "The thermal evolution of metakaolin geopolymers: Part 2 - Phase stability and structural development," *Journal of Non-Crystalline Solids,* vol. 353, pp. 2186-2200, 2007.

[60] P. R. Griffiths and J. A. de Haseth, *Fourier Transform Infrared Spectromery*

Hoboken, NJ: Wiley, 2007.

[61] N. Jaggi and D. R. Vij, "Chapter 9 Fourier transform infrared spectroscopy," in *Handbook of Applied Solid State Spectroscopy*, D. R. Vij, Ed., ed New York: Springer, 2006.

[62] P. J. Hore and C. L. John, "NMR principles," in *Encyclopedia of Spectroscopy and Spectrometry*, Oxford, England: Elsevier, 1999, pp. 1545-1553.

[63] N. E. Jacobsen, *NMR Spectroscopy Explained*. Hoboken, NJ: Wiley, 2007.

[64] E. J. Nassar, E. C. O. Nassor, L. R. Avila, P. F. S. Pereira, and A. Cestari et al., "Spherical hybrid silica particles modified by methacrylate groups," *Journal of Sol-Gel Science and Technology,* vol. 43, pp. 21-26, Jul 2007.

[65] H. Xu, *Geopolymerization of aluminosilicate minerals*, Ph.D. dissertation, Univeristy of Melbourne, Australia, 2002.

[66] J. Klinowski, S. Berger, and S. Braun, "A highly siliceous structural analog of zeolite-Y - high-resolution solid-state Si-29 and Al-27 NMR-studies," *Inorganic Chemistry,* vol. 22, pp. 63-66, 1983.

[67] W. Loewenstein, "The distribution of aluminum in the tetrahedra of silicates and aluminates," *American Mineralogist,* vol. 39, pp. 92-96, 1954.

[68] B. H. W. S. Jong, C. M. Schramm, and V. E. Parziale, "Polymerization of silicate and aluminate tetrahedra in glasses, melts, and aqueous-solutions .4. aluminum coordination in glasses and aqueous-solutions and comments on the aluminum avoidance principle," *Geochimica Et Cosmochimica Acta,* vol. 47, pp. 1223-1236, 1983.

[69] P. Duxson, J. L. Provis, G. C. Lukey, S. W. Mallicoat, and W. M. Kriven et al., "Understanding the relationship between geopolymer composition, microstructure and mechanical properties," *Colloids and Surfaces a-Physicochemical and Engineering Aspects,* vol. 269, pp. 47-58, Nov 2005.

[70] W. M. Kriven, J. L. Bell, and M. Gordon, "Microstructure and microchemistry of fully-reacted geopolymers and geopolymer matrix composites," *Advances in Ceramic Matrix Composites IX,* vol. 153, pp. 227-250, 347, 2003.

[71] Z. Yunsheng, S. Wei, and L. Zongjin "Synthesis and microstructural characterization of fully-reacted potassium-poly(sialate-siloxo) geopolymeric cement matrix," *Aci Materials Journal,* vol. 105, pp. 156-164, Mar-Apr 2008.

[72] R. R. Lloyd, J. L. Provis, and J. S. J. Van Deventer, "Microscopy and microanalysis of inorganic polymer cements. 2: The gel binder," *Journal of Materials Science,* vol. 44, pp. 620-631, Jan 2009.

[73] H. L. Wang, H. Li, and F. Yan"Synthesis and mechanical properties of metakaolinite-based geopolymer," *Colloids and Surfaces a-Physicochemical and Engineering Aspects,* vol. 268, pp. 1-6, Oct 31 2005.

[74] M. Rowles and B. O'Connor, "Chemical optimisation of the compressive strength of aluminosilicate geopolymers synthesised by sodium silicate activation of metakaolinite," *Journal of Materials Chemistry,* vol. 13, pp. 1161-1165, 2003.

[75] M. A. Glinicki and M. Zielinski, "Depth-sensing indentation method for evaluation of efficiency of secondary cementitious materials," *Cement and Concrete Research,* vol. 34, pp. 721-724, Apr 2004.

[76] I. Belena and W. Zhu, "Nanoindentation study of Na-geopolymers exposed to high temperatures," in Proc. *Nanotechnology in Construction 3,* pp. 169-174, 437, 2009.

[77] O. Burciaga-Diaz, J. I. E. Gatcia, R. A. Aguilar, and A. Gorokhovsky, "Statistical analysis of strength development as a function of various parameters on activated metakaolin/slag cements," *Journal of the American Ceramic Society,* vol. 93, pp. 541-547, Feb 2010.

[78] J. Temuujin, R. P. Williams, and A. Van Riessen, "Effect of mechanical activation of fly ash on the properties of geopolymer cured at ambient temperature," *Journal of Materials Processing Technology,* vol. 209, pp. 5276-5280, Jul 2009.

[79] Z. H. Zhang, X. Yao, H. Zhu, S. Hua, and Y. Chen, "Preparation and mechanical properties of polypropylene fiber reinforced calcined kaolin-fly ash based geopolymer," *Journal of Central South University of Technology,* vol. 16, pp. 49-52, Feb 2009.

[80] K. Nihara, "New design concept of structural ceramics - ceramic nanocomposites," *Nippon Seramikkusu Kyokai Gakujutsu Ronbunshi-Journal of the Ceramic Society of Japan,* vol. 99, pp. 974-982, Oct 1991.

[81] J. Lankford, "Indentation microfracture in the palmqvist crack regime - implications for fracture-toughness evaluation by the indentation method," *Journal of Materials Science Letters,* vol. 1, pp. 493-495, 1982.

[82] B. R. Lawn, "Indentation of ceramics with spheres: A century after Hertz," *Journal of the American Ceramic Society,* vol. 81, pp. 1977-1994, Aug 1998.

[83] G. R. Anstis, P. Chantikul, B. R Lawn, and D. B. Marshall, "A critical-evaluation of indentation techniques for measuring fracture-toughness .1. direct crack measurements," *Journal of the American Ceramic Society,* vol. 64, pp. 533-538, 1981.

[84] M. W. Barsoum, Ed., *Fundamentals of Ceramics*. New York: Taylor & Francis Group, LLC, 2003.

[85] J. L. Bell, P. Sarin, P. E. Driemeyer, R. P. Haggerty, and P. J. Chupas et al., "X-ray pair distribution function analysis of a metakaolin-based, KAlSi2O6 center dot 5.5H(2)O inorganic polymer (geopolymer)," *Journal of Materials Chemistry,* vol. 18, pp. 5974-5981, 2008.

[86] A. Palomo and F. P. Glasser, "Chemically-bonded cementitious materials based on metakaolin," *British Ceramic Transactions and Journal,* vol. 91, pp. 107-112, Jul-Aug 1992.

[87] A. Sindhunata, *A conceptual model of geopolymerisation*, Ph.D. dissertation, The University of Melbourne, Australia, 2006.

[88] V. C. Farmer, "The infrared spectra of minerals," *Mineralogical Society Monogram,* vol. 4, pp. 50, 1988.

[89] M. Alkan, M. Oktay, M. M. Kocakerim, and M. Copur, "Solubility of chlorine in aqueous hydrochloric acid solutions," *Journal of Hazardous Materials,* vol. 119, pp. 13-8, Mar 2005.

[90] P. De Silva, K. S. Crenstil, and V. Sirivivatnanon, "Kinetics of geopolymerization: Role of Al2O3 and SiO2," *Cement and Concrete Research,* vol. 37, pp. 512-518,

Apr 2007.

VITA

Name:	Hyunsoo Kim
Address:	c/o Dr. Miladin Radovic Department of Materials Science and Engineering Texas A&M University College Station, TX, 77843-3003
Email Address:	c14469@gmail.com
Education:	B.S., Weapons Engineering, Korea Military Academy, 2004 M.S., Material Science and Engineering, Texas A&M University, 2010